Aircraft Noise Model Improvement by Calibration of Noise-Power-Distance Values using Acoustic Measurements

Rebekka (R.C.) van der Grift

Delft University of Technology

TU Delft

knowledge & development centre
Mainport Schiphol

Aircraft Noise Model Improvement by Calibration of Noise-Power-Distance Values using Acoustic Measurements

by

Rebekka (R.C.) van der Grift

to obtain the degree of Master of Science
at the Delft University of Technology.
to be defended publicly on Thursday January 27, 2022 at 14:00.

Student number:	4341279	
Project duration:	February 1, 2021 – January 27, 2022	
Thesis committee:	Prof. dr. ir. M. Snellen,	TU Delft, supervisor
	Prof. dr. D. G. Simons,	TU Delft
	Dr. A. Bombelli,	TU Delft
	Ir. F. Dijkstra,	KDC

An electronic version of this thesis is available at `http://repository.tudelft.nl/`.

TU Delft

Preface

Aircraft noise and its impact is a daily discussion subject in the aviation industry. It is a tangible subject, while also being a large technical challenge. This drove me to start my thesis in aircraft noise modelling and measurement. Over the last year, I came in contact with many experts in this research field and had interesting discussions on the topic of aircraft noise. I would like to thank these people who helped me in the making of this thesis.

First of all, I would like to thank the ANCE department of the TU Delft and especially my daily supervisor Mirjam Snellen, who guided me through the project with her knowledge on the topic. The regular meetings we had were always informative and helpful, but also encouraging, which left me more passionate about the topic of aircraft noise than before. I would also like to thank Dick Simons for his critical reviews and the help with the statistics applied in this research. This helped me to bring the research to a higher level.

I would like to thank Ferdinand Dijkstra for his supervision on behalf of the KDC and the many discussions on the value of noise modelling and measurement and how my research can contribute to the industry and the communities.

A special thank you is in order to Max Heilig from LVNL, whose work I got to proceed. The weekly meetings we had, with many useful and detailed discussions on noise modelling and calibration, were extremely helpful in bringing this thesis to a successful end.

Further, I would like to thank Wouter Dalmeijer from Amsterdam Airport Schiphol for his critical view during our meetings and for the access to the ANOMS application, for without this research would not be possible.

I also would like to thank KLM, and mainly Gerry, for the help and access to the Aircraft Condition and Monitoring System data. This data was key to a successful and innovative research.

Finally, I would like to thank my friends and family for their support during this busy year. When starting my thesis one year ago, I never imagined the passion I would develop for the subject of aircraft noise modelling and measurement. My thesis project has been an educational, but most of all fun learning experience and I look forward to continuing in this field.

Rebekka (R.C.) van der Grift
Delft, January 13, 2022

Contents

List of Figures

List of Tables

Nomenclature

Symbols

α	Absorption coefficient	m^{-1}	h	Altitude	ft
β	Elevation angle	°	h_m	Microphone height	m
Δ_I	Engine installation correction	dBA	L_A	A-weighted Sound level	dBA
Δ_F	Finite segment correction	dBA	$L_{A_{max}}$	Maximum A-weighted sound level	dBA
Δ_{imp}	Impedance correction	dBA	L_{DEN}	Day-Evening-Night L_A	dBA
Δ_V	Duration correction	dBA	M	Mach number	-
ϵ	Bank angle	°	m	Mass	kg
γ	Flight path angle	°	$N1$	Rotational speed	rpm
Λ	Lateral adjustment	dBA	P	Power spectral density	Pa^2/Hz
ψ	Angle of the aircraft and the observer	°	p_e	Effective pressure	Pa
			Q	Reflection coefficient	-
φ	Phase shift	-	R	Lift to drag ratio	-
a	Acceleration	m/s^2	R	Pearson correlation coefficient	-
DI	Directivity Index	θ	r	Distance	m
f	Frequency	Hz	T	Temperature	$C°$
F_n	Thrust force per engine	lb	V_C	Calibrated airspeed	kts
f_s	Sampling frequency	Hz	W	Acoustic power	$Watt$
g	Gravitational constant	m/s^2	W	Weight	lb

Abbreviations

$ACMS$	Aircraft Condition and Monitoring System.
$AEDT$	Aviation Environmental Design Tool.
$ANCON$	Aircraft Noise Contour.
$ANOMS$	Airport Noise and Operations Management System.
$ANoPP$	Aircraft Noise Prediction Program.
ANP	Aircraft Noise and Performance.
$BADA$	Eurocontrol Base of Aircraft Data.
BPF	Blade Passing Frequency.
$ECAC$	European Civil Aviation Conference.
FDR	Flight Data Recorder.
GTF	Geared Turbofan.
$ICAO$	International Civil Aviation Organisation.
ILS	Instrument Landing System.
INM	Integrated Noise Model.
$MFCC$	Mel Frequency Cepstral Coefficients.
MWU	Mann-Whitney-U test.
$NADP$	Noise Abatement Departure Procedure.
NMT	Noise Monitoring Tower.
$NOMOS$	Noise Monitoring System.
NPD	Noise Power Distance.
$OSPL$	Overall Sound Pressure Level.
PBL	Pressure Band Level.
PWL	Power Watt Level.
RH	Relative Humidity.
$RMSE$	Root Mean Square Error.
SAE	Society of Automotive Engineers.
SEL	Sound Exposure Level.
SNR	Signal to Noise Ratio.
SPL	Sound Pressure Level.

Introduction

The aviation industry is growing. Every day more aircraft take-off and land on airports around the world and with that a growing impact on the environment. In regions around airports, aircraft noise is causing annoyance and adverse health effects for people in those communities. Government regulations are in place to limit these effects and reduce the impact of aviation noise. This is done by limiting the amount and times of flight operations and adapting their respective routes. The noise impact of these flights is calculated with aircraft noise models. Aircraft noise modelling can be done on multiple levels of detail, but the most common approach for large scale noise calculations is based on simple empirical relations called Noise-Power-Distance (NPD) tables. The noise values are measured for multiple aircraft power settings and distances between aircraft and observer positions. Inaccuracies in input data can cause 20-30% area contour differences [1]. The need for accurate noise models is thus important.To validate these model calculations, validation is performed by comparing the results with measurements, but often large (unexplained) differences are measured. For better noise predictions, the differences between model results and measurements must be reduced.

In this research, methods to improve aircraft noise modelling by calibration of NPD values is done. The research objective is as follows:

> "The research objective is to minimise differences between noise model results and measurements by creating a method to accurately calibrate the models' input parameters using acoustic measurements."

This research objective will be fulfilled by splitting the topic into four sections. The first part is a literature review. To understand the (dis-)advantages and accuracy of noise models, an in-depth study is performed. The current best-practice methods with respect to modelling and measuring aircraft noise are analysed. This research will work with the ECAC Doc.29 model [2] and the measurements from the Noise Monitoring System (NOMOS) placed around Schiphol Airport. The second part of this research is to find a reliable method to gather model input information. For a large number of historical flights, the distance and power settings are derived through RADAR and acoustic data, respectively. This data is validated using the Aircraft Condition and Monitoring System (ACMS) aboard multiple flights. Thirdly, a comparison with measurements needs to be made. An analysis of the reliability of each measurement is performed after which a comparison with the model calculations can be carried out. In the final part of the research objective, the model is calibrated by altering the NPD values to improve the models' accuracy.

In this report the thesis is documented in three parts. In Part I the main research methods, results and conclusions are given in a paper format. In Part II, the results of a literature study on the topic of the research are presented. This literature study is previously graded under AE4020. Finally, in Part III, supporting chapters that are complementary to the research paper are given. In chapter 1, a more extensive analysis of the used methods and results are given for the B737-800. After which in chapter 2 and 3 the methods used in the paper are repeated for the B737-700 and A330-300, respectively.

I

Paper

Aircraft Noise Model Improvement by Calibration of Noise-Power-Distance Values using Acoustic Measurements

Rebekka (R.C.) van der Grift
Delft University of Technology, 2629 HS Delft, The Netherlands

Aircraft noise and its impact is one of the biggest challenges the aviation industry faces today. At airports, the number of operations and the flight routes are driven by the noise impact on the surrounding communities. To predict the expected aircraft noise levels around airports, noise models are used. The accuracy of these models is thus of great importance. This research aims to improve aircraft noise modelling by validation and calibration of the main input parameters using acoustic measurements. This research is focused on the Doc.29 aircraft noise model. This is an empirical model, based on Noise-Power-Distance (NPD) tables, which is convenient for fast computations of a large number of flight operations. The data set used consists of take-off measurements of the B737-800 gathered around Schiphol airport. To validate and calibrate the model with measurements, all input parameters should be correct to be able to identify where deviations come from. The power parameter thrust is an important input, but often not exactly known. The N1 rotational speed of the engines can be used to estimate the used thrust. An estimation of the N1% is performed by finding the fan tones from acoustic measurements. The found N1% is validated with Aircraft Condition and Monitoring System data (ACMS) from the measured flights. The estimation resulted in an average 4% root mean square error with the ACMS data. When using the estimated N1% as input for thrust, differences between model results and measurement are still found. These differences are assumed to be caused by errors in the NPD table. This allows altering the entries in the NPD table by adding the found differences from the measurements reduces the mean error to less than ±0.2 dBA and providing a 20-30% reduction in standard deviation. Another method of model improvement is done by looking at the measurements which have been standardised to reference conditions. The relation between thrust setting and sound level showed to be less dominant than originally expected from the NPD table. From these newfound thrust-noise relations, new NPD tables are created. This caused a 30-40% reduction in standard deviation, reducing the variation found between noise measurements and model results significantly. Next to an improvement in best-practice noise modelling, the methods described in this research give insight into the creation and validation of NPD values.

I. Introduction

THE aviation industry is growing and with it the noise nuisance of communities around airports. To predict the effects of noise, noise models have been established which calculate the expected noise heard on the ground from (a set of) aircraft. These noise models are, for example, used to regulate the number of operations or create new flight routes to prevent too much noise at certain times and locations. Models used for these practices are empirical models, based on measurements. These types of models have fast computation times, which is beneficial for a large number of operations. As these models have a great impact on the planning and growth of the aircraft industry, accuracy is needed.

In Europe, a harmonised approach for noise modelling was deemed important, as such the ECAC Doc.29 was developed [1–3]. These documents contain the methods of calculating aircraft noise following the current best-practice standards and a method to verify the model. This method of calculating aircraft noise has been in place since the ‘60 and updated throughout the years to take newer aircraft models and discovered effects into account.

Previous studies related to the validation of models such as Doc.29 were performed [4, 5], but deviations between model and measurements remained. The mean differences between model results and measurements can be reduced by calibrating the Noise-Power-Distance (NPD) values [6]. This proved effective, but even for similar aircraft flying at the same distance from the microphones, variations are measured. The variation of measurements of landing aircraft could partly be explained by a difference in engine setting or speed [7, 8]. The variation and the effect this has on take-off operations is yet to be investigated. As engine noise is deemed dominant during take-off, this information is valuable.

Therefore, this paper is focused on take-off operations. To limit the scope, the research is shown for the B737-800, but more aircraft types are analysed.

The research objective of this paper is to improve aircraft noise modelling by evaluating the Doc.29 input parameters and calibrating the model using acoustic measurements. To do this, the structure of this paper is as follows: In section II the current practice of noise modelling using Doc.29 and the measurement system are discussed. Section III explains the method and validation of retrieving accurate thrust input. After which section IV describes the model results and the comparison to the measurements. These measurements are then used in section V to calibrate and improve the model. Finally, in section VI the conclusions and recommendations following this research are drawn.

II. Current practice

In current practice, the prediction of aircraft noise impact is done on large scales. Large airports, like Amsterdam Airport Schiphol (AAS), have noise monitoring systems in place around the airport. General reports of these measurements are written, but single event comparison and validation of model results with measurements is limited. To gain a better understanding of how the Doc.29 model works and what its limitations are, an in-depth analysis of its inputs is performed. Further, when comparing model results to measurements from the Noise Monitoring System (NOMOS) around Schiphol Airport, the characteristics and uncertainties of the microphones need to be known. In this section, these subjects are discussed.

A. Doc.29 model

In the ECAC developed Doc.29, calculation instructions on how to model perceived noise on the ground is given. These model techniques are following the best-practise guidelines and are applied worldwide. Doc.29 works similar to the Aviation Environmental Design Tool (AEDT) and the Dutch Noise Model (NRM). These so-called empirical models are based on measurements and have an accuracy of 1 to 2 dB for locations calculated directly beneath the flight path [9]. The model is used for calculations of, for example, L_{DEN} (Day-Evening-Night) contours of airports. The accuracy is deemed accurate enough when producing contours. However, on a single event level, these deviations can become quite significant [10].

Best practice models such as Doc.29 make use of Noise Power Distance (NPD) tables. As the name suggests, it gives the noise level for combinations of power (lb) and distance (ft). NPD tables are given for EPNL, $L_{A,max}$, PNLTM and Sound Exposure Level (SEL) for both approach and departure operations. In this research, the focus is on $L_{A,max}$ and SEL as these are commonly used for contour calculations. These noise levels are empirically gathered through a number of measurements and standardised for standard atmosphere and a reference speed of 160 kts in accordance with AIR-1845 [9]. These measurements are often done during certification of the aircraft and are then extrapolated for all values in the NPD table.

The inputs and outputs of the Doc.29 model are illustrated in Figure 1. The aircraft and operation types are necessary to find the correct NPD table. After which the distance and power inputs are needed to find the corresponding noise level. The exact distance is logarithmic inter-/extrapolated from the NPD distances to find the correct noise level, while the power is inter-/extrapolated linear from the NPD power values. Lastly, weather information is needed to find the attenuation correction. More on corrections to the NPD table is discussed in section II.A.2.

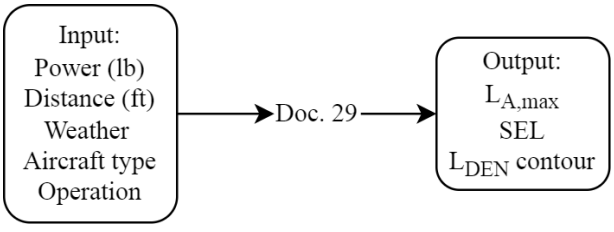

Fig. 1 Main input and output of the Doc.29 model.

1. Thrust input parameter

As mentioned, the model requires two main input parameters: power and distance. Distance is found from the (expected) flight path of the aircraft. The power estimation, however, is a bit more difficult. Although many studies on

how to estimate power from historical flights are being performed, a lack of operational data is still present. For thrust estimation methods based on aircraft performance, information about the weight and aerodynamic properties of the aircraft is needed. In multiple studies these parameters are estimated. In Strümpfel and Hübner [11] ADS-B data and the Base of Aircraft Data (BADA) [12] are used with 11% accuracy for thrust estimation.

For the modelling of future flights, an estimation of the used thrust profile is needed. This is done by what we call procedural steps. For each flight phase (take-off, climb-out etc.), a power setting is assumed. A few default steps can be found in the Aircraft Noise and Performance (ANP)* database of which an example is given in Table 1. These steps are different for aircraft in varying weight ranges. The weight of the aircraft is based on the expected distance that the aircraft has to fly and thus the amount of fuel it is carrying. The table is for the first stage length of 0-500 nm (926 km) and thus the lightest modelled aircraft.

Table 1 Default thrust procedural steps for B737-800 with stage length 1.

Step Number	Step Type	Thrust Rating	Flap_ID	End Altitude (ft)	Rate of Climb (ft/min)	End CAS (kt)
1	Takeoff	MaxTakeoff	T_05			
2	Climb	MaxTakeoff	T_05	1000		
3	Accelerate	MaxTakeoff	T_05		1885.7	181.7
4	Accelerate	MaxTakeoff	T_01		2112	204.8
5	Climb	MaxTakeoff	T_00	2040		
6	Climb	MaxClimb	T_00	3000		
7	Accelerate	MaxClimb	T_00		1891.3	250
8	Climb	MaxClimb	T_00	5500		
9	Climb	MaxClimb	T_00	7500		
10	Climb	MaxClimb	T_00	10000		

The thrust rating can be calculated using the engine parameters, also given in the ANP database, and Equation 1. This equation calculates the corrected net thrust F_n using the coefficients from Table 2, the calibrated airspeed V_C, altitude of the aircraft h and the temperature at the aircraft position T. For a standard atmosphere, this results in Figure 2.

$$\frac{F_n}{\delta} = E_0 + F_0 V_C + G_A h + G_B h^2 + HT \tag{1}$$

Table 2 Engine parameters for the B737-800 for different flight phases.

ACFT_ID	Thrust Rating	E (lb)	F (lb/kt)	Ga (lb/ft)	Gb (lb/ft2)	H (lb/ °C)
737800	IdleApproach	649	-3.3	0.0118	0	0
737800	MaxClimb	22403.5	-27.2645	0.305603	0	0
737800	MaxClimbHiTemp	26593.3	-26.293	-0.078	0	-174.4
737800	MaxTakeoff	26089.1	-29.1098	0.143559	0	0
737800	MaxTkoffHiTemp	30143.2	-29.773	-0.029	0	-145.2

*https://www.aircraftnoisemodel.org/

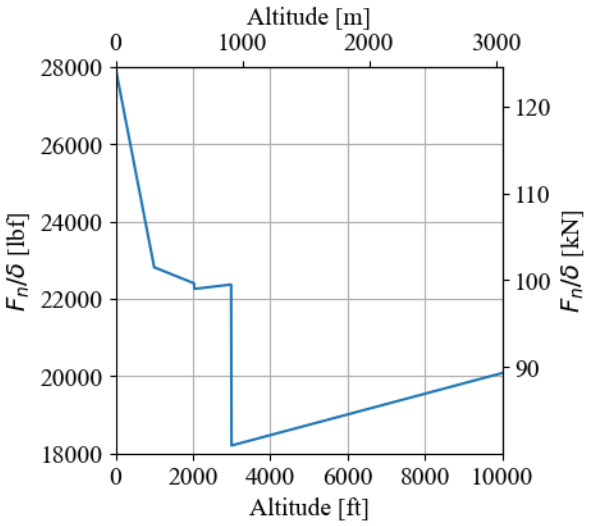

Fig. 2 Standard thrust setting during departure of B737-800 for stage length 1.

2. Correction terms for Noise Power Distance values

The NPD tables are given for most aircraft types but are often generalised. For example, the B737-700 and B737-800 make use of the same NPD table. When an aircraft type does not have its own table, a substitution is found. To account for the differences between the aircraft while using the same NPD values, correction factors are used. These correction factors are a general $\Delta L(dBA)$ that is applied to all NPD values for departure or approach. Two methods exist and are both given by Doc.29. The first is a correction factor based on its ICAO code. The other method is based on the configuration of the aircraft (engine-frame combination) using the EASA Type Certificate Database and its noise record number. These noise record numbers can be found in national registers such as the Dutch aircraft register[†] for each specific aircraft tailnumber. This second method is used for this research as this is the preferred method [2].

The weather correction is for the change in atmospheric attenuation of sound with changing atmosphere. This correction factor is applied by calculating $\Delta L_A(T, p_a, h_{rel}, d_i)$ for every distance d_i in the NPD table and adding those values to the existing table. ΔL_A is the difference in absorption between the sound level at the measurement atmosphere $L_{A,atm}$ and the sound level in reference standard atmosphere $L_{A,ref}$ (101325 Pa, 15 °C, 80% relative humidity). This factor is calculated by removing the standard atmospheric attenuation $\alpha_{n,ref}$ and calculating the new α_n for every frequency band n. This is done by using the given engine spectrum from the ANP database, which contains the expected sound levels of the frequency bands at 1000ft from the aircraft. In Equation 2 the weather correction factor is calculated by subtracting the attenuation corrections for each of the 17 frequency bands n and summing them for a single ΔL_A in dBA.

$$\begin{aligned} \Delta L_A(T, p_a, h_{rel}, d_i) &= L_{A,atm}(T, p_a, h_{rel}, d_i) - L_{A,ref}(d_i) \\ &= 10log \sum_{n=17}^{40} 10^{(L_{n,atm} - \alpha_n d_i)/10} - 10log \sum_{n=17}^{40} 10^{(L_{n,ref} - \alpha_{n,ref} d_i)/10} \end{aligned} \tag{2}$$

Next to this absorption correction, the impedance correction is also applied using Equation 3. Acoustic impedance ρc is a measure of how a medium resists against the propagation of sound through it. This is often a very small number, but important for locations where the atmosphere is significantly different. ρc is calculated using the pressure ratio δ and the temperature ratio θ as seen in Equation 4.

$$\Delta_{impedance} = 10log\left[\frac{\rho c}{409.81}\right] \tag{3}$$

$$\rho c = 416.86\left[\frac{\delta}{\theta^{1/2}}\right] \tag{4}$$

[†]https://www.ilent.nl/onderwerpen/luchtvaartuigregister

Next to general NPD corrections, some corrections are calculated for different segments in flight. As the NPD values represent a steady, straight and level flight along an infinite flight path, deviations from this have to be corrected. This means that for every segment of the flight path, these correction factors are calculated and applied. This is done as these are not general corrections but based on, for example, the speed of the aircraft or the relative angle between the aircraft and the observer. In Equation 5 and 6, the method of calculating the segment values for $L_{A,max}$ and SEL are given, respectively. The correction factors ($\Delta_V, \Delta_I(\phi), \Lambda(\beta, l), \Delta_F$) will be further explained below.

$$L_{A,max,seg} = L_{A,max}(P, d) + \Delta_I(\phi) - \Lambda(\beta, l) \tag{5}$$

$$SEL_{seg} = L_{AE,seg} = L_{E\infty}(P, d) + \Delta_V + \Delta_I(\phi) - \Lambda(\beta, l) + \Delta_F \tag{6}$$

To find the final $L_{A,max}$, the maximum segment value $max(L_{A,max,seg})$ is taken. The final SEL, or $L_{A,E}$, is calculated by summing all L_{AE} segment values:

$$L_{AE} = 10log\Big(\sum 10^{L_{AE,seg}/10}\Big) \tag{7}$$

The position of the engines affects the directionality of the sound produced by the aircraft due to reflection, refraction and scattering. That is why an engine installation correction Δ_I is produced to take these effects into account. The effect is a correction based on the depression angle ϕ, which is comprised of the elevation angle β and bank angle ε. This is calculated by Equation 8, where a,b, and c are coefficients based on the location and type of engine.

$$\Delta_I(\phi) = 10log\Big[\frac{(a \cdot cos^2\phi + sin^2\phi)^b}{c \cdot sin^2 2\phi + cos^2 2\phi}\Big] \tag{8}$$

The NPD data is defined as a function of distance directly underneath the aircraft. Any lateral deviation has an effect on the propagation of sound. In Doc.29 these effects are summarised as the lateral adjustment $\Lambda(\beta, l)$ which is the adjustment between the observed noise level with the free-field noise level. The modelling of this so-called ground effect is further described in SAE AIR-5662 [13]. The modelling is based on experimental data. In Equation 9 the simplified formula for the lateral adjustment is given, where $\Gamma(l)$ is the distance factor and $\Lambda(\beta)$ the long-range air-to-ground lateral attenuation. This last factor is 0 for $\beta > 50°$.

$$\Lambda(\beta, l) = \Gamma(l)\Lambda(\beta) \tag{9}$$

For sound exposure levels (SEL), the duration of the measurement becomes important. The SEL value is defined as the area underneath the $L_A(t)$ curve from 10 dBA $L_{A,max}$ downtime on either side of the peak. The NPD values are set for a fixed reference speed V_{ref} of 160 kts. Any deviation of average speed during the segment V_{seg} from V_{ref} will result in longer or shorter event times and thus different SEL levels. This duration correction Δ_V is given by Equation 10.

$$\Delta_V = 10log(V_{ref}/V_{seg}) \tag{10}$$

Next to the duration correction, the length of each segment is also important. The NPD SEL values are the values for the total event for a flight along an infinite flight path. To find the contribution of each segment to that total event, a finite segment correction Δ_F is applied. This correction is based on the energy fraction F of each segment. A more detailed explanation can be found in section 4.5 in Doc.29 Vol.2 [2].

B. NOMOS measurements

For this research, measurements from the Noise Monitoring System (NOMOS) around Schiphol airport are used. NOMOS is a network of over 40 unattended continuous Noise Monitoring Towers (NMTs). The system has been in use since 1993 and is equipped with class 1 microphones, which have an uncertainty of 0.7-0.9 dB for elevation angles above 60°[14]. These microphones are placed on 6-10 m high poles at different locations. As NOMOS is originally meant to inform the public and not for academic purposes, the locations of the NMTs are often in communities. This is not advantageous as this increases the chance of background noise and reflections from buildings. The exact locations can be found on the NOMOS website.[‡]

Most of these NMTs have a threshold of 60 dBA, meaning that a noise event is only registered when the noise exceeds that threshold. It is noted that these measurements often contain background noise, thus to get a clean data set,

[‡]https://noiselab.casper.aero/ams/

only measurements with a $L_{A,max} > 70dBA$ are taken into account to reduce the chance of having false measurements. Further, only measurements where the aircraft has an elevation angle $\beta > 60°$with respect to the NMT are taken into account. This is to reduce the uncertainty of the lateral attenuation and the microphone itself in line with the ISO 20906 requirements [15]. This also reduces the chance of measuring background noise events, as the matching of aircraft is more likely to be correct. Lastly, only measurements made during weather conditions specified by the ISO 20906 are taken into account ie. no precipitation and a wind speed of less than 10 m/s.

The NMTs considered in this research are deemed suitable and can be seen in Table 3 with their corresponding number of measurements for the B737-800. Some locations are surrounded by trees or buildings. This is good to be aware of when analysing the results. All microphones are placed on a 10 meter mast unless specified different.

Table 3 NMTs used for this research and its corresponding number of valid measurements for the B737-800.

NMT	# measurements	Characteristics
10	5	Trees present
12	8	Trees present
13	6	Trees present
14	23	Buildings present
19	12	Trees present
29	7	On a 4 story roof, 6 meter mast
30	53	On a 8 story roof, 6 meter mast
34	164	Buildings present
40	372	Free field
41	49	Free field
94	96	On a parking lot, 4 meter mast
Other	21	-
Total	**816**	

The data set of the B737-800 used in this study consists of different engine types. In Table 4 the different engine types and their corresponding number of measurements are given. The engine information is gathered from the EASA database.[§] The main difference between the standard, /3 and E-models is its shape to fit newer aircraft. The maximum thrust and rotational speed remain the same. This engine information will be used in section III to find the correct thrust setting of each aircraft.

Table 4 Number of measurements per engine types of B737-800.

Engine type	# measurements	$N1_{max}$[104% rpm]	$F_{n,max}$[lb]
CFM56-7B24	365	5380	24200
CFM56-7B24/3	170	5380	24200
CFM56-7B24E	39	5380	24200
CFM56-7B26	39	5380	26300
CFM56-7B26/3	14	5380	26300
CFM56-7B26E	144	5380	26300
CFM56-7B27	11	5380	27300
CFM56-7B27/3	10	5380	27300
CFM56-7B27/3B1F	6	5380	27300
CFM56-7B27E	18	5380	27300
Total	**816**		

[§]https://www.easa.europa.eu/downloads/7795/en

III. Estimating thrust from acoustic measurements

For Doc.29 and other best-practice methods, thrust is a key input parameter. To validate the model, it is thus of great importance that the correct thrust is used. As the thrust of aircraft is dependent on the weather, flight path, weight of the aircraft and more, an accurate method to derive the thrust used during measurements is needed. For this research, the method described by Merino-Martinez et al [16] is expanded on.

A. N1 estimation

Aircraft noise is a combination of multiple sources i.e., airframe noise and engine noise. Airframe noise typically gives low-frequency broadband noise, while engine noise is more complex. The fan of the engine rotates at a specific speed, producing a tonal sound called the blade passing frequency (BPF). The fan is connected to the low-pressure turbine, also called N1. The N1 parameter is often used by engine manufacturers and pilots to determine the currently delivered thrust from the engine [16]. For the input to the model the relative rotational speed $N1\%$ is needed. This is found by:

$$N1\% = \frac{BPF \cdot 60}{n_{blades} \cdot N1_{max}} \tag{11}$$

To find the fan tone in the audio file of the flyover, the signal is cut into one-second pieces and Fourier transformed. This signal is then analysed in a specific frequency range. As departing aircraft produce a high thrust, the range of 70%-100% of maximum rotational speed $N1_{max}$ is set as the range of expected values. From gathered flight data this proved to be a reasonable range for most aircraft in the first part of the flight. This is translated to a specific frequency band. For each second the BPF where maximum energy is noted is determined. As the rotational speed of the engines does not make sudden jumps, the search frequency band is narrowed by looking at the previously found points. This is to prevent extreme outliers by background or buzzsaw noise. For the entire signal, this results in estimates for N1% as a function of time.

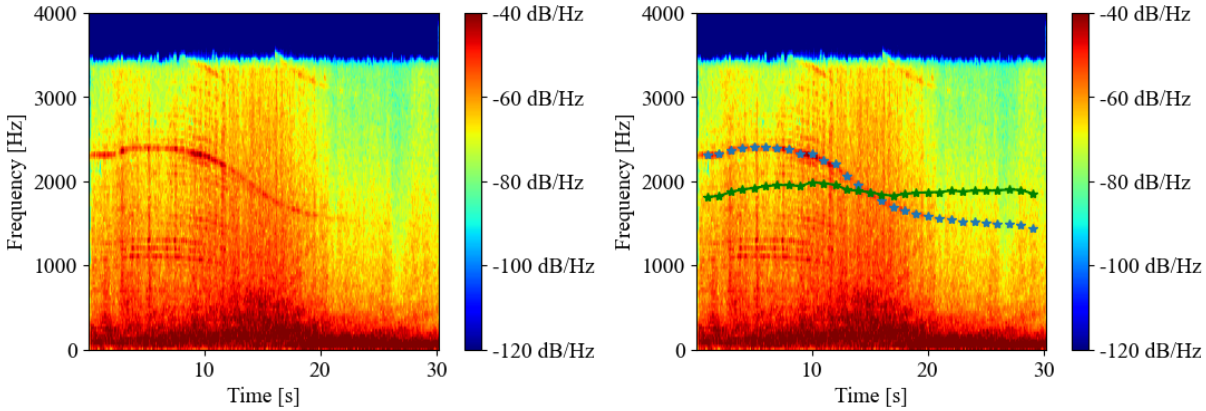

(a) Spectrogram of flyover measurement of B737-800. **(b) Found BPF of flyover measurement of B737-800.**

Fig. 3 Spectrograms of flyover measurement of B737-800.

Figure 3a shows a spectrogram for a flyover measurement and a few things are noted. The first are the overtones in the spectrogram. These tones are multiples of the original tone and are attributed to the higher harmonics. It is thus important to only look for noise peaks in the expected frequency range to avoid finding an over- or undertone.

Another effect that is clearly visible in this figure is the Doppler effect resulting in a changing frequency with the relative speed of the aircraft to the observer. The fan tone at the source is often constant for certain parts of the flight, but the perceived frequency may change. The aim is to eliminate these effects by making use of the RADAR data of the corresponding flight.

$$\frac{f}{f'} = 1 + \frac{dr/dt}{c} \tag{12}$$

Here dr/dt is the change in distance between the aircraft and the NMT per second. The frequency correction is sensitive to speed and location changes. This is why discrepancies in RADAR data can cause unwanted effects and precaution

should be taken. In Figure 3b the found frequencies are shown in blue and the corresponding so-called dedopplerised frequencies in green.

To get a smooth line from these raw dedopplerised data points, multiple methods of fitting are applied. When taking the raw data points, the input to the model becomes sensitive to outliers, causing unwanted effects on the noise calculation. Three types of fitting are applied to the datasets and are compared to the ACMS data: averaging the datapoints, n-order polynomial fit and a moving median filter (Hampel filter). The moving median filter was found to perform best in the irregular datasets that these measurements give. This method will be further applied in this research.

Lastly, a problem occurred with a small percentage of datasets. When a clear fan tone is not visible in the spectrogram, the search algorithm finds random values in the expected range, resulting in a scattered plot. To counteract these events, all measurements with a large standard deviation within their found $N1\%$ is discarded.

For validation of this method, the found $N1\%$ is compared to the $N1\%$ obtained from the Aircraft Condition and Monitoring System (ACMS) data gathered from departing flights of KLM. The ACMS logs all parameters important to the functioning of the aircraft. For this research, the two main parameters used are the rotational speed N1% and the fuel flow to the engines.

To check if the medians of the two $N1\%$ distributions are equal, the Mann-Whitney-U test (MWU) is used. This tests the null hypothesis that the distribution underlying the measured $N1\%$ is the same as the distribution underlying the $N1\%$ of the ACMS. This test is an alternate test to the T-test and is used when the samples to be compared cannot be assumed normally distributed, which is often the case for the data gathered from the mp3 files. From this test, a p-value is found that represents the confidence interval of the tested hypothesis. When $p < 0.05$, there is a 95% confidence that the null hypothesis is rejected and the two distributions are different. The MWU test is applied to all flyover measurements.

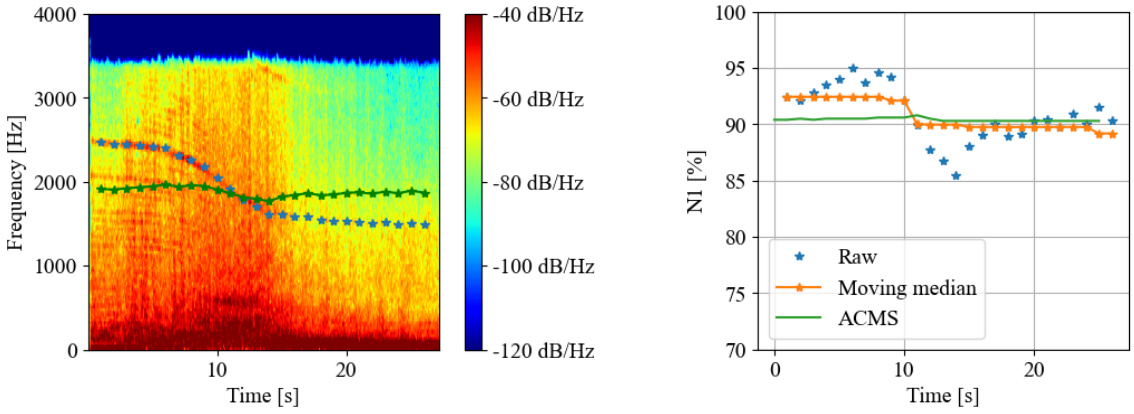

(a) Spectrogram of flyover measurement of B737-800. **(b) Found N1% of flyover measurement of B737-800.**

Fig. 4 N1% estimation method and validation.

In Figure 4 a typical flyover measurement of a B737-800 is given. Figure 4a is a spectrogram with the found frequencies of the fan tone. In this figure also the dedopplerised frequencies are given in green. In Figure 4b the corresponding $N1\%$ of this measurement is given with a moving median filter applied on the raw data points. This is compared to the ACMS data and a p-value of 0.56 is found when using the MWU-test, validating the measurement. The Root Mean Square Error (RSME) of this measurement is 2.02%, falling in an acceptable error margin.

This validation is done for all available ACMS files and their corresponding measurements. Due to the scarcity of ACMS data, these measurements are not adhering to all requirements mentioned in section II.B, for example, the weather requirements or the 60 degree incidence angle requirement. In total, a set of 37 valid audio files were available for the B737-800. The results can be seen in Table 5. Interesting to see is that more than 50% of the measurements do not pass the MWU-test. The results are quite different when looking at per NMT basis. For NMTs with a high percentage of MWU-test passing, the average RMSE is higher. This gives conflicting results.

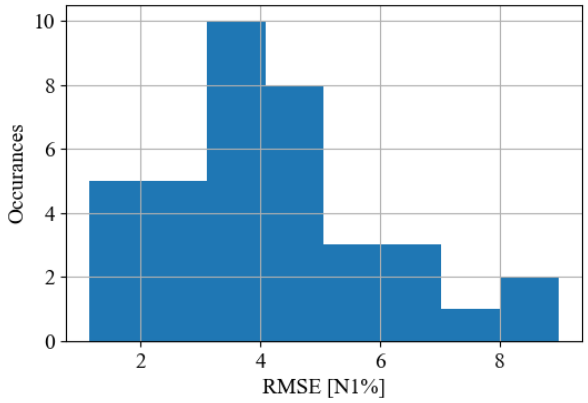

Fig. 5 Histogram of RMSE of $N1\%$ measurements of the B737-800.

Table 5 Results of comparison of found $N1\%$ with ACMS data of the B737-800.

NMT	#	p>0.05	RMSE [$N1\%$]
2	5	2	6.5
10	9	5	3.1
25	2	1	5.4
34	2	0	4.9
40	11	6	4.2
94	8	0	3.2
Total	**37**	**12**	**4.1**

The histogram of the found RMSE between the $N1\%$ measurements and the ACMS data is given in Figure 5. The maximum error is below 9% and does not occur often. NMT 2, with an average high RMSE, is not further used in the data set for this reason. A 4% uncertainty in $N1\%$ can lead to an approximate 800 lb uncertainty for the B737-800, which is less than the 1500-2000 lb uncertainty for conventionally used methods [17]. That is why an average error margin of 4% is deemed acceptable for this research and this method will be further applied.

B. N1 to thrust

The N1% to thrust conversion is not as straightforward as one might think. From literature and conversations with pilots, it is found that N1%:F% is not a 1:1 conversion, but often exponential. The 80%-100% N1 increase is a much larger percentage in kN than 60%-80%. The $N1\%$ to thrust conversion can be done with several methods presented in this section.

1. N1% to thrust using engine parameters

The method given by Doc.29 is based on engine parameters given in the ANP database [2]. The corrected net thrust F_n/δ is then calculated using Equation 13.

$$\frac{F_n}{\delta} = E_0 + F_0 V_C + G_A h + G_B h^2 + HT + K_3\left(\frac{N1\%}{\sqrt{\theta_T}}\right) + K_4\left(\frac{N1\%}{\sqrt{\theta_T}}\right)^2 \tag{13}$$

In this equation, E_0, F_0, G_A and H are engine constants and the constants K_3 and K_4 can be derived from installed engine data. This equation takes into account the temperature and pressure differences of the atmosphere and the effect it has on the efficiency of the engines. Unfortunately, these constants are not available for most common aircraft types. Currently, these parameters are only available for the A330-300 and the B777-200, which excludes most of the commercial aircraft departing and landing at Schiphol. Further, this method is not suited for landing aircraft [18].

2. N1% to thrust through fuel flow

To be able to use the $N1\%$ parameter for noise modelling of other aircraft, a $N1\%$-thrust relation is needed. A good measure for thrust is the fuel flow used by the engines as fuel is the potential energy that is converted to thrust. At the certification of new engines, their fuel use and emissions are measured for different thrust settings at standard atmosphere and documented in the ICAO engine emission database.[¶] In ACMS data, $N1\%$ and fuel flow to each engine is given per time step, from which a relation between the two can be found.

To find a relation between N1% and fuel flow, ACMS data is gathered for multiple flights departing from Schiphol. This is done for a good comparison to departure noise events under similar altitudes and weather. The $N1\%$ efficiency is also dependant on the atmospheric pressure and temperature as seen in the equation for the A330-300. That is why

[¶]https://www.easa.europa.eu/domains/environment/icao-aircraft-engine-emissions-databank

each ACMS datapoint is corrected to standard atmospheric relations. This is done using the pressure correction δ and temperature gradient θ_T. For all engine types, a different relation is found. The most common engine for the B737-800 is the CFM56-7B24 with a $N1_{max}$ of 5380 rpm and maximum rated thrust $F_{n,max}$ of 107.6 kN. The found relation can be seen in Equation 14 and is visualised in Figure 6a.

$$fuelflow[kg/s] = 1.328e^{-4} * (N1\%)^2 - 1.698e^{-3} * (N1\%) + 7.308e^{-2} \tag{14}$$

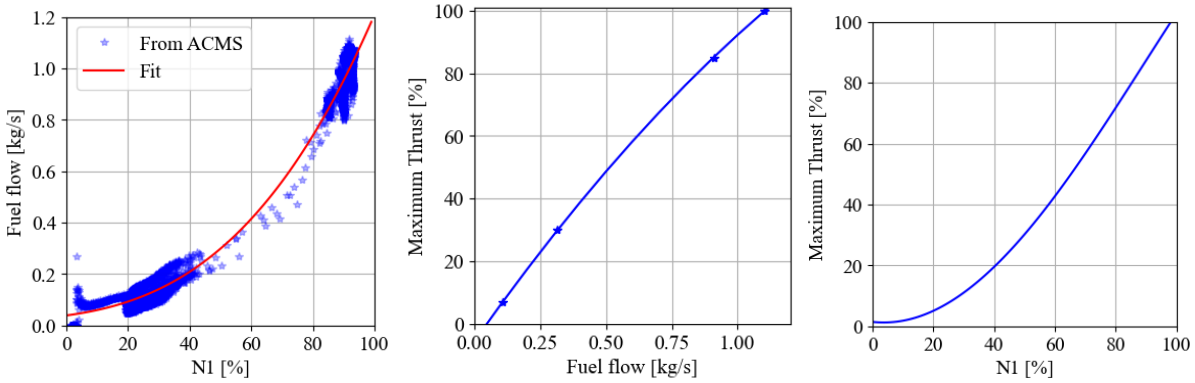

(a) Fit from ACMS data for fuelflow N1% relation

(b) Relation between % of maximum thrust to fuel use from ICAO database.

(c) Found relation between N1% and % of maximum thrust.

Fig. 6 Relations used for determining the N1% to thrust conversion.

Together with the fuel flow to percentage of maximum thrust $F_{\%}$ from ICAO visualised in Figure 6b, a relation between $N1\%$ and $F_{\%}$ can be found in Figure 6c. This relation is then used to converse the found $N1\%$ data points to thrust using Equation 15. As each measurement is taken in different atmospheric conditions and the NPD table thrust values are given in corrected thrust, the found F_n is corrected using a new pressure correction δ.

$$\frac{F_n}{\delta}[kN] = F_{\%} * F_{n,max} \tag{15}$$

3. Comparison of N1%-thrust relations

The sonAIR model that is used by EMPA (Switzerland) is removing thrust as uncertainty as a whole. They use $N1\%$ as a direct input into the model without conversion to thrust [19]. The advantage of this method is that the measurements can be directly validated. In Zellmann et al [20] the measured unweighted sound pressure levels L_p are given for a few 1/3 octave bands as a function of $N1\%$. These are taken from ground measurements of the A330-301 for different angles measured from the nose of the aircraft. Unfortunately, these values cannot be directly compared to the current research results, due to the difference in noise metrics. Further, from these graphs, limited information in $N1\%$ and frequency range is available. For the information that is present in Zellmann et al [20], similarities were found with the NOMOS measurements. The relation between $N1\%$ and L_p for the 2 kHz band at 90°can be seen in Figure 7 for a distance of 170 m from the source.

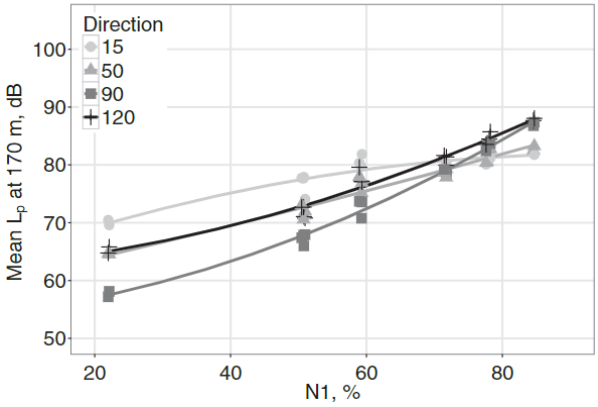

Fig. 7 Relation between $N1\%$ and L_p for 2 kHz 1/3 octave measurements at 170m of the A330-300 [20].

The previously mentioned $N1\%$ to thrust relations, i.e. using the formula from the ANP database and using the fuel flow from the ACMS data, are conversed to a $N1\%$-$L_{A,max}$ relation. These relations are plotted against a set of NOMOS measurements for the A330-300 in Figure 8. Interesting to see is that two clusters are formed in the take-off procedure in terms of $N1\%$ setting. This is corresponding to the two types of derated climb procedures that are also found during the research of EMPA [18]. A validation of both conversion methods is needed to draw conclusions on the accuracy.

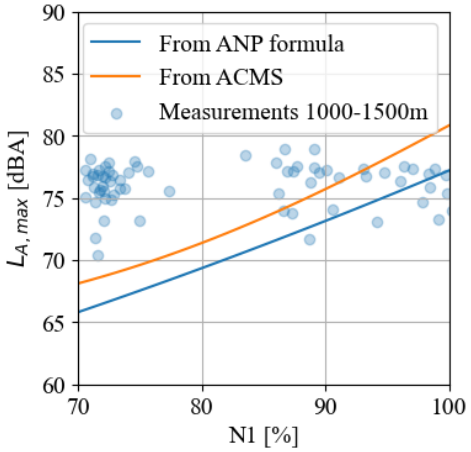

Fig. 8 $L_{A_{max}}$ for 1250m with respect to N1 for the A330-300.

C. Baseline data set using N1%

The data set used for this research consists of approximately 20,000 measurements of the B737-800 for the year 2021. Out of these measurements, only 816 are considered to fall within the requirements stated in section II. These measurements are evaluated with the above-described method and are coupled to measurements. In Figure 9a this data set is visualised by plotting the $L_{A,max}$ versus the estimated $N1\%$ and the distance of the aircraft to the NMT at the time of the measured $L_{A,max}$. In Figure 9b this same data set is plotted for the SEL values. On the x-axis, a clear relation of decreasing measured sound levels with increasing distance is visible, as expected. On the y-axis, however, a relation is not immediately visible. The effect of the increase in $N1\%$ is not directly visible in the measurements.

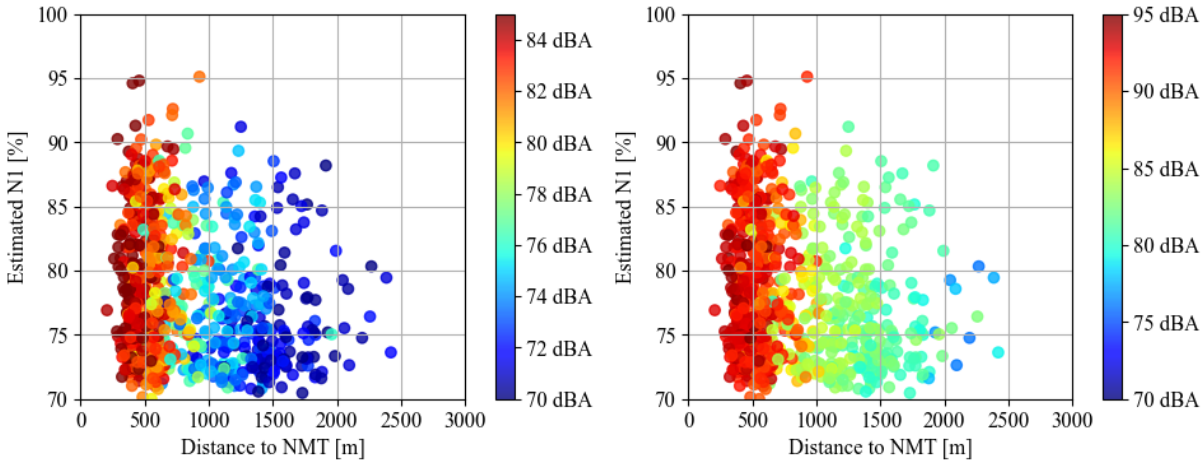

(a) $L_{A_{max}}$ measurements with respect to N1. **(b) SEL measurements with respect to N1.**

Fig. 9 Sound level of measurements of B737-800 with respect to distance and N1.

To analyse the effect of $N1\%$ on the sound level, the measurements are grouped by distance and the estimated $N1\%$ is plotted against the measured sound levels shown in Figure 10. For some distances, a positive correlation is visible in the plotted linear fit, while for others there seem to be no correlation present.

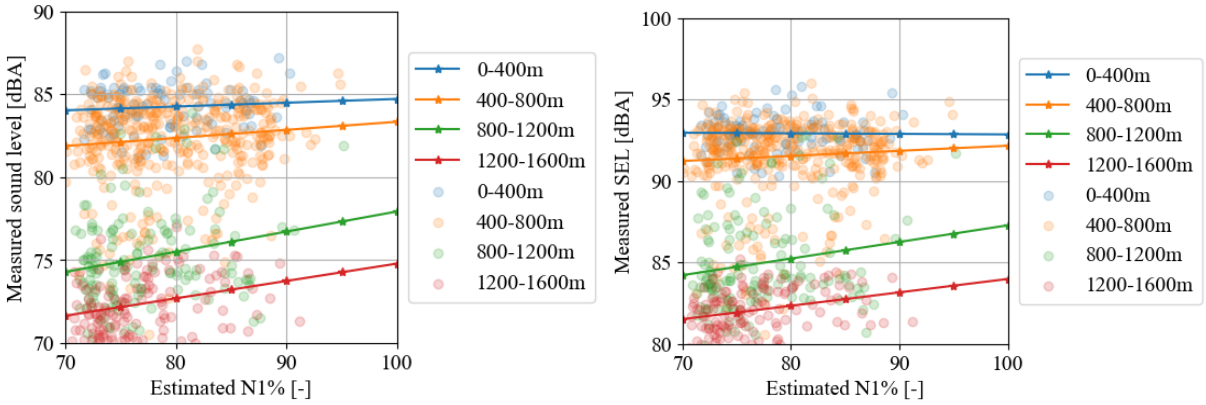

(a) Fit of $L_{A,max}$ to N1% data grouped per distance. **(b) Fit of SEL to N1% data grouped per distance.**

Fig. 10 Analysis of the B737-800 N1% with respect to measured $L_{A,max}$ and SEL grouped per distance.

IV. Model data comparison

The data gathered for the B737-800 is put into the Doc.29 model. The predictions of this model can be directly compared to the measurements taken by NOMOS. The differences found from this comparison are analysed to be able to find the cause of the deviation in the model. This direct comparison is looked at in section IV.A. To be able to compare the measurements to their corresponding entry in the NPD table, the measurements need to be standardised. This is further discussed in section IV.B.

A. Differences model and measurement

As mentioned before, the NOMOS measurements provide $L_{A_{max}}$ and SEL, so these will be the main parameters that the model results will be compared to. In Figure 11, the measurements are set out against the model results. The corresponding parameters can be found in Table 6, where μ is the average difference between the model result and

its corresponding measurement of all data points in the set. The μ is defined by Equation 16 and σ is the standard deviation of the differences between model result and measurement. A negative μ means an underestimation of the model, while a positive μ represents an overestimation.

$$\mu = L_{model} - L_{measurement} \tag{16}$$

Table 6 Mean and standard deviation of the model results minus the measurements.

	μ [dBA]	σ [dBA]
$L_{A_{max}}$	-0.24	3.24
SEL	0.13	3.09

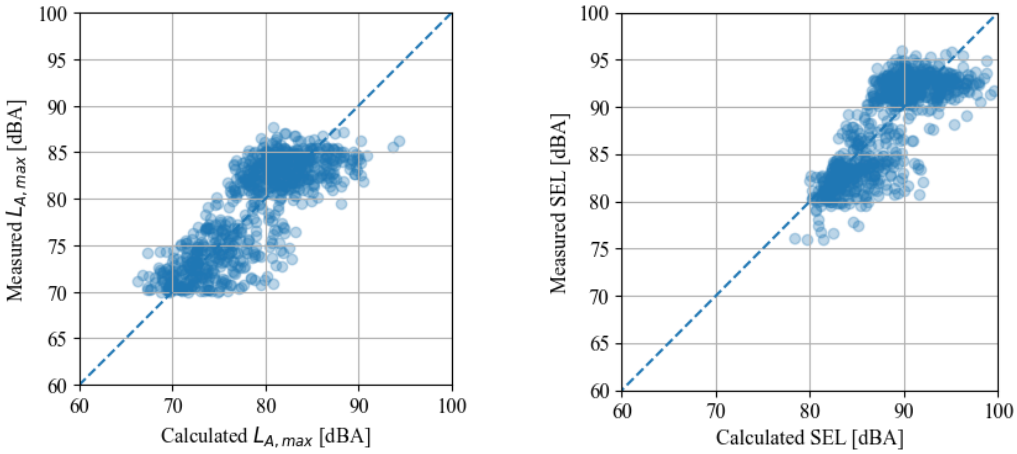

(a) $L_{A_{max}}$ measurements compared to model results. **(b) SEL measurements compared to model results.**

Fig. 11 Measurements of B737-800 with respect to model results.

A slight offset is immediately visible, but to find where the problems in the calculations lie, the differences are analysed. In Figure 12, the found differences between model results and the NOMOS measurements are plotted for the distance and power parameter. Here, again, a positive Δ represents an overestimation of the model, while negative Δ is an underestimation. In the plots with the estimated power setting, a clear trend line is seen. This gives the suspicion that the source of error is attributed to the power estimation. In the plots, Pearson's correlation coefficient R is given. This R represents the factor of linear relation of the two variables and is given by Equation 17. An R of 0 means no correlation, while an R of -1 or 1 is a full negative and full positive correlation, respectively. Often values below -0.5 and above 0.5 are seen as a notable correlation. Following this guideline, the estimated thrust setting and the found differences have a notable correlation.

$$R_{ij} = \frac{C_{ij}}{\sqrt{C_{ii}C_{jj}}} \tag{17}$$

In the graphs in Figure 12, the p-value is also given. A p-value tests the Null-hypothesis that there is not a relationship between the two data sets. When the p-value < 0.05, the hypothesis is rejected and a relationship is likely. These p-values give the same result as the Pearson correlation coefficient for the analysed parameters.

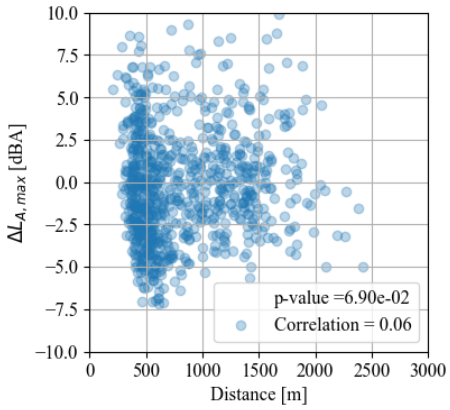

(a) Differences in $L_{A_{max}}$ with respect to distance.

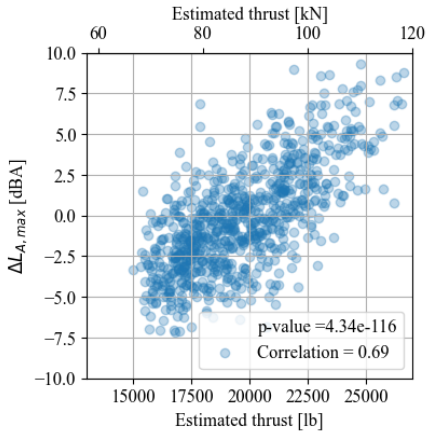

(b) Differences in $L_{A_{max}}$ with respect to power setting.

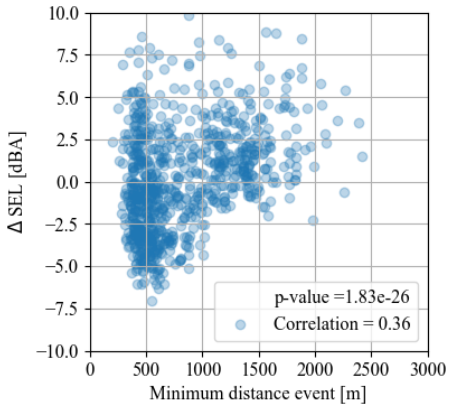

(c) Differences in SEL with respect to distance.

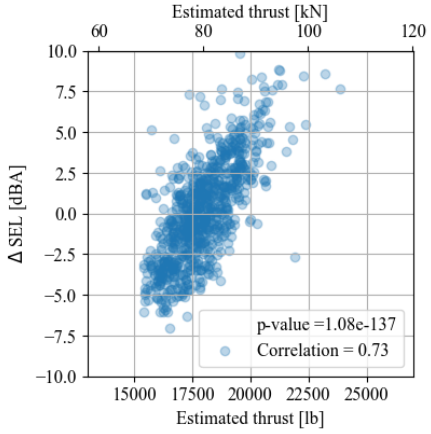

(d) Differences in SEL with respect to power setting.

Fig. 12 The differences between model results minus measurements with respect to different parameters.

B. Standardised measurements

As mentioned in section II.A, the Doc.29 model works from a standard NPD table with correction factors applied. To be able to compare these NPD values to the found measurements, the measurements have to be standardised to match the NPD conditions. This is done by inverting the correction factors applied and propagating back to a standard distance.

For $L_{A_{max}}$ measurements, these correction factors are rather straightforward. The applied engine-frame model, impedance, engine installation and lateral attenuation correction are subtracted from the measurement. The weather correction is a bit more difficult. Each measurement is taken under different weather conditions and at a different distance. To convert the measured values to those corresponding to a standard atmosphere and standard conditions is not trivial. Using the frequency spectrum of the acoustic measurement and the measured weather conditions, attenuation rates can be calculated. Unfortunately, NOMOS mp3 files are sampled with a sampling rate of 8000Hz, meaning that the information above 4000Hz is unknown. This makes the spectral information of the measurement not useful for the backward calculation of the attenuation. To still be able to take atmospheric effects into account, a method is developed to find the attenuation. The only spectral information of the aircraft known comes from the ANP database, where the standard engine spectrum at 1000ft (305m) is given. The assumption is made that this spectrum is correct. Now the following steps are taken.

The first step is to get the theoretical spectrum $L_{n_{theory}}(d_0)$ at 1m from the source d_0 using Equation 18. In this equation the geometrical spreading and the atmospheric absorption are subtracted using the absorption coefficient for all

frequency bands f_n for reference atmospheric conditions $\alpha_{n,ref}$.

$$L_{n_{theory}}(d_0, f_n, \alpha_{n,ref}) = L_{n_{theory}}(305, f_n, \alpha_{n,ref}) + 20log(305) + 305\alpha_{n,ref} \tag{18}$$

This source spectrum is then used to calculate the theoretically spectrum that would be heard the measurement location d_{NOMOS} using Equation 19. The atmospheric absorption coefficient for the weather conditions at time of the measurement $\alpha_{n,NOMOS}$ is used for this. After which the theoretically measured overall A-weighted sound pressure level $L_{A,theory}(d_{NOMOS}, \alpha_{NOMOS})$ is calculated using Equation 20.

$$L_{n_{theory}}(d_{NOMOS}, f_n, \alpha_{n,NOMOS}) = L_{n_{theory}}(d_0, f_n) - 20log(d_{NOMOS}) - d_{NOMOS}\alpha_{n,NOMOS} \tag{19}$$

$$L_{A,theory}(d_{NOMOS}, \alpha_{n,NOMOS}) = 10log\Big(\sum_{n=17}^{40} 10^{L_{n_{theory}}(d_{NOMOS}, f_n)/10}\Big) \tag{20}$$

For step 3, the expected measurement spectrum $L_{n_{theory}}(d_{NOMOS}, f_n, \alpha_{n,NOMOS})$ is now known. This is, however, not exactly the same as the measured spectrum. As mentioned before, the latter is unknown, but the measured overall A-weighted sound pressure level $L_{A_{NOMOS}}(d_{NOMOS}, \alpha_{NOMOS})$ is known. The difference between the two ΔL_A is given by:

$$\Delta L_A = L_{A_{NOMOS}}(d_{NOMOS}, \alpha_{NOMOS}) - L_{A_{theory}}(d_{NOMOS}, \alpha_{NOMOS}) \tag{21}$$

The measured spectrum is assumed to be the theoretical spectrum plus an additional factor $dL(f_n)$.

$$L_{n,NOMOS}(d_{NOMOS}, f_n, \alpha_{NOMOS}) = L_{n_{theory}}(d_{NOMOS}, f_n, \alpha_{NOMOS}) + dL(f_n) \tag{22}$$

When plugging this value into the measured spectrum equation, the following relations are found.

$$\begin{aligned} L_{A,NOMOS}(d_{NOMOS}, \alpha_{NOMOS}) =& 10log\Big(\sum_{n=17}^{40} 10^{L_{n,NOMOS}(d_{NOMOS}, f_n, \alpha_{NOMOS})/10}\Big) \\ =& 10log\Big(\sum_{n=17}^{40} 10^{\frac{L_{n,theory}+dL(f_n)}{10}}\Big) \\ =& 10log\Big(10^{dL/10}\sum_{n=17}^{40} 10^{\frac{L_{n,theory}}{10}}\Big) \end{aligned} \tag{23}$$

$$dL(f_n) = 10log\Big(10^{L_{A_{NOMOS}}(d_{NOMOS}, \alpha_{NOMOS})/10} / \sum_{n=17}^{40} 10^{\frac{L_{n,theory}}{10}}\Big) = \Delta L_A \tag{24}$$

Thus the difference between measured and calculated L_A is the same as the additional factor defined in Equation 22. From this, the spectrum is known at distance d_{NOMOS}. The measured sound can be propagated back to the source using the attenuation coefficient during measurement conditions α_{NOMOS} as seen in Equation 25.

$$L_{n_{NOMOS}}(d_0, f_n, \alpha_{NOMOS}) = L_{n_{theory}}(d_NOMOS, f_n, \alpha_{NOMOS}) + \Delta L_A + 20log(d_{NOMOS}) + d_{NOMOS}\alpha_{NOMOS} \tag{25}$$

With a measured source noise, the noise level at a standard NPD distance d_i can be calculated for reference weather conditions α_{ref}, giving a standardised L_A.

$$L_{n_{NOMOS}}(d_i, f_n, \alpha_{ref}) = L_{n_{NOMOS}}(d_0, f_n, \alpha_{NOMOS}) - 20log(d_i) - d_i\alpha_{ref} \tag{26}$$

$$L_{A,NOMOS}(d_i, \alpha_{ref}) = 10log\Big(\sum_{n=17}^{40} 10^{\frac{L_{n,NOMOS}(d_i, \alpha_{ref}}{10}}\Big) \tag{27}$$

Standardising the SEL measurement is more difficult as this value is comprised of multiple segment values (and multiple segment corrections) instead of an instantaneous value. The total SEL is calculated as a cumulative of all segments in the event using Equation 28. During this research, the segment length is four seconds, corresponding to the

RADAR data points. To be able to standardise the SEL measurement, each segment contributing to the event must be corrected separately as each segment has different distances, power, speed and other correction factors.

$$SEL(dBA) = 10log\Big(\sum_{segments} 10^{SEL/10}\Big) \tag{28}$$

From the NOMOS measurements, only a single value for SEL is shown. It is thus not known what the contribution of each segment to the total SEL value is. An approximation must be made to find this contribution to be able to calculate the finite segment correction factors that need to be subtracted from the measurement. This is done through the same method described above, depicted in Equation 29.

$$\begin{aligned} SEL_{seg,NOMOS} =& SEL_{seg,model} + \Delta SEL \\ =& SEL_{seg,model} + (SEL_{OASPL,NOMOS} - SEL_{OASPL,model}) \end{aligned} \tag{29}$$

Further difficulties arise when propagating the standardised SEL value to a reference distance from the NPD table. When the slant distance is shorter, but the aircraft flies at the same speed, the event is expected to be shorter and thus the SEL will be lower. This is expected to cause an overestimation of SEL level for short distances (200 and 400 ft) and an underestimation for larger distances. For the B737-800 data set the measurements durations are plotted against the minimum distance in Figure 13. These durations are obtained from the NOMOS measurements and are set for 10dB(A) downtime from $L_{A,max}$. As a relation is not immediately visible, the SEL values are not further standardised.

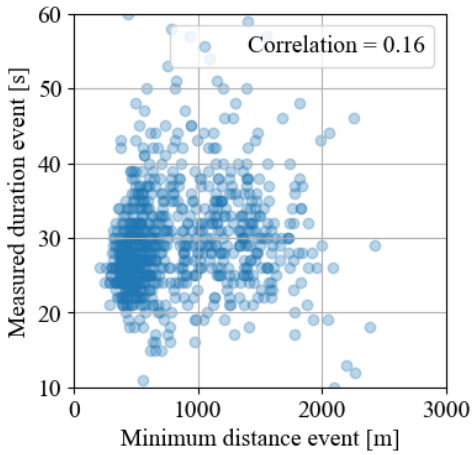

Fig. 13 Measurement duration versus minimum slant distance.

Applying all correction factors and propagating all measurements to a reference distance of 1000 ft (305m) gives updated values for the noise levels of the reference distance. A fit is found for these measurements and outliers are determined with the w-test and subsequently removed from the data set [21]. The resulting relation between the noise levels and thrust is shown in Figure 14. Something that is immediately visible is the flattened line with respect to the NPD values. It seems the measured sound level is not strongly dependent on the estimated thrust. In the NPD table, ten reference distances are given in the range of 200 to 25000 ft. For each of these reference distances, a thrust to noise level relation is made. The relations for these distances are similar to the ones given in Figure 14. The derived relations will be applied in section V.

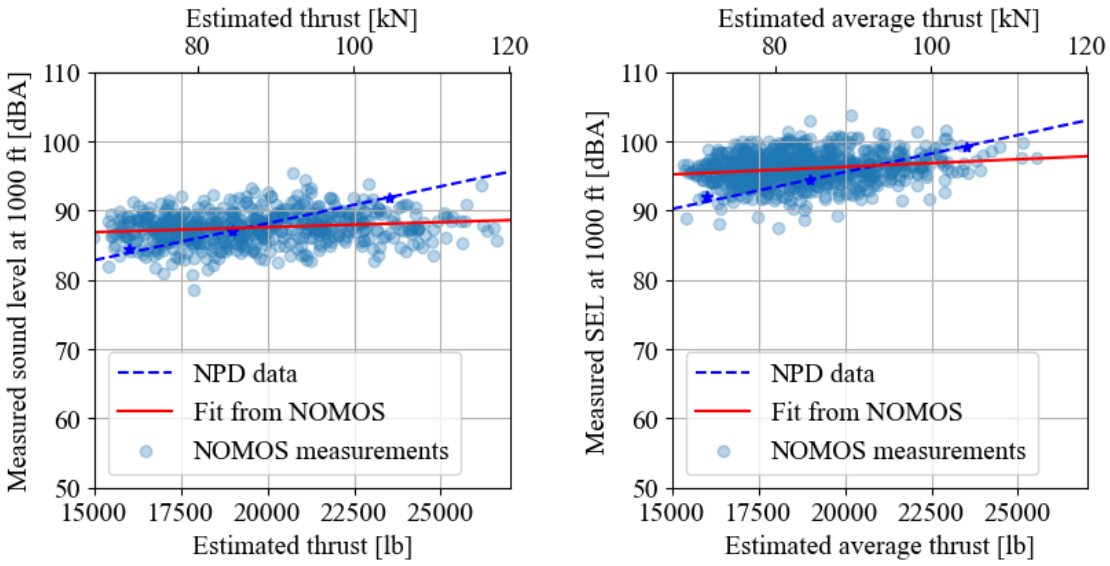

(a) $L_{A_{max}}$ **measurements standardised for 1000 ft.** **(b) SEL measurements standardised for 1000 ft.**

Fig. 14 Measurements of B737-800 standardised to a reference distance.

V. Calibration of Noise Power Distance table

The use and accuracy of NPD values is a widely discussed topic. According to Filippone, NPD has a "lack in scientific basis on their own" [22]. As mentioned before, the way NPD values are retrieved, have some remissness. In many studies where the model results are compared to measured values and systematic errors occur, the NPD values are mentioned as a source for error. Giladi and Menachi [23] showed a difference from the AEDT model and measurements up to 4-7 dB. Following this result, they suggest a correction of the NPD tables as well as take-off profiles. A way to improve the model outcome with respect to the measurements is to calibrate the NPD values, as considered in section II.

A. Average calibrated model

Studies that validate and calibrate the NPD values are limited. Sari et al. [24] used year-round long term noise measurements L_{DEN} (Day-Evening-Night) for calibration of Doc.29. The differences in L_{DEN} between the model and the measurements were added to the model. Trow and Allmark [6] showed a method to use single event differences between the model results and the measurements. The thrust and location of the aircraft with respect to the measurement station was modelled and matched to an NPD value. The average difference from multiple flights is taken and the corresponding value in the NPD table is adjusted. These corrections are then inter- or extrapolated over the entire table. The disadvantage of this approach is that it is strongly affected by outliers [17]. Although differences remained, the calibrated model results when using this approach were more accurate than when long term noise measurements were used in Sari et al. [24]. When using these newfound NPD values for contour calculations, a narrower, elongated SEL footprint was found [6]. This calibration method is repeated for Schiphol airport using NOMOS measurements and has proven to be effective [17].

The method from Trow and Allmark [6] used procedure profiles as thrust input and assumed them correct. In this research, a more accurate method for finding the thrust input is given. Even then, a difference between model and measurement remained. To get the most accurate model possible, calibration of these NPD values is performed. The previously mentioned method is repeated and the average differences are added to their corresponding values in the NPD table. As the noise value used during modelling is an interpolation between the neighbouring distances and thrust settings, these neighbouring values are also altered, so that the logic of the table is kept. A value in the NPD table is only altered when more than two measurements are present for that entry in the NPD table. This can cause some measurements to not be taken into account but will reduce the influence of outliers. In Table 7 the amount of measurements for each entry are given. The average differences corresponding to these measurements are given in

Table 8. This results in a new NPD table given in Table 9 with the old NPD values between brackets.

Table 7 Number of measurements in each entry of the NPD table

Power Setting (lb)	200ft	400ft	630ft	1000ft	2000ft	4000ft	6300ft	10000ft	16000ft	25000ft
10000	0	0	0	0	0	0	0	0	0	0
13000	0	0	0	26	3	0	0	0	0	0
16000	0	0	3	132	84	29	0	0	0	0
19000	0	0	2	101	103	68	9	0	0	0
23500	0	0	1	15	12	21	1	2	0	0

Table 8 Average differences between model results and measurement per NPD value for $L_{A,max}$.

Power Setting (lb)	200ft	400ft	630ft	1000ft	2000ft	4000ft	6300ft	10000ft	16000ft	25000ft
10000	-	-	-	-	-	-	-	-	-	-
13000	-	-	-	-3.3	-2.1	-	-	-	-	-
16000	-	-	2.4	-2.1	-1.6	-2.0	-	-	-	-
19000	-	-	3.3	1.2	0.1	0.3	-1.5	-	-	-
23500	-	-	8.0	5.1	5.1	4.9	4.6	-2.6	-	-

Table 9 NPD table for $L_{A,max}$ calibrated using average differences.

Power Setting (lb)	200ft	400ft	630ft	1000ft	2000ft	4000ft	6300ft	10000ft	16000ft	25000ft
10000	95.2	87.9	83.6	78.8	71.3	63.0	57.3	50.4	44.2	36.9
13000	98.1	91.0	86.7	**85.3**(82.0)	**77.7**(74.5)	**68.4**(66.3)	60.7	53.9	46.9	39.6
16000	100.5	93.7	**86.9**(89.3)	**86.8**(84.6)	**79.2**(77.3)	**70.9**(69.2)	**65.5**(63.5)	56.8	49.4	42.1
19000	102.7	96.0	**89.0**(91.7)	**87.8**(87.1)	**79.7**(79.7)	**71.8**(71.7)	66.1	**61.1**(59.5)	52.2	44.9
23500	107.2	100.9	96.5	**90.2**(91.9)	**83.5**(84.7)	**75.0**(76.8)	**68.4**(71.4)	64.6	57.7	50.4

For this calibration, the data set is divided into a calibration and validation data set. 75% of the measurements is put into the calibration data set, while 25% is used for the validation data set. This deviation is made using a random seed in Python. The calibration data will be used to form a new NPD table, after which this table will be used to run both data sets.

This results in the new average mean μ and standard deviation σ given in Table 10. A scatter plot of the new calculated maximum sound level can be seen in Figure 15c and 15d. A few things are noted. The first is that the calibration data set does not go to an exact mean 0 dBA difference. This is due to a few extreme outliers that can be seen in Table 8. Because these are single values in their NPD entry, the NPD value is not altered, but the measurement is still in the calibrated data set. The mean differences between model results and measurements μ after calibration are very small values, so these are deemed insignificant. More interesting is the reduction in standard deviation for both the calibration and the validation data set. A smaller standard deviation, together with a smaller total deviation, makes the single event model predictions more reliable, thus an improvement to the model.

Table 10 Results for the baseline and calibrated model using the average correction method.

	Data set	$L_{A,max}$ [dBA]		SEL [dBA]	
		μ	σ	μ	σ
Baseline	Calibration	-0.28	3.16	0.11	3.11
	Validation	-0.11	3.47	0.20	3.05
Calibrated	Calibration	-0.08	2.59	-0.01	2.27
	Validation	0.05	2.60	0.20	2.27

B. Standardised measurements calibrated model

A new method to create calibrated NPD tables is developed. In this new method, the old tables are not altered based on the found differences between model and measurement, but to look at the basis of NPD table creation. As mentioned before, a lack of scientific basis is often seen in the NPD tables. In this method, the standardised measurements, as discussed in section IV, are used to create a new NPD table. This is done by finding a polynomial fit through the standardised noise measurements versus power plots for every distance in the NPD table. One of those fits for 1000 ft is shown in Figure 14. The order of polynomial fit is found through the reduced chi-squared χ^2_ν statistic. For all distances in this data set the linear fit came out as best, which is in line with the current NPD assumptions where measured sound level increases linearly with increasing power setting.

A new NPD table is made based on these fits through the measurements and their corresponding thrust setting for every reference distance present in the NPD table. This results in 10 linear fits, each containing the 5 thrust settings. A disadvantage of this method is the lack of data of the lower thrust setting range, as departing aircraft do not often fly with only 50% thrust. That is why the lower 2 thrust settings are kept linear with respect to the newfound thrust levels for continuity sake. This method leads to a new NPD table, as seen in Table 11, fully based on measurements and not depending on existing NPD values. The more horizontal trend lines, as visible in Figure 14, when compared to the original NPD values result in a smaller relation between thrust and expected noise level. A hypothesis for this large difference in thrust-noise level relation is that the engine models used today are different from the engine models used during the original NPD table creation. The engine type for which the NPD table is used for the B737-800 is a CFM56-7B. The newest version (-27) has a maximum rated thrust of 1.3 times higher than the older version (-22), giving quite a large difference in operational use. For newer engine models, general correction factors are set, as discussed in section II. These factors are applied over the entirety of the NPD table and do not take into account the changes in engine noise for different thrust settings. For example, the effects and efficiency of liners, which are present in the newer models to reduce tonal noise, is still being researched. The newer engines may be more noise efficient when it comes to higher thrust levels. When looking at the average of the model results minus the measurements μ, the general correction factor used by Doc.29 seems to be correct. This is, however, not the case when looking at single events.

Table 11 NPD table for $L_{A,max}$ calculated using standardised measurements.

Power Setting (lb)	200ft	400ft	630ft	1000ft	2000ft	4000ft	6300ft	10000ft	16000ft	25000ft
10000	101.6	95.4	91.2	86.8	80.0	72.6	67.3	61.6	55.2	48.4
13000	101.7	95.5	91.3	86.9	80.1	72.7	67.5	61.7	55.3	48.5
16000	101.9	95.6	91.5	87.1	80.2	72.9	67.6	61.9	55.5	48.7
19000	102	95.8	91.6	87.2	80.4	73.0	67.8	62.0	55.6	48.8
23500	102.3	96.0	91.8	87.5	80.6	73.2	68.0	62.2	55.8	49.1

Implementing this new NPD table into the Doc.29 model gives the results shown in Figure 15e and 15f. The new mean averages and standard deviations are given in Table 12. Although the μ for $L_{A,max}$ reduces to almost 0 dBA for the calibration data set, the μ for SEL is overcompensated. This could be caused by the assumptions made during standardisation as discussed in section IV.B. For both noise metrics, the standard deviation decreased by about 35% for both the calibration and validation data set.

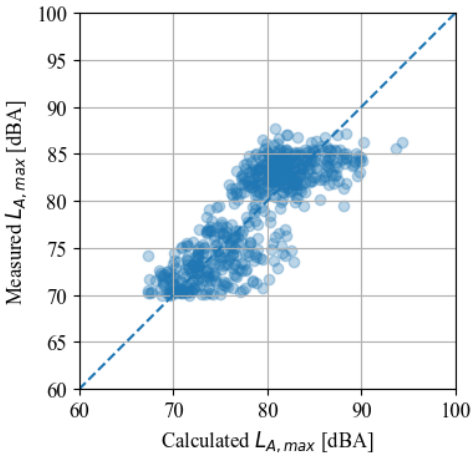

(a) $L_{A_{max}}$ **calibration data set baseline**

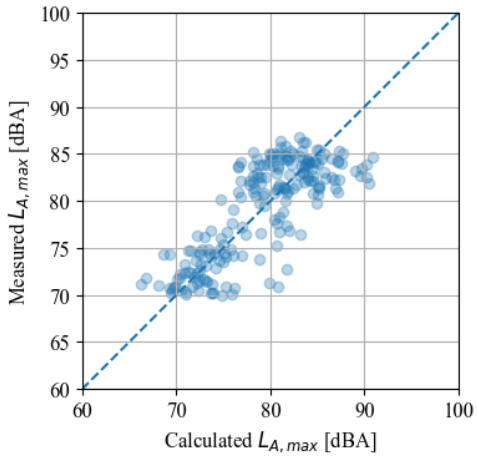

(b) $L_{A_{max}}$ **validation data set baseline.**

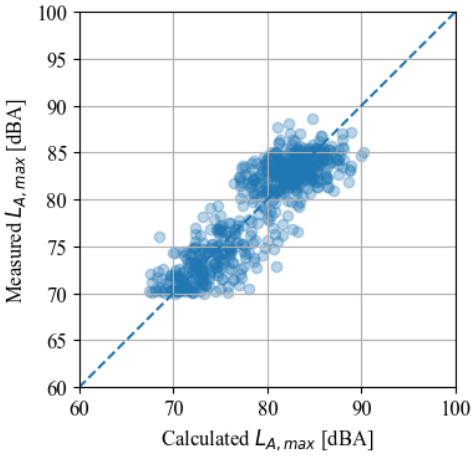

(c) $L_{A_{max}}$ **calibration data set calibrated using average differences.**

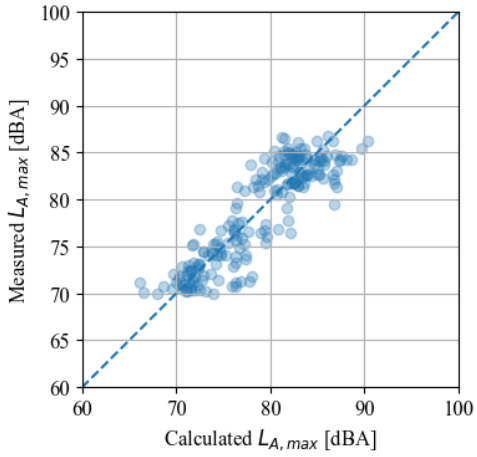

(d) $L_{A_{max}}$ **validation data set calibrated using average differences.**

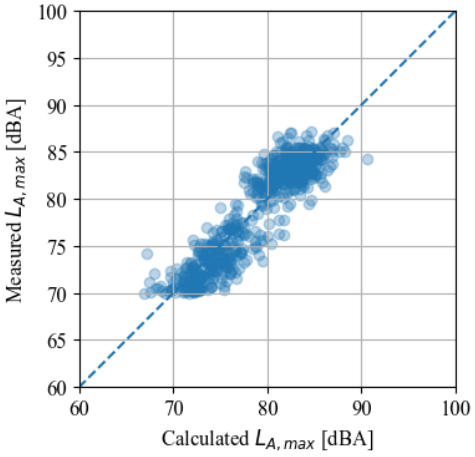

(e) $L_{A_{max}}$ **calibration data set calibrated using standardised measurements.**

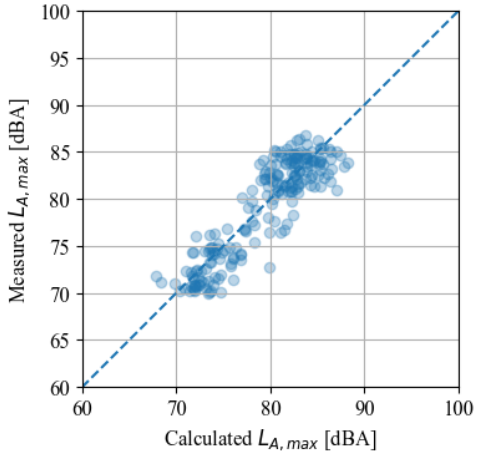

(f) $L_{A_{max}}$ **validation data set calibrated using standardised measurements.**

Fig. 15 Calibration and validation data set before and after calibration using both calibration methods.

Table 12 Results for the baseline and calibrated model using the standardised measurements.

	Data set	$L_{A,max}$ [dBA]		SEL [dBA]	
		μ	σ	μ	σ
Baseline	Calibration	-0.28	3.16	0.11	3.11
	Validation	-0.11	3.47	0.20	3.05
Calibrated	Calibration	-0.02	2.10	-0.29	2.08
	Validation	0.16	2.29	-0.09	2.13

C. Effect on contour

Doc.29 primary use is the calculation of aircraft noise impact on areas surrounding airports. This is done through calculations over a grid for a large number of flights, creating L_{DEN} contours. These contours are dependent on the flight path and profile of each aircraft trajectory and the NPD table. The calibration of the NPD values thus affects the calculated contours. For sake of simplicity, the SEL contour of a single flight is plotted in Figure 16a using the flight path and N1% setting of ACMS data. The contour of the same flight with the calibrated NPD values are visible in Figure 16b and 16c for the average differences and the standardised measurement calibration methods, respectively.

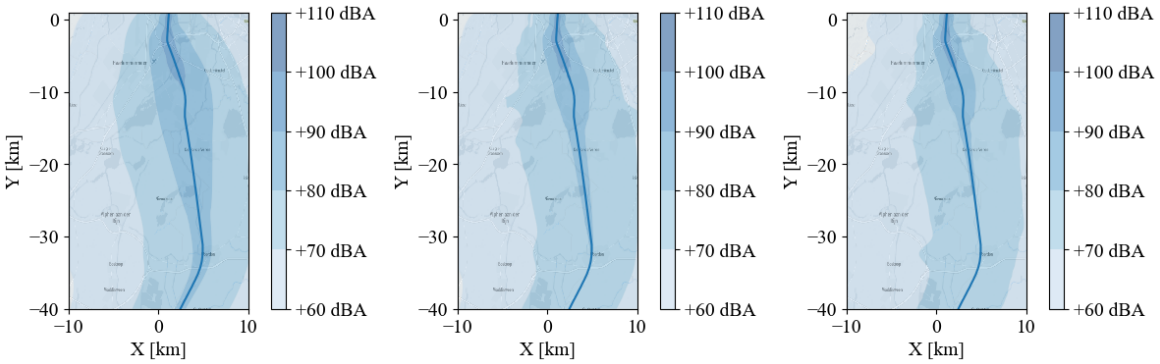

(a) SEL contour for baseline model. **(b) SEL contour for model calibrated using average differences.** **(c) SEL contour for model calibrated using standardised measurements.**

Fig. 16 SEL contours for baseline and calibrated models.

As expected, the use of calibrated NPD values affects the contour, some more than others. In Figure 17, the differences between the baseline and calibrated models are depicted. Here a negative Δ (blue) shows that the calibrated model predicts a lower SEL value than the baseline model, while a positive Δ (red) predicts a higher SEL value.

The calibration method which uses average differences to alter certain values in the NPD table has a clear effect on these parts of the flight. As there are few measurements for the larger distances, these NPD values are not altered, which results in no differences in these areas. The second calibration method gives similar results for the areas close to the flight path, but differences are seen. This method predicts a higher noise level for lower thrust settings and a lower noise level for higher thrust settings when comparing it to the current NPD values. This results in a lower modelled noise level during the high thrust phases (climb-out around y=-10km) and a higher modelled noise level in later stages of flight when trust is reduced. Further, it is interesting to see is that for close distances to the flight path, the noise is expected to be lower than what the baseline model predicts, while for the larger distances from the flight path, the baseline model underestimates the noise.

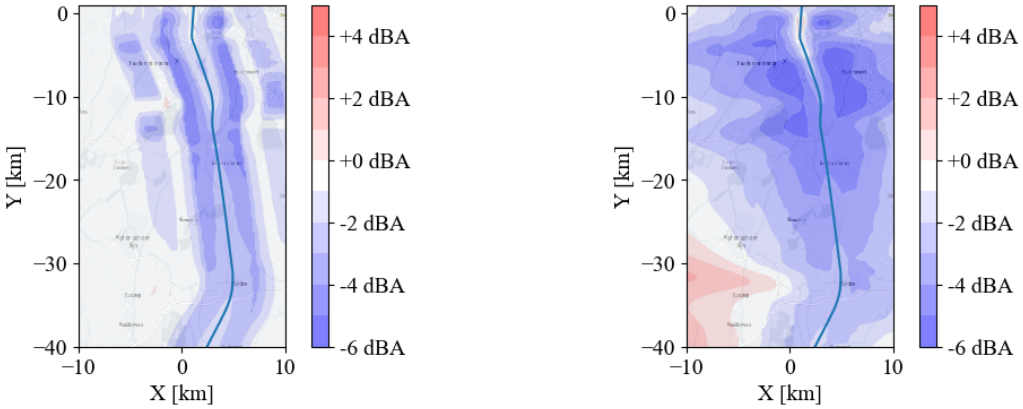

(a) Difference in SEL contour for model calibrated using average differences.

(b) Difference in SEL contour for model calibrated using standardised measurements.

Fig. 17 Difference in SEL contours between baseline and calibrated models.

D. Discussion

Calibration of NPD values has a positive effect on the found differences between model en measurement. For this specific data set, the mean difference was already quite low (-0.28 dBA difference for $L_{A,max}$) and with a standard deviation of 3.16 dBA which is an acceptable variation when compared to other best-practice methods. Improvement of this model is thus mainly focused on the reduction of the small offset and decrease in variation. This last part will increase the accuracy of single event modelling.

Although both methods perform well, differences are found. Both methods fail to calibrate the entire model to a 0.0 dBA difference, but both decrease the standard deviation. The method using average differences has a better effect on the average differences, while the methods using standardised measurements decreases the standard deviation more. A reason for this can be the more pointed approach of the average calibration method, focused on this specific data set, while the other method used a more generalised approach. For the independent data set used for validation, also improvements are visible for both methods. As both methods are not a perfect calibration, a trade-off between the two can be made to reduce the mean error or the standard deviation. Iteration of the calibration resulted in even smaller average differences (± 0.01 dBA) but did not reduce the standard deviation further. From previous studies, it is found that the variation due to weather effect, next to atmospheric attenuation effects, is about 2 dB [7, 25]. This could explain part of the remainder of the variation seen after calibration.

For both calibration methods, a larger data set is preferred. Due to the strict measurement requirements set, measurements at the larger distances are left out as these are not surpassing the 70 dBA threshold. Furthermore, it is expected that the fan tone becomes less noticeable for large distances due to the attenuation of high frequencies. Measurements for the lowest and highest distances, but also for more different thrust settings are needed to validate the methods used and to make grounded conclusions on the NPD values. As mentioned in section IV.B, the standardised SEL measurements are based on a few assumptions due to a lack of acoustic data for the higher frequencies. These assumptions have to be validated for a larger data set, as this is not extensive enough, but shows promising results to be repeated in follow-up research.

VI. Conclusion

In this paper, several methods to improve aircraft noise predictions are given. This is done by evaluating the input parameters of the best-practice model Doc.29. First, the uncertainty of the thrust input to the model is reduced by estimating the N1% thrust setting of the aircraft during the measurement through a spectral analysis of the fan tone. Validation of the N1% estimates is based on data from the Aircraft Condition and Monitoring System (ACMS). With an average root mean square error of 4%, the thrust estimation method is accurate to use in this model.

The second input for the Doc.29 model that is evaluated is the Noise-Power-Distance (NPD) table. These NPD values are found through (certification) measurements and are used in all best-practice methods. The NPD values are

evaluated by comparing measurements with model results with the actual thrust setting and distance, i.e. not making use of the default flight profiles. By reducing the chance of errors in these input parameters, a remaining part of the differences can be attributed to errors in the NPD values. For the B737-800 data set of around 800 departing flights, the mean offset was under ±1 dBA, while the standard deviation σ of these differences was around 3.2 dBA. For the improvement of this baseline model, two calibration techniques are applied to the NPD values. To evaluate and validate the calibration techniques, the data set is divided into a calibration and validation data set of respectively 75% and 25% of the measurements. The first calibration technique, based on the study of Trow and Allmark [6], altered the existing NPD values by adding the average differences found between the measurements and model results. This method proved efficient in reducing the small offset to 0 dBA and the standard deviation by 20-30%.

The second calibration method developed in this paper is not based on model predictions, but rather on measurements directly. All measurements in the data set were standardised to reference conditions as used in the NPD table. From these measurements, interesting conclusions were drawn. The relation between thrust setting and sound level showed to be less dominant than originally expected from the NPD table. The measurements in this research showed that a 20% thrust increase at 1000 ft (305m) resulted in a less than 1 dBA increase in measured maximum noise level. This is significantly less when comparing this to the expected 4 dBA increase found from the original NPD table. Applying these new relations to create a new NPD table resulted in an improvement of the standard deviation of found differences by 30-40%. For this method, the small offset was not reduced, but as these mean differences are smaller than ±0.3 dBA, these differences are deemed insignificant.

The two calibration methods both improve model predictions, but different results are obtained. In the first method, only the NPD entries matching the measurements are altered, while for the second method all new NPD entries are created. The first method is a more pointed approach, while the second method is more generalised. This results in a better reduction of average differences when using the first method, but a larger reduction in standard deviation when applying the second method.

Calibration of NPD values can improve Doc.29 model predictions on a single event level by having more accurate estimations. Next to an improvement to the best-practice noise model, the methods described in this research gives insight into the creation and validation of NPD values. Repetition of this research, but also additional research into this topic is advised for larger data sets and full range acoustic measurements to verify made assumptions.

Recommendations

A few recommendations for additional research are mentioned in this paper to improve this research. Next to that, research topics for follow-up studies are provided here.

Firstly, to improve best-practice noise modelling, a sensitivity analysis of the N1% setting with respect to flight phases, but also weather and weight of the aircraft is advised. A better understanding of the variation in thrust setting will help model single future flights more accurately and also improve the development of noise abatement procedures. This study could be combined with the promising results of the sonAIR model from EMPA, which is based purely on N1% settings instead of thrust.

Secondly, a larger measurement campaign for more extreme thrust and distance cases is necessary. Many measurements are used in this method, but only the ones above 70 dBA with an incidence level above 60 degrees, limiting the scope of this research. This causes a lack of information in the lower thrust and/or higher distances range. Research should be conducted to find a reliable method to check if these lower noise levels are indeed aircraft measurements. Also, as fan tones consist of high frequencies, these dampen out more quickly than the lower frequency broadband noise. It should be looked into how large the distance between the observer and the aircraft can be to still get a reliable fan tone estimate from the acoustic measurement. This larger data set could then be used to validate the entire NPD table.

Next, in this research, it is assumed that the correction factors applied by Doc.29 are correct and any deviations found after the correct thrust and distance input is caused by the NPD values. This is something to look further into. The corrections applied for the standardisation are also based on these corrections and other general assumptions due to the lack of measurement data in the higher frequency range (above 4000 Hz). Calibration can be done more accurately when full-range measurements are known. This will have a positive influence on the standardisation of the measurements as more accurate weather corrections and SEL corrections can be calculated.

Finally, the effect the positional information has on the dedopplerisation is large. During this research, RADAR and ground RADAR (ASTRA) was evaluated. Differences up to 100 meters were found between them, which resulted in a possible error of 10% N1. It is recommended that the research is repeated with other positional data sources such as ADS-B.

References

[1] "CEAC Doc 29 4th Edition Report on Standard Method of Computing Noise Contours around Civil Airports. Volume 1: Applications Guide," Tech. rep., European Civil Aviation Conference, Dec. 2016.

[2] "CEAC Doc 29 4 th Edition Report on Standard Method of Computing Noise Contours around Civil Airports. Volume 2: Technical Guide," , Dec. 2016.

[3] "CEAC Doc 29 4th Edition Report on Standard Method of Computing Noise Contours around Civil Airports. Volume 3, Part 1-Reference Cases and Verification Framework," , Dec. 2016.

[4] Hogenhuis, R., and Heblij, S., "Trendvalidatie van Doc.29 berekeningen," Tech. rep., NLR, Oct. 2018.

[5] Rhodes, D. P., and Ollerhead, J. B., "Aircraft Noise Model Validation," , 2001.

[6] Trow, J., and Allmark, C., "The benefits of validating your aircraft noise model," Euronoise, 2018.

[7] Simons, D. G., Snellen, M., van Midden, B., Arntzen, M., and Bergmans, D. H. T., "Assessment of Noise Level Variations of Aircraft Flyovers Using Acoustic Arrays," *Journal of Aircraft*, Vol. 52, 2015, pp. 1625–1633. https://doi.org/10.2514/1.C033020.

[8] Snellen, M., Merino-Martínez, R., and Simons, D. G., "Assessment of noise variability of landing aircraft using phased microphone array," *Journal of Aircraft*, Vol. 54, 2017, pp. 2173–2183. https://doi.org/10.2514/1.C033950.

[9] "SAE-AIR-1845A - Procedure for the Calculation of Airplane Noise in the Vicinity of Airports," Tech. rep., Society of Automotive Engineers, 2012. URL https://doi.org/10.4271/AIR1845A.

[10] Rhodes, D. P., White, S., and Havelock, P., "Validating the CAA aircraft noise model with noise measurements," Tech. rep., Environmental Research and Consultancy Department, CAA, 2002.

[11] Struempfel, C., and Hübner, J., "Aircraft Noise Modeling of Departure Flight Events based on Radar Tracks and Actual Aircraft Performance Parameters," *DAGA 2020 46. Jahrestagung für Akustik*, 2020. URL https://www.researchgate.net/publication/340461180.

[12] Poles, D., "EUROCONTROL Base of Aircraft Data (BADA) Aircraft Performance Modelling Report," , Mrt 2009.

[13] "AIR5662 - Method for Predicting Lateral Attenuation of Airplane Noise," Tech. rep., Society of Automotive Engineers, Oct. 2019.

[14] Soede, W., "Technische beschrijving vliegtuig geluidmeetsystemen: Luistervink, Nomos, Sensornet," , June 2012.

[15] "ISO 20906: Acoustics - Unattended monitoring of aircraft sound in the vicinity of airports," Tech. rep., International Organization for Standardization, 2009. Reviewed and confirmed in 2020.

[16] Merino-Martínez, R., Heblij, S. J., Bergmans, D. H. T., Snellen, M., and Simons, D. G., "Improving Aircraft Noise Predictions Considering Fan Rotational Speed," *Journal of Aircraft*, Vol. 56, 2018. https://doi.org/10.2514/1.C034849.

[17] Heilig, M. A., "Aircraft Noise: Modelling & Measuring Using aircraft noise measurements for noise model prediction improvement," , July 2020.

[18] Schwab, O., and Zellmann, C., "Estimation of Flight-Phase-Specific Jet Aircraft Parameters for Noise Simulations," *Journal of Aircraft*, Vol. 57, 2020, pp. 1111–1120. https://doi.org/10.2514/1.C035779.

[19] Jäger, D., Zellmann, C., Schlatter, F., and Wunderli, J. M., "Validation of the sonAIR aircraft noise simulation model," *Noise Mapping*, Vol. 8, 2021, pp. 95–107. https://doi.org/10.1515/noise-2021-0007.

[20] Zellmann, C., Schäffer, B., and Wunderli, J. M., "Aircraft Noise Emission Model Accounting for Aircraft Flight Parameters," *Journal of Aircraft*, Vol. 55, 2018, pp. 682–695. https://doi.org/10.2514/1.C034275.

[21] Teunissen, P., Simons, and Tiberius, *Probability and Observation Theory: an Introduction*, Delft University of Technology, Faculty of Aerospace Engineering, 2006.

[22] Filippone, A., "Aircraft noise prediction," *Progress in Aerospace Sciences*, Vol. 68, 2014, pp. 27–63. https://doi.org/10.1016/j.paerosci.2014.02.001.

[23] Giladi, R., and Menachi, E., "Validating Aircraft Noise Models," *OpenSky Symposium*, Vol. 59, 2020. https://doi.org/10.3390/proceedings2020059012.

[24] Sari, D., Ozkurt, N., Akdag, A., Kutukoglu, M., and Gurarslan, A., "Measuring the levels of noise at the Istanbul Atatürk Airport and comparisons with model simulations," *Science of the Total Environment*, Vol. 482-483, 2014, pp. 472–479. https://doi.org/10.1016/j.scitotenv.2013.07.091.

[25] Heblij, S. J., Sindhamani, V., Arntzen, M., Bergmans, D. H. T., and Simons, D. G., "Noise attenuation directly under the flight path in varying atmospheric conditions," National Aerospace Laboratory, 2013.

II

Literature Study

1 Introduction

With an exception of the year 2020, the yearly number of passengers travelling by plane has increased. This increase in flight numbers results in a more prominent environmental effect caused by the aerospace industry. Aircraft noise plays an important role in the environmental pollution around airports. Many health aspects concerning noise are researched. Effects of noise on cardiovascular diseases, stress, hearing losses and more have been found [3]. Rules and policies to limit these consequences are based on aircraft noise models which predict the noise inflicted on a specific area for a certain number of aircraft operations. The models which are often used are called best-practice models and are based on Noise-Power-Distance (NPD) tables. Input into these models are very susceptible to change. Inaccuracies in input data can cause 20-30% area contour differences [1]. In a populated area, this can increase or decrease the number of people living in high noise area significantly. The need for accurate noise models is thus important, especially when it is used for policymaking.

Over the years, communities around the airport are experiencing more annoyance. During the past year where the number of flight movements dramatically decreased, the annoyance of communities did not drop with the same level.[1] This insinuates that the problem is more complex. According to a study performed by Lim et al [4], for the same aircraft noise level, communities in a high background noise level are less annoyed than communities in a low background noise level region. The overall reduction in the number of flights can cause the still present flights to become "more annoying". Another factor that plays a role is that the trust that communities have in noise models, is decreasing and the pressure to use measurements instead is increasing [5]. Generally, people have more credence in measurements.

The aim of this literature study is to gain knowledge of the latest developments in the research field of aircraft noise modelling and measurement. This includes, but is not limited to, finding results and applications of best-practice methods, but also the pitfalls and conflicting opinions on these best-practice and other methods. Finally, a research gap to base the upcoming research on is to be found.

In this literature study the latest developments and implementations of the aircraft noise modelling process are discussed. In chapter 2 the basic principles of sound and sound modelling are discussed. This is important as a basis to understand the rest of the research. In chapter 3 the different types of noise models are discussed. How these work, their (dis-)advantages, their input parameters and how they are used around the world. In chapter 4 the research related to aircraft noise measurements and their uncertainties and application is elaborated on. The model and measurements need to be verified and validated. Studies related to this can be read in chapter 5. This chapter 5 also presents the research into model calibration with the use of measurements. Finally, in chapter 6, the literature study is wrapped up with a statement of the research gap and the planned research following this study.

[1] https://bezoekbas.nl/wp-content/uploads/2020/12/Bas-Tussentijdse-rapportage-2020.pdf

2

Acoustic Basis

To gain a basic understanding of how sound is created, propagates and is measured, the literature study starts at the basis of acoustics. The principles in this chapter are important for the understanding and implementation of noise modelling and measurement. In the first section, the sound sources and how to quantify them are explained. After that in section 2.2, the propagation of sound through the air is discussed. The final step is the measurement of sound. These corresponding noise levels can be quantified with multiple noise metrics as explained in section 2.3.

2.1. Sound sources

Sound can be described as a sum of pressure waves with a specific frequency and amplitude propagating through a medium such as water or air. Something that produces a sound is called a sound source. For an aircraft, the sources can be engines, flaps, the landing gear or other parts. Each sound source has an acoustic power (W) under specific conditions. This acoustic power level commonly ranges from 0 to $10^8 Watt$. This can be defined as a Power Watt Level (PWL) in dB and is given as:

$$PWL = 10log_{10}\Big(\frac{W}{W_0}\Big) \tag{2.1}$$

with $W_0 = 10^{-12} Watt$. A typical value of PWL for a jet engine is 160 dB. How the signal shape is described can be done on several levels. For instance in the time domain (section 2.1.1) and in the frequency domain (section 2.1.2).

2.1.1. Time domain

The disturbance in pressure these sound waves cause, is the reason sounds can be heard and measured. This is commonly done by taking the effective pressure p_e and calculating the total Sound Pressure Level (SPL) using Equation 2.2.

$$SPL = 10log_{10}\Big(\frac{p_e^2}{p_{e_0}^2}\Big) \tag{2.2}$$

Here the reference effective pressure p_{e_0} is $2 \cdot 10^{-5}$Pa. In the case of multiple sound sources, the effective pressures of all sources are added to create an Overall SPL (OSPL) value as can be seen in the equation below for two different sources.

$$OSPL = 10log_{10}\Big(\frac{p_{e_1}^2 + p_{e_2}^2}{p_{e_0}^2}\Big) = 10log_{10}\Big(10^{SPL_1/10} + 10^{SPL_2/10}\Big) \tag{2.3}$$

This method is useful to be able to model an aircraft as a single sound source while having multiple sound-making components. The equation

2.1.2. Frequency domain

Each sound wave can also be described as a set of waves with different frequencies and amplitudes. To calculate the SPL for specific frequencies, the signal is Fourier transformed to the frequency domain. It is common to divide the sound into 43 1/3-octave bands each with a centre frequency of $f_i = 10^{i/10}$ Hz with i the number of the 1/3-octave band. For each frequency band, the sound pressure level is calculated. This is denoted as the Pressure Band Level (PBL) in dB and is calculated using Equation 2.4.

$$PBL = 10log_{10}\left[\frac{P(f)\Delta f}{p_{e_0}^2}\right] \tag{2.4}$$

Where $P(f)$ is the power spectral density in Pa^2/Hz and Δf the width of the frequency band in Hz. The overall SPL is again calculated similar to the OSPL for multiple sources using Equation 2.5.

$$OSPL = 10log_{10}\left[\sum_{i=1}^{n} 10^{SPL(f_i)/10}\right] \tag{2.5}$$

2.1.3. Directionality

While each source produces a specific (set of) frequencies and pressures, it can also give the sound a direction. For simple noise models, aircraft are modelled as an unidirectional sound source, meaning the sound is uniformly distributed around the aircraft. In reality, the engines have strong directional properties as can be seen in Figure 2.1. The effect of directionality in the calculation of the SPL can be accounted for with a correction factor, the Directivity Index $DI(\theta)$. Next to the directionality of sources themselves, other parts of the aircraft can influence the direction of the sound produced. For example, shielding of the engine noise by the wings can limit the sound from propagating upwards when the engine is installed under the wing.

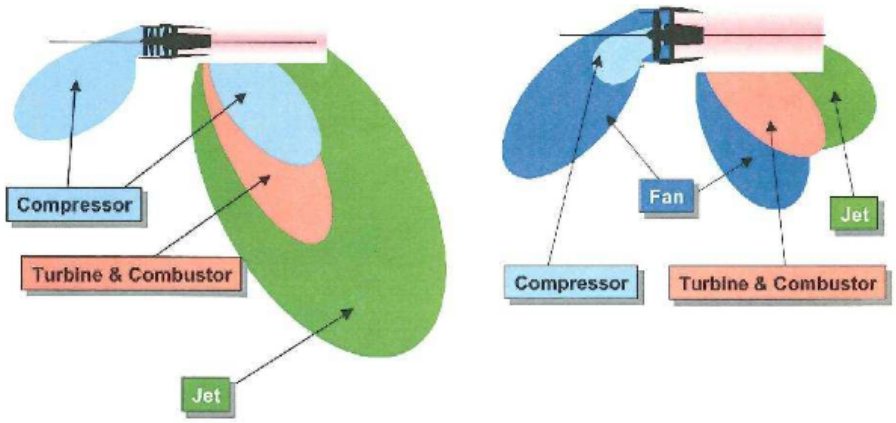

Figure 2.1: Directionality of sound from a turbojet (left) and turbofan (right) engine [6].

2.2. Sound propagation

When sound travels from a source to an observer, multiple effects take place. The effect of spherical spreading is discussed in section 2.2.1. In section 2.2.2 the absorption of sound in air is explained. In section 2.2.3 the reflection of sound on surfaces and specifically the ground effect is discussed. Finally, in section 2.2.4 the Doppler effect is explained.

2.2.1. Spherical spreading

When the sound source is assumed to be a point source, the sound wave propagates in all directions. The energy contained in the wave thus spreads over an area that increases with distance from the sound source. The larger the distance from the observer, the bigger the spread and the lesser amount of acoustic energy reaches the observer. This is visualised in Figure 2.2. This propagation follows the inverse square law since the acoustic energy is spread over the surface of the sphere when free field conditions apply. The SPL at distance r can be calculated using Equation 2.6.

$$SPL(r) = SPL(r = 1m) - 20log_{10}(r) \tag{2.6}$$

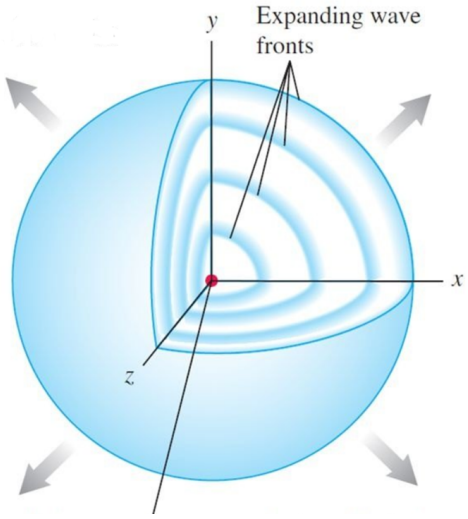

Figure 2.2: Spherical spreading of sound of a point source.

Note that this is for a uniform point source without directionality. Further is this effect not dependent on the medium in which the sound travels.

2.2.2. Sound absorption in air

As sound propagates through a medium such as air, reactions with it result in the absorption of energy by the medium. This is due to the friction of the pressure wave and the vibrational relaxation processes of the molecules. Where the spherical spreading is uniform over the frequency domain, the absorption coefficient α is not. For higher frequencies of the wave, this friction is also higher and the absorption is stronger. This is for example easily noticeable when a party is being thrown across the street. The low sounds of the bass are the frequencies that will keep you up at night. The absorption for the different frequencies due to vibrational relaxation and thermoviscous absorption processes are visible in Figure 2.3a. In this figure, α_x is the absorption coefficient of the specific process. For all processes, the higher frequencies damp out faster.

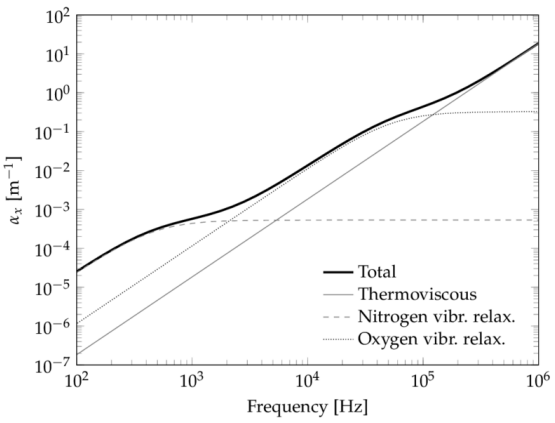

(a) Absorption coefficient for air with a temperature of T = 293.15 K and relative humidity of RH = 70%. [7]

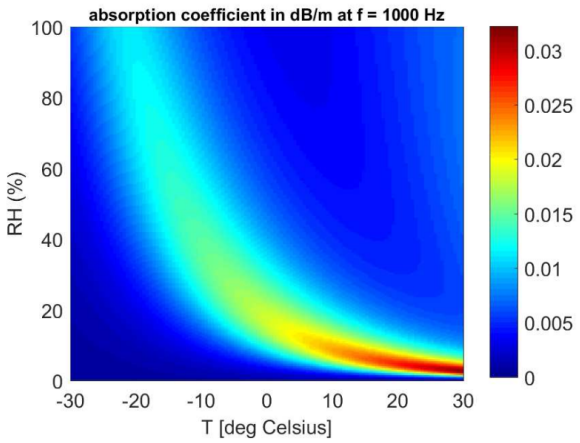

(b) Change in absorption coefficient for different temperatures and relative humidity. [6]

Figure 2.3: Change in absorption coefficient α

Absorption is also affected by the relative humidity (RH) of the air because water molecules act as catalysts for the relaxation process. When water molecules and other molecules in the air, such as nitrogen or oxygen,

collide, these air molecules get knocked into a different vibrational energy state. If the RH is higher, and thus more water molecules present in the air, these collisions happen faster and an equilibrium is reached earlier. The water molecules act as a catalyst. This decreases the relaxation time τ_m and thus decreases the absorption coefficient. [7] The temperature also has an influence on the absorption coefficient as can be seen in Figure 2.3b.

In ISO 9613 [8] the standard on how to calculate the absorption coefficient is given for noise propagation calculations. This method takes into account the different frequencies, air pressures and molecular compositions and gives the absorption coefficient α in dB/m. With this coefficient, the attenuation factor δL_t in dB can be calculated and the influence of the atmosphere on the modelled sound can be found.

2.2.3. Sound reflection

Sound, just as any other wave, can diffract and reflect on surfaces. Diffraction is an important phenomenon to investigate when applying shielding for sound such as walls next to a highway. In common aircraft flyovers, however, this is not of high importance. Reflection on the other hand is. When measuring aircraft noise with a microphone, the observer position should take notice of reflective surfaces around it, such as buildings, to avoid measuring reflective sound. A reflective surface that is always present, is the ground. For aircraft flyovers, the so-called "ground effect" can have an influence on the measurements. Measurement devices (microphones) are often mounted to a tripod or pole. The ground effect is when a sound wave reflects on the ground into the microphone. This results in two waves arriving at the microphone, the direct wave and the reflected wave, as can be seen in Figure 2.4. This could lead to a doubling of measured effective pressure (translated to 6 dB) or cancellation of sound depending on the angle between the source and the microphone. With Equation 2.7 the difference in SPL of this effect can be calculated. In this formula, the direct path, r_1 and the reflected path, r_2, are calculated from the height H and ground distance s. Q is the reflection coefficient of the surface and is dependent on the surface impedance and reflection angle. |Q|=1 for a perfectly reflecting surface.

$$\Delta SPL(r,\theta) = 10log_{10}\left[1+\left(\frac{r_1}{r_2}\right)^2|Q|^2+2\left(\frac{r_1}{r_2}\right)|Q|cos\left(\frac{4\pi f}{c}h_m sin(\psi)+\varphi\right)\right] \tag{2.7}$$

Often for calculations where the aircraft is far away, r_1 is assumed equal to r_2. Further is the phase shift φ assumed to be zero. This leads to the simplified Equation 2.8.

$$\Delta SPL(r,\theta) = 10log_{10}\left[1+|Q|^2+2|Q|cos\left(\frac{4\pi f}{c}h_m sin(\psi)\right)\right] \tag{2.8}$$

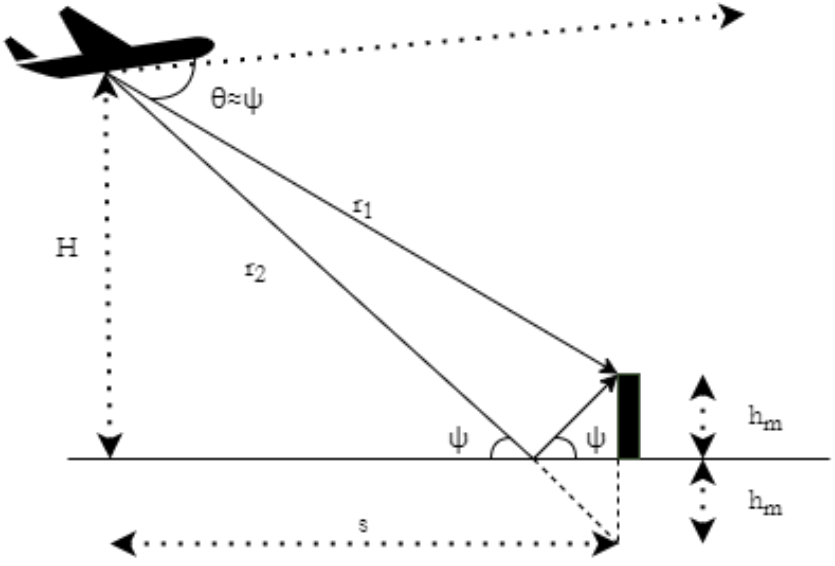

Figure 2.4: Ground effect of a reflecting sound signal when measuring with a microphone of height h_m.

In ISO 20906 [9], rules regarding the placement of microphones for aircraft noise measurements are stated to prevent these effects. The measurement location should be free of obstruction above an elevation angle

of 20°from the ground. Further there should not be any reflective surfaces within 10m of the measurement location. To minimise the ground effect, the microphone should be placed at least 6m above the ground. In chapter 4, ISO 20906 and noise measurement requirements will be further elaborated on.

2.2.4. Doppler effect

The frequency of a sound is determined by the speed and the wavelength of the sound wave. In air, the speed of sound is relatively constant but the spread of the wave is also determined by the relative speed between the observer and the source. The change in observed frequency as a result of this relative speed difference is attributed to the so-called Doppler effect. In Figure 2.5 an aircraft is seen flying over the observer. The sound wave headed to the observer is compressed by the speed of the aircraft in the same direction, resulting in a higher frequency observed than the source produces. This change in frequency can be calculated with Equation 2.9.

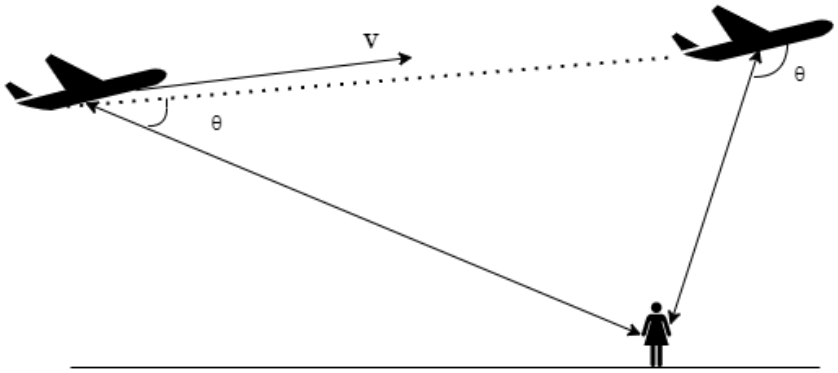

Figure 2.5: Flyover of an aircraft and its relative angle θ to the observer to calculate the Doppler shift.

$$\frac{f'}{f} = \frac{1}{1 - Mcos(\theta)} \tag{2.9}$$

In this equation f is the emitted frequency, f' is the observed frequency, M is the relative speed as a Mach number and θ is the angle between the observer and the aircraft. In a typical flyover, the emitted frequency and speed are constant and the observant is stationary. The angle θ is changing constantly, resulting in a constantly changing observed frequency. In Figure 2.6 a clear fan tone and its Doppler shift is visible. The determination of this fan tone and Doppler shift will be further elaborated on in subsection 3.2.2.

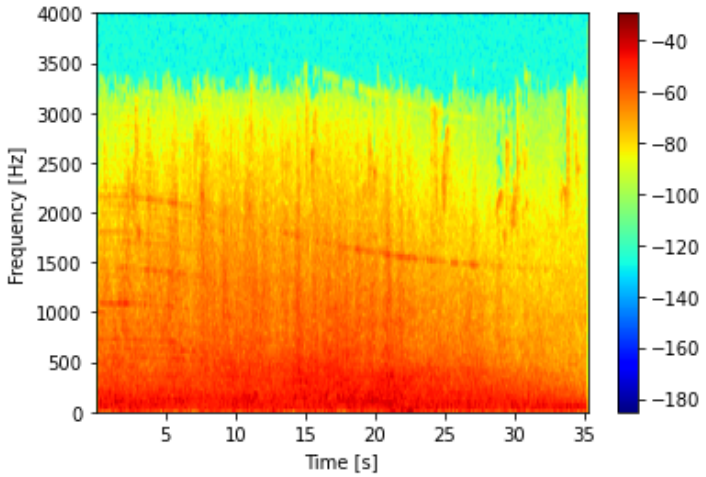

Figure 2.6: Spectrogram of an aircraft flyover measurement with clear engine fan tone with Doppler shift.

2.3. Noise metrics

Even though pressure differences are measurable, noise is often a more subjective experience. The human ear has selective hearing and does not experience every frequency in a broadband sound as evenly loud. The same is for the time duration of the sound. The consequence of this is the numerous forms noise metrics.

2.3.1. A-weighting

The first and most common form to take into account the human perception of noise is the A-weighting. This A-weighting amplifies sound around 1000 Hz while dampening sounds outside the audible spectrum and is based on the 40 phon line.[1] For specific frequencies in the sound a weighing function is applied. This is given by Equation 2.10.

$$\Delta L_A = -145.528 + 98.262 \cdot log_{10}(f) - 19.509 \cdot (log_{10}(f))^2 + 0.975 \cdot (log_{10}(f))^3 \tag{2.10}$$

A broadband signal can be adapted by taking the ΔL_A for multiple frequencies and calculate the overall A-weighted sound pressure level L_A (in dBA) using Equation 2.11. In Figure 2.7a this weighting is applied on a broadband signal for each 1/3-octave band. The unit of this metric is dBA (red line) while the original signal is presented in dB (black line).

$$L_A = 10log_{10}\left[\sum_i 10^{\frac{SPL(i)+\Delta L_A(i)}{10}}\right] \tag{2.11}$$

When looking at the aircraft flyover OSPL, the result of A-weighting is shown in Figure 2.7b. The maximum measured SPL is 95 dB, while the maximum A-weighted sound level $L_{A_{max}}$ is 84 dBA. This is the result of the high negative value of the weighting Equation 2.10 for low frequencies. The broadband signal of an common aircraft flyover contains a high amount of these lower frequencies and are thus corrected when applying A-weighting.

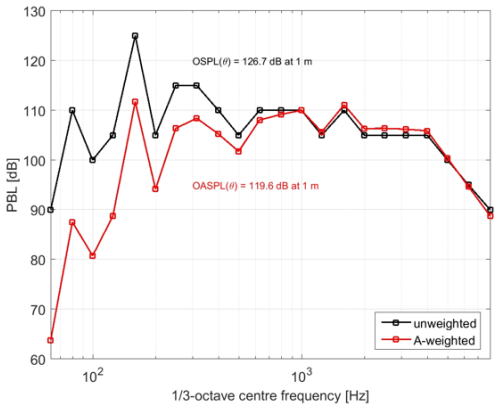

(a) Effect of A-weigthing on the frequency spectrum of an aircraft flyover.

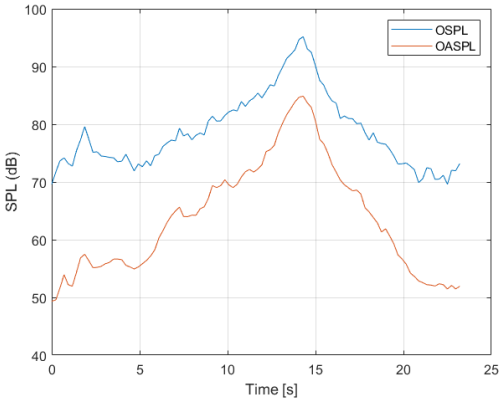

(b) Effect of A-weighting on the time-series of an aircraft flyover.

Figure 2.7: Effect of A-weighting on the time-series of a flyover

2.3.2. SEL

The second important aspect of the perception of noise is the duration of the noise event. A metric commonly used to measure aircraft flyovers is the Sound Exposure Level (SEL) in dBA. To calculate the SEL, the $L_A(t)$ curve is integrated over the time of the event. The SEL value contains the same amount of energy as the total noise event.

$$SEL = 10log_{10}\left[\int_0^T 10^{L_A(t)/10} dt\right] \tag{2.12}$$

To find the right time frame to integrate over, the 10 dBA downtime is used. From a noise event, the maximum sound level is found $L_{A_{max}}$. The moments the L_A curve crosses the threshold of 10 dBA below $L_{A_{max}}$ is the start and end position of the event. This is depicted in Figure 2.8. This assumption can be made as only the upper part of $L_A(t)$ contributes to the integral.

[1] 0 phon is the threshold of hearing and 120 phon corresponds to the threshold of pain.

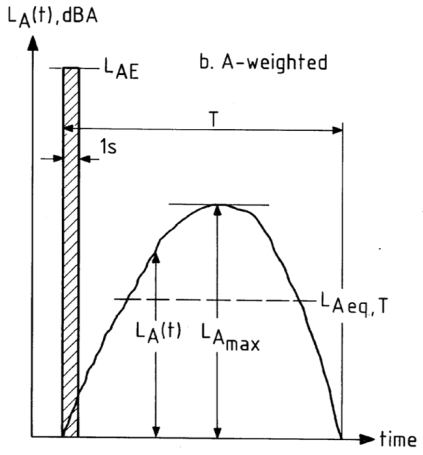

Figure 2.8: Definition of L_{AE} of a noise event.

2.3.3. L_{DEN}

Next to the frequency and the duration of the noise, the time of day people experience the noise is of great importance. An aircraft flyover during night time is creating a higher annoyance than a flyover during the day. The noise metric L_{DEN} takes into account the time of the day of the event and applies appropriate weighting to each event. If the event takes place during the day (07:00-19:00), no additional weighting is applied. During the evening (19:00-23:00) an additional 5 dBA is applied to each event. During night time (23:00-07:00) a weighting of 10 dBA is applied. The value for L_{DEN} in dBA is then calculated using Equation 2.13.

$$L_{DEN} = 10log_{10}\left[\frac{1}{86400}\sum_{i=1}^{N} 10^{\frac{SEL_i+W_i}{10}}\right] \tag{2.13}$$

Where SEL_i is the dBA value of the flyover of the i^{th} event and W_i the appropriate weight penalty.

The L_{DEN} is a good metric for the environmental load of an airport to its surroundings. Studies relating to health effects take into account this metric [3] and is also used for policymaking and putting restrictions on the number of operations. The L_{DEN} is often visualised as a contour surrounding the airport. For Schiphol, an example of the model output and its visualisation is shown in Figure 2.9.

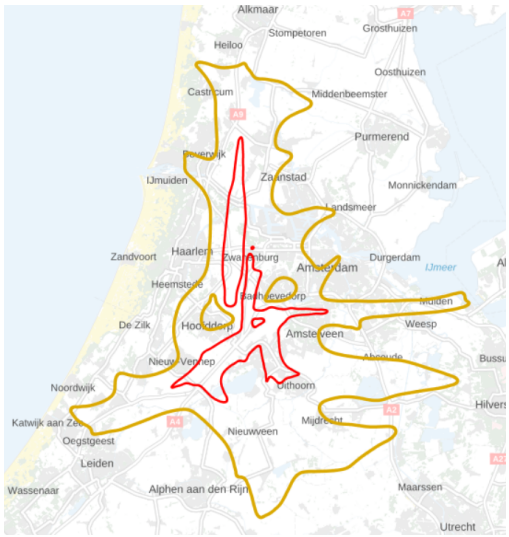

Figure 2.9: L_{DEN} of aircraft noise around Schiphol airport [2016][2].

[2]https://www.atlasleefomgeving.nl/geluid-vliegverkeer-2016-lden

3

Noise models

To be able to predict the noise emitted by an aircraft, noise models are developed. In this chapter, the different types of noise models and their application are discussed in section 3.1. The input parameters for these models and their influence are discussed in section 3.2.

3.1. Types of noise models

Research in noise modelling of aircraft and the effect on the population has been done since mid 20th century when the commercial aviation industry took flight. To accurately reflect the noise produced by different aircraft, multiple types of models have been developed. Aircraft are complex sound sources, as mentioned in section 2.1, and thus require extensive research to predict its noise and the propagation of this noise. In this section, the different types of models and their application are discussed. In section 3.1.1 the differences between non-empirical and semi-empirical models are explained and their use in today's practice, while in section 3.1.2 the operation of fully empirical models and their application are discussed.

3.1.1. Non-empirical and Semi-empirical models

The first type of noise models is the fully non-empirical models. These models are based on pure mathematical calculations containing flow dynamics (aerodynamics) and sound propagation calculations. In these models, every aspect of the airframe and engine needs to be modelled such as the trailing edge of the wing done in [10]. The advantage of this type of modelling is that for the development of new aircraft, the noise impact can be taken into account and even optimised. The disadvantage is however that research of every aspect is timely and the modelling of this noise is computationally expensive.

That is why simplification is often applied in the form of measurements. These result in fully empirical models (further discussed in section 3.1.2) and semi-empirical models. The semi-empirical models combine the mathematical formulas for different engine and airframe characteristics with coefficients obtained through measurements. A review of the current developments in this area is given by Filippone [11]. The advantage of these type of models is that they can accurately predict the type of noise produced (frequency and sound level) and distinct the different sources while still being computationally achievable with a normal computer. This is useful for parametric noise optimisation of new aircraft designs [12]. Famous programs that use this approach are the Aircraft Noise Prediction Program (ANoPP) developed by NASA.[1] Here the distinction is made for 4 airframe noise sources; the wing (trailing and leading edge), the landing gears, the tailplane and the fuselage. The necessary input parameters are the geometry of the aircraft and the flight speed. For engine noise prediction, more detailed input parameters are necessary, which are often not available.

In Germany, the German Aerospace Institute (DLR) created the SIMUL model where individual noise components (airframe, jet and fan) are modelled with data gathered from wind tunnels and dedicated flyover events as described in Guérin et al [13]. In Pott-Pollenske et al [14], these measurements are compared to the model and could lead up to a 6 dB difference. Especially the higher frequencies were underestimated. These types of extensive measuring campaigns are a good source of information to improve the (semi)-empirical models.

[1] https://software.nasa.gov/software/LAR-19861-1

3.1.2. Empirical models

Unfortunately, for large models with a great number of aircraft movements, semi-empirical models are too time and computationally expensive. Therefore the most common (best-practice) models are the fully empirical models. As the name already states, noise prediction is based on measurements and historic values. It often makes use of the so-called Noise-Power-Distance (NPD) tables. In these tables the known noise level (in dBA) is given for specific distances from the aircraft to the observer and power (thrust) setting of each aircraft. These values are found through certification testing for departures and arrivals and can be found in the Aircraft Noise and Performance (ANP) database.[2] The effects of the propagation of sound through the air, as explained in section 2.2, is already incorporated into these values. If the atmospheric conditions differ from the standard ISO conditions of 15 °C and 80% humidity, adjustment factors should be added. Together with a few simple mathematical expressions, the empirical models can predict noise exposure quickly. The accuracy of these models is 1 to 2 dB for locations calculated directly beneath the flight path [15]. For aircraft flying at a low incidence angle, this accuracy is reduced [16]. The overall lower accuracy is often deemed sufficient when comparing it with the faster computation time.

In many countries around the world, empirical noise models are developed. A widely used model is the Integrated Noise Model (INM) created by the Federal Aviation Administration (FAA). This model is now replaced with the Aviation Environmental Design Tool (AEDT).[3] This model is based on the guidance material of the Society of Automotive Engineers (SAE) [15] and the International Civil Aviation Organisation (ICAO) Annex 16 [17]. This tool is easy to understand and widely used for US airports and in research studies such as Giladi and Menachi [18] and Strümpfel and Hübner [19]. The accuracy of the AEDT is not specified but is estimated to be ±1.5 dB [16]. This accuracy is dependent on the input variables for the model. How these parameters vary and how it influences the model is further discussed in section 3.2. The Aircraft Noise Contour (ANCON) model used in the UK is based on the same principles as the INM and is considered best-practice.

A slightly different approach is used in Switzerland, where the FLULA model is developed [20]. This model is based on flyover measurements taken with single microphones. From these measurements, polynomial functions are derived to predict the aircraft source noise. The Swiss Federal Laboratories for Materials Science and Technology (EMPA) is currently working on an improved model called the sonAIR.[4] A new set of more than 11,000 flyover measurements and cockpit information is used to provide this model with source data. These measurements were taken for locations in the vicinity of the airport and larger distances. Zellmann et al [21] created a method to divide the sound source in airframe and engine noise into two linear regression models. This is done by linking the real aircraft configurations and engine settings with the measurements. Together with the noise propagation model sonX[5], which takes into account atmospheric properties, spherical spreading and the ground effect, the noise experienced by the observer can be predicted. This method from EMPA is more detailed than the current best-practice method but still fully empirical and less computationally hard than the semi-empirical methods. The disadvantage of this method is the high amount of data necessary to create and update it.

For Schiphol, noise modelling translated to the "Nederlands Reken Model" (NRM), which has been in use since 1967 [22], and is also based on the principles of the INM. Over the past decades, the need to have a harmonised noise modelling approach through Europe surfaced. The European Civil Aviation Conference (ECAC) produced the Doc.29 model with an approach based on best-practice noise modelling [2]. How to implement this model and how to verify it are explained in Volume 2 [23] and Volume 3 [24] of Doc.29, respectively. The implementation of Doc.29 on Schiphol is discussed in Heblij et al [25]. Here the assumptions made in the model and the used programs are elaborated on. In Hogenhuis and Heblij [26] the results of the NRM and Doc.29 models are compared with respect to the noise measurements taken by the continuous NOise MOnitoring System (NOMOS) which is placed around Schiphol. More on NOMOS will be discussed in section 4.3. Doc.29 predicted the aircraft noise more accurate, but a difference with the measurements remained. The minimisation of these differences is key to an accurate model. As best-practice models are very susceptible to changing input variables, these will have to be evaluated thoroughly. In this literature study, the focus will be on the Doc.29 model.

[2] https://www.aircraftnoisemodel.org/
[3] https://aedt.faa.gov/
[4] https://www.empa.ch/web/s509/sonair
[5] https://www.empa.ch/web/s509/sonx

3.2. Noise model input parameters

As mentioned before, the main input parameters for the best-practice noise models are the thrust setting of the aircraft and the distance to the observer. This distance over time can be found through the flight path of the aircraft which can be a standard route or taken from radar data. Multiple studies on finding the correct input information and the consequences on the models were performed. The studies related to the influence of the flight path on the predicted noise are discussed in section 3.2.1. The effect of changing thrust and how to find the right input is discussed in section 3.2.2. The influence of the weather is shown in section 3.2.4. Finally, the NPD values and how they are obtained are given in section 3.2.3.

3.2.1. Flight path

The flight path of an aircraft is the route it takes (latitude and longitude) and altitude over time. Specific height profiles for climb and descent and waypoints are often used by airports for air traffic management purposes. When modelling a noise contour, the spreading of aircraft along a route can be calculated using a standard deviation [2]. The L_{DEN} is then calculated for a large set of aircraft over time. For single events, however, a deviation from the modelled route can give higher differences when comparing it with measurements. In Strümpfel and Hübner [19] the results of the AEDT model with real (RADAR based) and modelled flight tracks are compared. It is shown that the real flight tracks provide a much more accurate noise footprint when comparing it to measurements in all cases except for a location lateral from the aircraft trajectory. This is confirmed in the study of Giladi and Menachi [18] modelled with the Doc.29 standard. The default flight tracks were less accurate than the real RADAR based tracks. Especially for take-off procedures the differences with modelled and measured noise were visible. For landings, where an Instrument Landing System (ILS) is used, the deviations from the flight track and thus the noise measurements were less visible [27]. The study of Zaporozhets [28] also proved this by modelling the different height profiles and their corresponding SEL contours.

3.2.2. Thrust

The thrust setting is a more difficult parameter to find. It can be found through standard departure and arrival profiles with the corresponding thrust settings in the ANP database. For take-off or climb procedures, thrust is often modelled for its maximum. However, this is regularly not the case as a reduced thrust setting saves on engine life [29]. The estimation of the correct thrust setting is thus of great importance as real thrust data is not freely available. That is why multiple studies are dedicated to finding the thrust setting from other data sources.

Aircraft performance thrust estimation

Thrust can be estimated with the aircraft performance data such as speed, flap settings and weight of the aircraft. The speed of an aircraft can be gathered from RADAR or ADS-B data, but flap settings and weights of an aircraft are still not openly available. A weight estimation given by Doc.29 is based on the stage length of departing aircraft or on the maximum landing weight for arriving aircraft [2]. A standard set of flap settings can be found in the ANP database for specific procedural steps. Strümpfel and Hübner [19] used ADS-B data and Eurocontrols Base of Aircraft Data (BADA) to estimate the weight and thrust of the aircraft. The weight at take-off is based on the safety speed V_2 of the climbing aircraft and some aerodynamic properties using Equation 3.1. In this equation, the lift coefficient $C_{L,max,1+F}$ is dependant on the flap setting F.

$$m_{v_2} = \frac{V_2^2 \cdot \rho \cdot S \cdot C_{L,max,1+F}}{1.13^2 \cdot 2 \cdot g} \tag{3.1}$$

The aircraft thrust along the trajectory is calculated using the BADA BEAM model. The BADA fuel consumption model provides coefficients to calculate the changing mass along the trajectory and updating the weight of the aircraft for the thrust model [30].

This method is validated with flight operational data and resulted in a 5.5% absolute mean deviation for the weight estimation and 11% for the thrust estimation. When using this thrust estimation in the AEDT model, the differences with measurements decreased when comparing it to standard procedural steps. This shows an improvement for noise modelling, but still, progress can be made.

In Alligier et al [31] the calculation is reversed and the thrust and weight of climbing aircraft are used to predict the trajectory. This is done using a point-mass model and the kinetic and potential forces. The unknown inputs for this model, the weight and thrust, are estimated using historical data and past trajectory points. This estimation is compared to the BADA standard model, but not validated with real-life data.

Heilig [32] used a different approach for the estimation of thrust taking into account the state of the aircraft at all times. In Equation 3.2 the thrust force per engine $F_n[lb]$ is calculated with the weight $W[lb]$, the drag to lift ratio $R[-]$, the flight path angle $\gamma[°]$, the bank angle $\epsilon[°]$, the acceleration $a[m/s^2]$ and the gravitational constant $g[m/s^2]$. In this research, the weight is calculated according to the maximum landing weight and stage length based methods described in Doc.29 [2]. The angles and the acceleration of the aircraft at any point can be extracted from RADAR data. The drag to lift ratio R, however, is more difficult to obtain as this aerodynamic coefficient is dependant on the flap setting, calibrated airspeed and altitude. In the ANP database, default procedural steps are found with flap settings and a value for R for each corresponding speed and altitude. Although this method is validated in Heilig [32] with data from an Aircraft Condition and Monitoring System (ACMS)[6], deviations in the estimated weight and flap setting remained.

$$F_n = F_{n,aero} + F_{n,potential} + F_{n,kinetic} = W\frac{R\frac{cos(\gamma)}{cos(\epsilon)} + sin(\gamma) + \frac{a}{g}}{N} \tag{3.2}$$

From Behere et al [33] the effect that the aircraft weight and thrust have on the noise model is analysed. This is performed with a sensitivity analysis on the AEDT. This resulted in quite intuitive results, such as a larger take-off weight creates an increase in noise contour and a reduced thrust setting, a decrease in noise contour. An interesting result from this study is the relative little changes in noise contours when a Noise Abatement Departure Procedure (NADP) is used. For some areas, the noise even increases when an NADP is used. A sensitivity analysis can assess previously described methods.

N1% parameter thrust estimation

Another method to estimate the thrust setting of an aircraft is to estimate the fan tones from spectral noise information [34]. The fan of an aircraft engine turns with a specific turn rate in rounds per minute (rpm). This fan is connected to the low-pressure turbine, powered by the low-pressure compressor, or the N1 spool. The turning fan creates a noise tone, which can be measured. The amount of rpm is often expressed as the percentage of the maximum rotational speed. This N1% has a strong correlation with the thrust setting of the engine. The equation for the corrected net thrust F_n/δ can be seen below.

$$\frac{F_n}{\delta} = E_0 + F_0 V_C + G_A h^2 + HT + K_3\left(\frac{N1\%}{\sqrt{\theta_T}}\right) + K_4\left(\frac{N1\%}{\sqrt{\theta_T}}\right)^2 \tag{3.3}$$

In this equation, E_0, F_0, G_A and H are engine constants, taken from the ANP database. The constants K_3 and K_4 can be derived from installed engine data. In the ANP database, for a small selection of aircraft engines, these parameters are given. Unfortunately, for several aircraft, this is not the case. For these aircraft a polynomial fit through the ACMS data can be set, linking the engine fuel flow and the N1% rotational speed [32]. The thrust per engine can then be calculated from this fuel flow using the constants from BADA for each specific engine type. The disadvantage of this method is the dependency on ACMS data, which is not freely available.

The study from Merino-Martinez et al [34] showed promising result when applying the above method for thrust estimation to a noise model. Also, the application done by Hooijmeijer [35] with NOMOS data files showed an improvement in noise prediction when comparing it with the use of procedural steps for thrust estimation.

A disadvantage of this method of thrust estimation is that a verified sound measurement is necessary. This limits this method to flights in the vicinity of airports where measurement locations are installed. When measuring the fan tone frequency of an aircraft flyby, the tone should be Doppler corrected with Equation 2.9. This can be done by matching the RADAR tracks with the audio file and finding the relative position and speed of the aircraft. As fan tones are directional, the orientation of the measurement location with respect to the aircraft is also important.

Another disadvantage of this method is the newest development in the aircraft engine industry: the Geared Turbofan (GTF) engine. A GTF engine has a reduction gearbox between the fan and the low-pressure turbine. Where a conventional turbojet engine has a rigid shaft between the fan and the turbine, in a GTF these components can move separately at different speeds. This is to not have the N1 spool be limited by the maximum fan blade tip speed. The fan speed thus not automatically specifies the N1, making the above described method very difficult. Bertsch et al [36] analysed the impact in noise when a GTF engine is installed. From this study, a noise reduction due to the reduced fan speed is found. A disadvantage is that the GTF engines have a higher weight due to the higher bypass ratio and thus bigger engines. This weight increase is

[6] An ACMS contains comparable data as to a Flight Data Recorder (FDR)

however predominated by the lower fuel consumption that can go up to 24% when using GTF [36]. Current aircraft with these GTF engines are the A320-neo, E190-E2 and the Bombardier C-series.[7] The advantages of GTF engines are great when comparing it to conventional turbofan engines and the GTF is expected to be widely implemented in the future.

3.2.3. NPD

The final input, and maybe even the most crucial part, of best-practice models, are the NPD tables. The current most complete database is the ANP database, which is updated with new aircraft and engine-frame configurations regularly. The values for the NPD table are gathered through certification testing according to ICAO standards (Annex 16)[17]. The measurements are taken at multiple points for flyover, lateral and approach for different thrust settings and distances as can be seen in Figure 3.1. Although the certification tests are done in a controlled environment, it is a limited set of distances and thrust settings. The other values in the NPD tables are interpolated and extrapolated from these certification tests. The evaluation of the NPD values is further discussed in chapter 5. The tables are given in EPNL, $L_{A,max}$ and SEL values. Michel [37] evaluates these EPNL levels with respect to physical parameters to be able to compare different noise levels of aircraft.

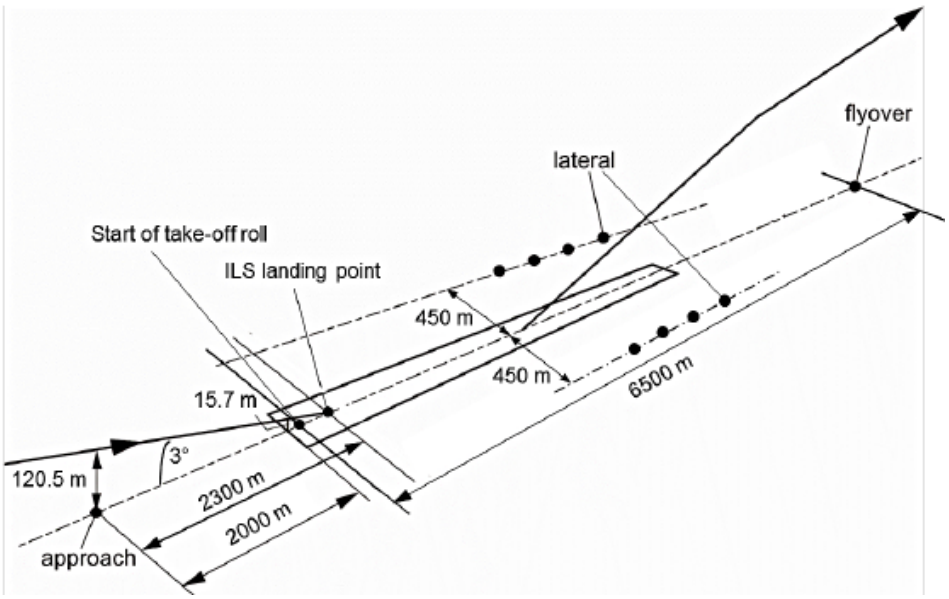

Figure 3.1: Measurement positions for noise certification test flights. Based on [37]

The sonAir model from Switzerland uses a different set of measurement data to provide their model with data. These measurements come from an extensive measurement campaign (2,600 close-by flights and 11,000 flights in the far-field) around Zurich airport and contain the most major aircraft.[8] For certification tests cockpit data is used to find the trust setting and distance to the observer. For the sonAir model measurements, this is done too but complemented with an optical tracking system and an N1 speed measurement.

3.2.4. Weather

The last set of variables to take into account is the weather. The values in the NPD tables are based on the standard atmosphere of 15°C and 80% relative humidity. As temperature and humidity of the air have a big effect on the propagation of sound [38], the modelled noise results will have to be corrected for the actual temperature and humidity. In Arntzen et al [39] the simplifications of atmospheric effects on the Doc.29 model are investigated. For year-long averaged models (for example the L_{DEN} noise contours) weather effects such as wind often cancel out. But for single event modelling, the effects of wind and temperature are significant and should be taken into account. Koster [40] showed a decrease in variability in differences between measurements from NOMOS and Doc.29 when applying actual meteorological conditions.

[7] https://aeroreport.de/en/innovation/geared-turbofan-how-the-engine-of-the-future-was-developed
[8] https://www.empa.ch/web/s509/sonair

4

Noise measurements

Noise models are made to predict the expected noise in an area. Measurements are often used to validate these models for research purposes or other reasons, for example to inform the public in that area. In this chapter, the types of noise monitoring stations and their (dis-)advantages are discussed in section 4.1. The influence of background noise on measurements and how to minimise this is discussed in section 4.2. Finally, in section 4.3, the specific measurement system NOMOS is discussed.

4.1. Noise monitoring stations

A Noise Monitoring Tower (NMT) is a sound measurement system on the ground, often on a pole or tripod. A distinction is made between supervised and unsupervised NMTs. A supervised NMT is a measuring location where a human observer is present to measure the (aircraft) sound source. These types of NMT are often short term and specific to certain research projects. The advantages of supervised measuring are that a sound can be directly linked to its source and any disturbances in the measurement are noted. The NMTs that are often placed around airports measure the sound levels continuously. The advantage of continuous noise measurements is the amount of data gathered from each NMT. The disadvantage of continuous measurement is that this is not profitable to do this supervised, as the number of man-hours it requires. This requires the use of unsupervised (or unattended) NMTs such as NOMOS. The requirements for these types of NMTs can be found in section 4.2.1. As the recorded measurements from these stations are no longer assigned to a source, an algorithm to distinct a noise and assign it to an aircraft need to be developed. The difficulty and uncertainties in event detection and aircraft identification are further discussed in section 4.2.2.

The type of noise measurement system is also different from an unattended NMT compared to a supervised NMT. With a supervised NMT, it is possible to use array microphones instead of a standard overall sound pressure meter. The array can be manually pointed to the source and gather more information about the type of sources. These arrays widely used in research such as that of Merino-Martinez et al [34] and Genesca et al [41]. This last research paper investigates the difference in measurements of the array pointed at the aircraft and a general sound level meter to find the influence of the background noise. The influence of background noise is discussed further in section 4.2. The most common sound level meter is a class 1 microphone which has an uncertainty of 0.7-0.9 dB for elevation angles above 60°[42]. For a class 2 microphone, a 1.1-1.4 dB uncertainty is accepted, but these are not in line with the ISO 20906 requirements [9].

In Shinohara et al [43] the uncertainty in year-round measurements of short term and continuous NMTs is measured. This is done with a set of temporary supervised NMTs at the same location as the unattended continuous NMTs around the airport of Narita. Through the standard deviation of the differences between the measurements, an error could be found. The standard deviation improved when multiple weeks of monitored measurements are taken in different seasons. The accuracy of these measurements was 1 dB. The comparison with unmanned noise monitoring stations showed that the influence of seasonality is strong and care should thus be taken in using only a short period of measurements. Filippone and Harwood [27] confirmed the seasonality influences and assigned them to the change in relative humidity. This research also pointed out the variations of the measurements ±10 seconds around the overhead position during a flyover. Care should thus be taken when SEL values are measured. White [44] performed a study into the uncertainty of the NMTs around London airport. These NMTs were positioned with a class 1 microphone and resulted in

a ±1.5 dB uncertainty. The uncertainty for the SEL measurements was lower than when $L_{A_{max}}$ is used.

4.2. Background noise

When taking noise measurements in urban areas, it is important to take the background noise level into account. This background noise could disturb the measurements, but could also create new non-aircraft noise measurements. The influence of the background level on the taken noise measurements and the difficulty in aircraft noise distinction is discussed in this section.

4.2.1. Measurement requirements

The effect of background noise on the measurements taken by an (unattended) NMT can be quite significant. In the research performed by Genesca et al [41], the influence of a high background noise environment resulted in a 5-8 dB difference between the aircraft noise measured by an array and the sound level measured by a standard sound level meter. As mentioned previously, an unattended continuous NMT often uses such a standard sound level meter. To prevent these errors in unattended continuous NMTs, a set of guidelines are presented in the ISO 20906: *"Unattended monitoring of aircraft sound in the vicinity of airports"* [9]. This is a report from the International Organization of Standardization, an organisation that publishes international standards on multiple subjects. ISO 20906 is followed by multiple models like Doc.29.

The first set of ISO 20906 requirements are about the location of the NMTs. It is specified that the microphone should be at least 10 m away from any reflective surfaces such as buildings. The microphone should also be placed at least 6 m above the ground. Further, should the field of view around the measurement site be free above 20°elevation angle from the ground to the aircraft [9]. Finally, the background noise level of the measurement location should be at least 10 dB lower than the noise level of the aircraft flyover event [17].

The second set of requirements describe the atmospheric condition during the event. In ISO 20906 [9], it is stated that the wind speed should be lower than 10 m/s. Although in Heilig [32], an 8 m/s maximum requirement yielded better results. Further, it should not be raining at the time of measurement. The temperature and humidity are often taken into account when modelling (see the previous chapter), but the ICAO Annex 16 [17] specifies a minimum temperature of -5 °C and a maximum of 35 °C for certification testing. Outside of these boundaries, the weather corrections are deemed unreliable. The same accounts for the relative humidity with boundaries between 20% and 95%.

For event detection, a different set of requirements are specified. As a continuous NMT measures the sound around it constantly, features in the measured sound are used to distinguish aircraft sound from background noise. According to ISO 20906, the noise is measured in $L_{Aeq,1sec}$ and is measured when it passes a set threshold. The event is then specified from 10 dB downtime from $L_{A,max}$ [9]. This is important when measuring the SEL of the event. Rhodes et al [45] also specifies the requirement that the elevation angle β between the NMT and the aircraft should be at least 60°. How aircraft are identified and coupled to measurements is further discussed in section 4.2.2.

The final set of requirements is about the instrumentation. As discussed in section 4.1, different types of microphones are used for different purposes. For an unattended NMT, ISO 20906 specifies that at least a class 1 standard sound level meter is used for the measurements [9].

4.2.2. Aircraft identification

The interpretation of the noise data is important to find the aircraft noise. When high background noise is present at the NMT, peaks in the L_A sound level could be attributed to multiple sources. Adams [46] reviews the complications of selecting a proper threshold level. A too high threshold can eliminate aircraft flyover noise, but a too low threshold can cause background sound sources to surface. The uncertainty in the identification of aircraft is assessed by Asensio et al [47]. This research showed an increase in false positives when a threshold system is used. To improve on matching measured sound events to aircraft flyovers, different techniques can be applied. A first method analysed by Asensio et al [47] minimised the aircraft identification uncertainty by using simple detection techniques by radar tracking. According to Giladi [48] using ADS-B data over conventional radar provides a more accurate result. This is due to the higher broadcast frequency (0.5s intervals for ADS-B versus 4s for radar). The accuracy of ADS-B data in the vertical plane is however not proven to be more accurate [49].

Other information caught by the microphone is the frequency spectrum. Dekoninck [50] measures the common aircraft frequencies (40-250Hz bands in specific) to see if it reaches the set threshold. As lower frequencies propagate further through the air, these measurements can be attributed to aircraft far away.

This resulted in being able to detect aircraft with a lower $L_{A_{max}}$ peak of 40 dBA. Spectral information is also used by Rosin and Barbo [51]. They use pattern recognition to look at specific descriptors in the audio signal such as harmonics below 1000Hz, which is corresponding with jet noise, and a peak (spectrum line) at around 2000 Hz for the fan tone. This study is applied around Paris Charles de Gaulle airport with continuous NMTs and improves the identification of aircraft by 5%.

Pattern recognition is more often used to identify aircraft sounds from background noise. Adams [52] shows different methods to characterise aircraft sound from background noise using a neural network for recognition of samples and the application of dynamic loudness. The study shows the big uncertainty in events and classification as some noise events are not fully community noise nor aircraft noise. Another method for neural networks is developed by Mariscal-Harana et al [53], where spectrograms are made from all noise events and the model is trained to recognise typical aircraft spectrograms.

A commonly used method in sound analysis, specifically voice recognition, is the use of Mel Frequency Cepstral Coefficients (MFCC). These MFCC represent the cepstrum (used in Fourier analysis for investigating periodic structures in the spectrum) on a mel-scale. This mel-scale is better in approximating the human auditory system with respect to the linearly-spaced frequency bands. The application of MFCC in pattern recognition of aircraft sound has been done by Asensio et al [54] and Klaczyński and Pawlik [55]. The study from Asensio et al was able to discriminate aircraft noise from background noise with 93% accuracy and decrease the signal-to-noise ratio (SNR) to 7 dB instead of the commonly used 15 dB [54]. Klaczyński and Pawlik created a method with a 90% accuracy in aircraft noise identification [55]. Overall this is a successful method of aircraft identification.

4.2.3. Measurement analysis/filtering

Even when aircraft are identified from measurements, it is not automatically a proper measurement. Next to the aircraft noise, the measurement can be contaminated with background noise. Much like the definition of SEL, background noise under 10 dB from $L_{A_{max}}$ is considered not to cause any disturbance. Nevertheless, sometimes during a flyover, community noise rising above that threshold is present at the same time. A measurement is thus not purely community noise nor can it be fully attributed to an aircraft. For example when a dog barks at the aircraft that is flying over the NMT. A method to filter out measurements with a high disturbance rate is thus necessary. This can be done through the frequency domain or the time domain.

Frequency filtering can be done to measure the presence of certain aircraft frequency and checking for their dominance. Much like pattern recognition discussed in the aircraft identification section 4.2.2. If a high energy level is present in a high frequency (>2500Hz), the measurement is likely to contain community noise. The disadvantage of this method is that community noise, such as cars, share the same low-frequency broadband noise as aircraft. Not all disturbances can be easily found.

For filtering in the time domain, a few key characteristics of flyovers can be looked for. The typical duration of the event and the rise and fall time of the sound level. Measurements much longer than the typical duration of the flyover will be discarded, while really short measurements are not registered as events. The slope of the sound level L_A can also be analysed. As aircraft typically come closer and move away from a NMT with a certain speed, the expected slope can be calculated. Short steep peaks in the measurement can be classified as non-aircraft sounds.

4.3. NOMOS

The research conducted after this literature study will focus on the NMTs in place around Schiphol airport, the Noise Monitoring System (NOMOS), which is active since 1993. NOMOS consists of 41 continuous unattended NMTs placed on different locations where aircraft noise is expected, see Figure 4.1. The placement is mostly according to the requirements specified in section 4.2.1, but often in urban areas which have reflective surfaces nearby or a high background noise level. The reason for this is that the system is currently mainly used as information to the public. The noise information is visible on the website run by CasperAero.[1] The maintenance and management of the NMTs are done by Brüel & Kjær.[2] Each NMT is equipped with a microphone of class 1 rating [42]. This is according to the ISO 20906 norm [9]. The microphones are calibrated two times a day by emitting a 90 dB(A) tone and adjusting the microphone accordingly. When the NMT is in the middle of a measurement at the scheduled calibration time, the calibration is skipped. Calibration errors often occur, resulting in the NMT not working properly for a 12 hour time period.

[1] nomos.schiphol.nl
[2] https://www.bksv.com/en

Figure 4.1: Location of currently active NOMOS NMTs[3].

4.3.1. Event registration

The noise event information is processed in the Airport Noise and Operations Management System (ANOMS) application (current version 9.8) managed by Envirosuite. For each NMT a threshold (in dbA) is set depending on the background noise level of that location. These thresholds are commonly set to 60 dBA, but these should be further analysed as the background noise of the NMTs is quite different. To be able to measure an event, the measured sound should pass the threshold for a minimum of 10 seconds and a maximum of 120 seconds. The measured $L_{A_{max}}$ should be at least 12 dBA higher than the background noise level and this must be the local maximum between 30 seconds before and after the peak. Otherwise, this peak is not the $L_{A_{max}}$ of the event. Lastly must the measured SEL be between $L_{A_{max}} + 7dBA$ and $L_{A_{max}} + 13dBA$. When all criteria are met, an event is registered with class 0.

For each noise event, the time, location, SEL, $L_{A_{max}}$, L_A over time, event duration, mp3 and to which flight the event is coupled is stored. A note has to be made for a few of these parameters. The L_A is only stored per average second ($L_{Aeq,1sec}$) and can differ in smoothness. Filippone and Hardwood noted that atmospheric turbulence can influence these measured noise levels [27]. Further is the mp3, which is stored, compressed with a sampling frequency of 8 kHz. This means that information found from this audio file is not reliable above 3500 Hz [34]. These files can thus not be used for determining the $L_{A_{max}}$ or SEL of the event as it is missing information of the higher frequencies. Per second of the event is also the dBA value per 1/3 octave band frequency visible in graph form up until 16 kHz. Although the human audible spectrum goes up to 20 kHz, aircraft rarely produces the high frequencies from 16-20 kHz. In addition is the atmospheric attenuation high for these frequencies and thus are less likely to reach the NMT. These higher frequencies are thus not of great importance when measuring aircraft noise.

[3] nomos.schiphol.nl

4.3.2. Event coupling

When an event is registered as class 0, the next step is to couple these events to aircraft. The event analysis is done on multiple factors including; the dB level of the event; the duration of the event; the rise and fall time of the event - how quickly the event gets loud and then quiet again; what traffic is in the sky close by to the NMT at the time of the event and the wind speed at the time of the event. Each event is then classified into one of the following classes:

0. - Original unprocessed class assignment when an event is imported
1. - Single local aircraft
2. - Multiple local aircraft
3. - Non-local aircraft
4. - Simultaneous local and non-local aircraft
5. - Community noise
6. - Simultaneous community and local aircraft
7. - Simultaneous community and non-local aircraft
8. - Wind noise
9. - Equipment malfunction

The most common classes are the class 1 event; where a noise event is attributed to a single aircraft flyover; and class 5, where noise from the community is detected. Although classes 6 and 7 exist, the identification program is not advanced enough to be able to recognise background noise through an aircraft noise event and are seldom used. A noise event is coupled to an aircraft if the track point was observed between 10 seconds before or after the peak of the noise event and the distance between the track point and the NMT is less than 2500m (8202ft). In the case that multiple aircraft are present within this distance and timeframe, the event is classified as class 2. Each event and operation is then coupled with a correlation ID. In the case of a class 2 event, the correlation ID is given to the closest aircraft operation.

4.3.3. Heathrow - ANOMS

A very similar system to NOMOS is the (similarly named) ANOMS system in place around London Heathrow airport. This consists of 50 alternating fixed and mobile NMTs. The advantage of having mobile NMTs is the flexibility in research applications. ANOMS is, same as NOMOS, a set of unattended continuous NMTs and equipped with class 1 microphones. Other than NOMOS, ANOMS is not only used for informing the public. Many studies, which make use of ANOMS for noise measurements, are performed around Heathrow. The UK's CAA is one of its bigger contributors to the research, mainly about validating and calibrating the models. In the next chapter, model validation and calibration will be discussed.

5

Model validation

The comparison of measured and modelled sound is not as straightforward as one might think. All parts of the modelling and measurement process need to be assessed and validated individually. In this chapter, the literature related to model and measurement verification and validation is discussed in section 5.1 and section 5.2, respectively. Further, the comparison and calibration of noise models will be discussed in section 5.3.

5.1. Model verification

To validate the model, all parts of the model need to be verified after which it can be compared to the measurements. The first verification necessary is the modelling technique and used implementation. As discussed before in chapter 3, the empirical best-practice models have increased uncertainty in prediction with respect to semi-empirical and non-empirical models. The advantage of the faster computation time makes these models useful for large airports. This modelling technique is well used in the industry and has proven to be successful. The implementation of the guidelines of best-practice modelling can be verified with certain test cases described in part 3 of Doc.29 [24]. Other methods are to use the already verified programs developed such as the AEDT.

The second verification is about the input parameters; aircraft performance data and the NPD values. According to Rhodes and Ollerhead [56] FDR (or ACMS) data is the "gold standard" when it comes to the validation process of aircraft performance data. The aircraft trajectory and thrust settings from historic flights can be used as input for the model and the noise measurements corresponding to these flights can be compared. Filippone [11], on the other hand, shows inaccuracies in FDR GPS position data up to two wingspans. As RADAR data and ADS-B also have their advantages and disadvantages, care should be taken in the verification of the flight tracks. Veerbeek and Bergmans [57] showed a verification of the flight tracks which are used around Heathrow airport. Using these tracks provided the best accuracy for noise modelling.

The method to calculate thrust also needs to be verified and the results validated. FDR data contains two key parameters that help validate the thrust results, the N1% and the fuel flow to each engine. With fuel consumption parameters from BADA, the used thrust from a flight can be calculated. The N1 thrust estimation technique can thus be easily validated. For the aircraft performance thrust estimation techniques, also the flap settings, flight angles and speeds are necessary to be validated. The angles can be calculated from track data or taken from ADS-B. The flap settings, however, need to be found from the FDR to be fully validated.

The last invalidated part of the noise model is the NPD data. The EU Directive 2015/996 states that the default settings of the noise models might be generating inaccurate results [58]. Researchers in the field suggest that the current NPD tables are too limited due to the strict test conditions of the ICAO noise certification process [59]. Only a small number of configurations is tested and only close to the airport. In reality, the flight envelope is much larger. These NPD tables only take two inputs, distance and thrust. The noise from the aircraft configuration such as the flap setting and landing gear is measured, but not available as input for the model. The NPD tables are interpolated and extrapolated from these select measurements. These assumptions can cause significant deviations with measurements [45]. If all other parts of the modelling and measurement process are validated, these NPD values can be assessed. This is further discussed in sec-

tion 5.3.

5.2. Measurement verification

Aircraft noise measurements have uncertainties that can be attributed to multiple factors. In the study of Filippone and Hardwood [27], measurements from the same operation and aircraft measured a 3dBA spread in $L_{A_{max}}$. To be able to verify noise measurements, these uncertainties need to be known and minimised. The first is the uncertainty of the instrumentation (microphones) itself. For a class 1 microphone, this uncertainty is already 0.7-0.9 dB [42]. With recurring calibration which follow the IEC 60942 norm [60], these effects can be minimised to 0.4 dB [61].

The second uncertainty that happens in measurements is the wrong identification of aircraft. Asensio et al [47] performed a study to determine the uncertainty that comes with aircraft identification and classification. This is done by measuring the exposure levels of all events at a NMT and classifying them as correctly identified aircraft sound events (true positive $L_{AE,tp}$) or wrongly identified sound events. For multiple time intervals, these test are performed and the ratio of correct identification is stored. With a Monte Carlo method the average identification uncertainty in dBA can be calculated from these ratios and exposure levels. For areas close to the airport, aircraft noise is dominant and the standard identification uncertainty u_{ident} is found to be less than 0.5 dBA. For areas far and not directly beneath the flight path, u_{ident} could lead up to 5.5 dBA. This could be reduced by 3 dBA when identification with RADAR tracking is used. The uncertainty can be even further reduced when promising methods described in section 4.2.2 are used.

The next set of uncertainties can be attributed to the fact that the measurements take place outside in an uncontrolled environment. The inherent imprecision of acoustic field measurements comes from weather effects such as atmospheric turbulence or wind. Often a standard deviation of 3 dB is taken to counter these effects [62][43]. Luckily in the last decade, the weather and sound propagation models improved. Together with the strict weather requirements discussed in section 4.2.1, an uncertainty of $\pm$0.5 dB is taken [44]. These standards also minimised the unwanted effects of ground reflection, which could disturb the measurements.

The last uncertainty in measurements is the influence of background noise during the measurement. If a threshold of 15 dB above background noise is taken, these effects are minimised, but not gone. Measurements can be filtered with the help of their audio files to recognise unwanted background noise as mentioned in section 4.2.3. This is however a time-consuming task and not further implemented by large companies such as NOMOS.

Summing up all the above discussed uncertainties makes continuous noise measurement verification a hard task. Rhodes [63] provides guidance for using measurements in noise model validation. It is recommended that at least two years of noise measurements are obtained for some measurement locations, so the average measured SELs may be compared for each year in order to demonstrate that the measured levels appear consistent and robust.

5.3. Calibration of NPD-values

The use and accuracy of NPD values is a widely discussed topic. According to Filippone, NPD has a "lack in scientific basis on their own" [11]. As mentioned before, the way NPD values are retrieved, have some remissness. In many studies where the model results are compared to measured values and systematic errors occur, the NPD values are mentioned as a source for error. Giladi and Menachi [18] showed a difference from the AEDT model and measurements up to 4-7 dB. Following this result, they suggest a correction of the NPD tables as well as take-off profiles. A way to improve the model outcome with respect to the measurements is to calibrate the NPD values.

The studies that validate and calibrate the NPD values is limited. In Sari et al [64] long term noise measurements are used for calibration after which short term measurements were used for validation. The calibrated model results were closer to the measurement, but a deviation of 2-7 dB remained. Trow and Allmark [29] showed a method to use single event differences between the model and the measurements. The thrust and location of the aircraft with respect to the measurement station was modelled and matched to a NPD value. The average difference from multiple flights is taken and the corresponding value in the NPD table is adjusted. These corrections are then inter- or extrapolated over the entire table. The disadvantage of this approach is that it is strongly affected by outliers [32]. Although differences still remained, the calibrated model results when using this approach was more accurate than when long term noise measurements were used [64]. When using these newfound NPD values for contour calculations, a narrower, elongated SEL footprint was found [29]. This calibration method is repeated for Schiphol airport using NOMOS measurements and

also proven to be effective [32].

The UK's ANCON model is one of the larger best-practice models that is being calibrated with measurements from the ANOMS measurement system. With these measurements, the database, which contains the NPD curves for the used aircraft in the UK, is checked and updated annually.[1] This method of calibration is proven to be effective in decreasing differences between model and measurement results on a large scale [45].

[1] https://www.caa.co.uk/Consumers/Environment/Noise/Features-of-the-ANCON-noise-modelling-process/

6

Conclusion

In the past decades, the research into noise modelling and measurement increased into a large research field. Especially with the large growth of commercial flights, the need for aircraft noise models and measurement surfaced. Even though the knowledge of physics behind noise sources and propagation is growing, there are still gaps and uncertainties in the models used. The more advanced non- and semi-empirical models are often traded off for fast predictive modelling of a large number of aircraft movements. The current challenges lie in the trade-off between fast predictive modelling and the accuracy with reality. In this literature study, the (dis-)advantages of different types of noise models and how they are applied around the world, is researched. Methods to improve best-practice (empirical) noise models and how to validate them with the use of measurements is also discussed. The uncertainty and applicability of noise measurements in noise modelling is a different field of study, thus also researched. In many cases, differences between model results and measurements remained after their respective study. Although the step to improve best-practice modelling by calibration with measurements has proven to be a step in the right direction, more question marks remain. In this research, a continuation of this work will be set out to fill the remaining research gap. The research gap can be distinguished on three levels: modelling accuracy, measurement analysis and calibration methods. As only landing procedures around Schiphol are currently analysed for comparison and calibration [32], this research will be focused on take-off procedures.

To improve the modelling accuracy, the literature presented in this study proved that the thrust estimation of the aircraft to be the most challenging part and easily susceptible to errors. For departing aircraft, the thrust estimation is even more crucial, thus the method described in Merino-Martinez [34] and applied by Hooijmeijer [35] will be used to estimate the N1 parameter. These methods showed improvement in the noise modelling, but validation was not yet performed. Together with the application of this method for this research, validation and verification of previous studies will have to be performed using FDR data.

The research gap left in the measurement analysis is the correct use of flyover measurements from NOMOS. A false coupling of aircraft to a measurement proved to be a large problem when comparing and calibrating the model. Even when an aircraft is correctly coupled, the measurement could be easily contaminated with background noise, resulting in different measured noise levels. To minimise faulty measurement, audio files should be analysed for the presence of typical aircraft frequencies as demonstrated by Dekoninck [50] and [51]. This way only measurements where aircraft frequencies are present and dominant will be used.

The final piece of the research gap that will be filled in this research is the method of calibration of the noise model. Current NPD calibration studies are limited to averaging the difference of measurements and the model outcomes and inter- and extrapolating this value over the entire table [32][29]. Testing the effect of different types of calibration methods will give new insight into how calibrated NPD tables are formed and what their influence is on the model outcomes. A rigid method is to be developed to create a validated approach on how to update your model.

With the work that will be done in this research, the stated research gap can be filled, alongside a contribution to the body of knowledge in the form of a validated method and model to analyse and predict aircraft noise more accurately. The effect of calibrated models will be further analysed by modelling the departure

procedures in place at Schiphol for the "old" and new input parameters. A model based on measurements will give a more accurate and dynamic tool, updated to the current situation.

III

Supporting material

1

Extensive analysis of methods and results

In this chapter, a more extensive analysis of the used methods and results are given. This chapter is seen as complementary to the paper given in Part I.

1.1. Thrust estimation

In this section, the method of finding the thrust of the aircraft during a flyover is further elaborated on. First, the influence positional data has on the thrust estimation is described in section 1.1.1. After that in section 1.1.2 the method of fitting the raw frequency data to a model input is given. Both these methods are applied in the research described in Part I.

1.1.1. Influence of positional data

Effect of position accuracy is extremely important for distance input to the model, but also for the dedopplerisation of the fan tone found from the acoustic measurement. Discrepancies in the RADAR data can be up to 75 meters, which affects the estimated N1%. During this research, ASTRA data, or ground RADAR, is used as an alternative input to the model. This is based on a sensor at Schiphol airport which reports positional data every second up to 6,000 ft (1,828 m). A 1 second update time compared to the 4 second update time from RADAR data is considered beneficial. In Figure 1.1 the positional data of a departing aircraft from runway 18L is plotted for RADAR and ASTRA data. For the distances further away from the Noise Monitoring Tower (NMT), large discrepancies between the two data sets are found. For this research, mainly the distances close to the NMT are of importance. In Figure 1.1c the graph is zoomed in on this specific distance. A deviation of about 100 meters is found between the RADAR and the ASTRA data.

The effect that this different data set has on the dedopplerisation of the frequencies is found in Figure 1.2. Although the found frequencies from the spectrum are the same, different outcomes are found for the N1% input. The one-second update frequency of ASTRA data seems to have an adverse effect in comparison to the much smoother RADAR data set. When comparing the results to the Aircraft Condition and Monitoring System (ACMS) data, the root mean square error (RSME) of RADAR data is less than for the ASTRA data. This effect was visible for most of the analysed flights. For now, the RADAR data is used for this research, but follow-up research using, for example, ADS-B data is advised.

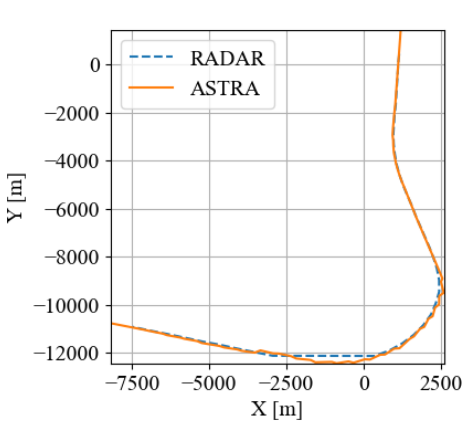

(a) Comparison between RADAR and ASTRA positional XY data.

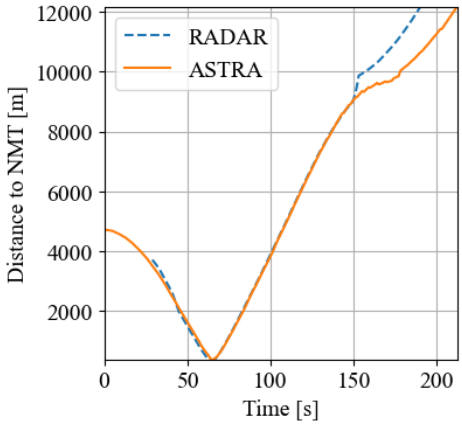

(b) Comparison between RADAR and ASTRA data for distance to a NMT.

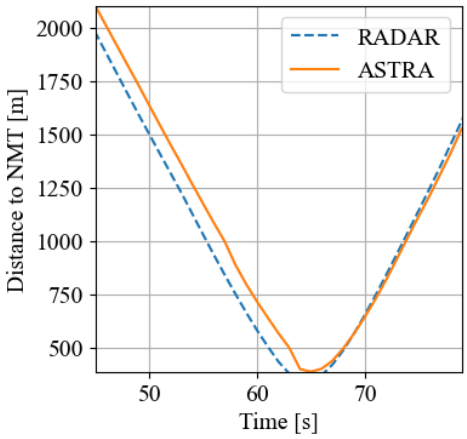

(c) Comparison between RADAR and ASTRA data for distance to a NMT.

Figure 1.1: Comparison between RADAR and ASTRA position data.

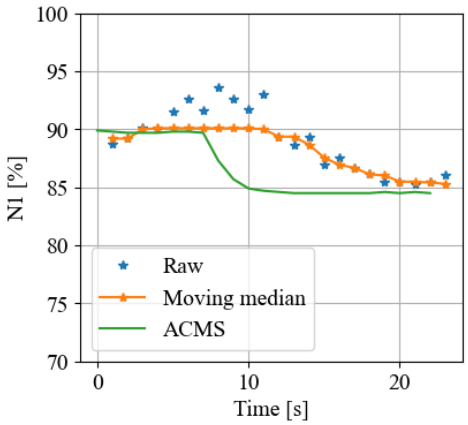

(a) Found N1% data points when using RADAR data (RMSE = 2.51%).

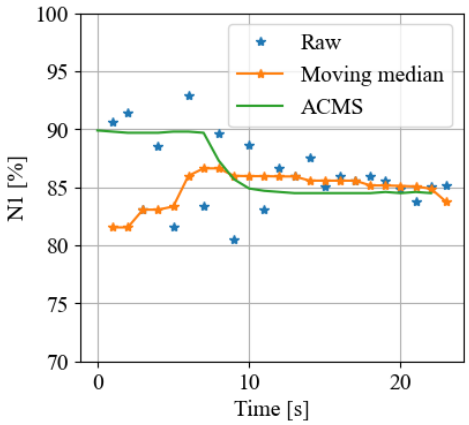

(b) Found N1% data points when using ASTRA data (RMSE = 3.69%).

Figure 1.2: Found N1% data points when using different positional data.

1.1.2. Fitting of found N1% datapoints

During the $N1\%$ estimation method, the frequencies for the fan tone are found for each second of the flyover measurement. These frequencies are dedopplerised and converted to their respective $N1\%$. These points are often not a smooth line due to unevenness of the measurement or RADAR data, causing sudden peaks or

drops in estimated thrust. This is of course not desirable as this would influence the noise level significantly. To get a smooth line from these raw dedopplerised data points, multiple methods of fitting are applied. Three types of fitting are applied to the data sets and are compared to the ACMS data. The first method is taking the average of the found points and fitting a linear regression on it. Unfortunately, from ACMS data is found that a thrust cutback or thrust increase is happening often during the departure phase as seen in Figure 1.3a, making this fit not as perfect as can be.

A second option was to fit a n-order polynomial through the data points. The order of the polynomial with the best fit was based on the reduced chi-squared statistics χ^2_ν.

$$\chi^2_\nu = \frac{\chi^2}{\nu} \tag{1.1}$$

In this formula χ^2 is the sum of differences between the measurements and the fit divided by the variance σ_i^2. The degree of freedom, ν is calculated by the number of observations n minus the number of fitted parameters m.

To find the best fit, a value of χ^2_ν around 1 is preferred as this means the fit matches the error variance found between the measurement points and the fit. A $\chi^2_\nu > 1$ indicates that the data is under fitted and the polynomial fit does not capture the data fully. A $\chi^2_\nu < 1$ means the data is over-fitted and the polynomial fit is probably fitting outliers in the data. Although this method often captured the shape of a thrust cutback, in more cases, it overshoots the actual curve, causing peaks in the thrust estimation. In Figure 1.3b a polynomial fit over the N1% points is shown. The RMSE for this specific example is only 1.57%. This is an improvement to just taking the average of all data points.

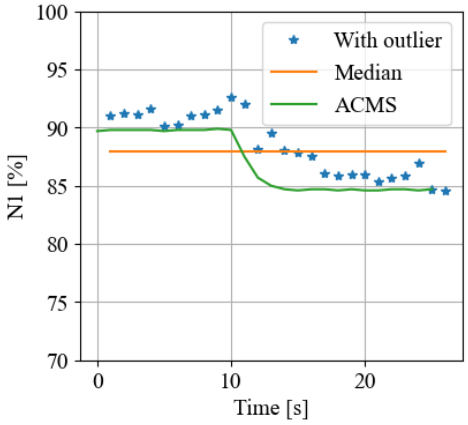

(a) Median fit of raw $N1\%$ data points. (RMSE=2.64)

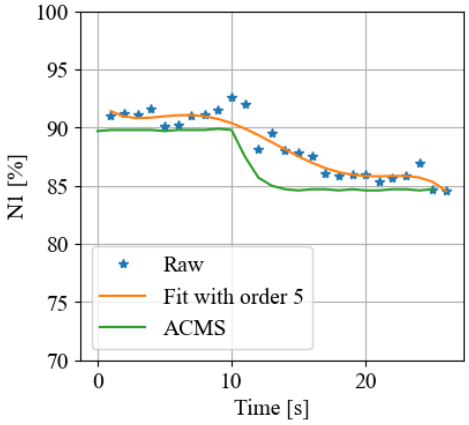

(b) Fit of 4th order polynomial through raw $N1\%$ data points.(RMSE=1.57)

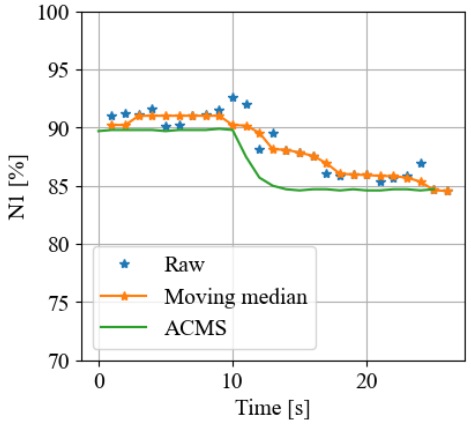

(c) Fit of raw $N1\%$ data points using Hampel filter. (RMSE=1.57)

Figure 1.3: Fitting methods for found $N1\%$ data points for B737-800 flyover.

Finally, a moving median filter was tried based on the Hampel filter. In this filter, a sliding window of size 9 is used to calculate the median absolute deviation (MAD) of each point considering the window. The MAD

is then multiplied by a Gaussian scale factor k and compared to the measurement. If the measurement differs more than three times the standard deviation, the measurement is considered an outlier and is replaced with the window median. For the example given in Figure 1.3c, the RMSE is 1.57, the same as for the polynomial fit. The moving median filter was found to perform best in the irregular data sets that these measurements give. So for the research, this method will be further applied.

1.2. Extensive analysis of the model results

Next to the evaluation of the NPD values and the errors in the thrust setting, a sensitivity analysis of other factors is applied. In Figure 1.4 the differences in $L_{A,max}$ between model results and NOMOS measurements are visualised for different periods during the day (Figure 1.4a) and for the different times in the year (Figure 1.4b). Although the median error is small, an effect of seasonality is visible. This could indicate an error with respect to the weather attenuation correction. Currently, the weather attenuation is calculated with respect to ground hourly weather data from the KNMI station. More in-depth knowledge of the weather at different altitudes could give a more correct attenuation correction. For now, these differences are not significant if year-round data is used for the evaluation of the model.

Another factor of influence on the noise characteristics can be the efficiency of the aircraft engines in colder weather. This can cause a difference in the $N1\%$ to thrust conversion and thus a difference in model input values. Specific engine characteristics need to be known to evaluate the effect on noise further.

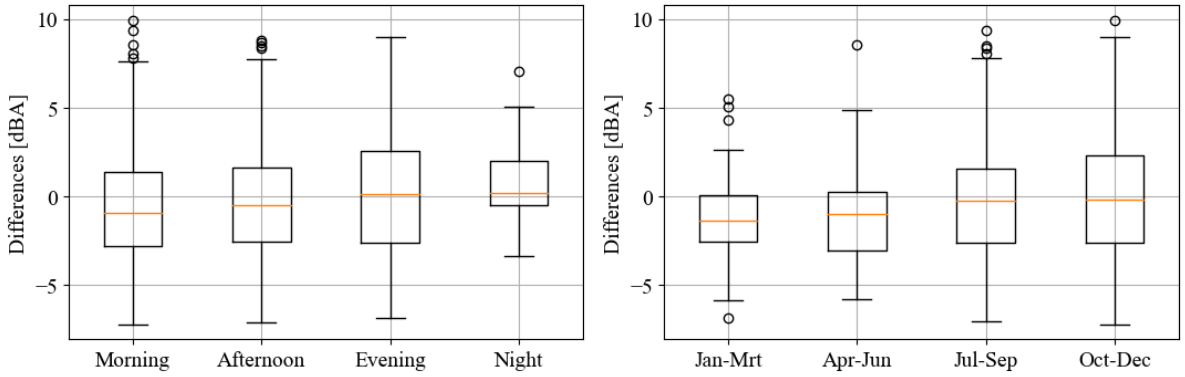

(a) Differences found for periods of the day.

(b) Differences found for different seasons

Figure 1.4: Boxplots of differences found between model results and measurements for $L_{A,max}$.

The next factor that is analysed is the location of the NMTs. In Figure 1.5 the differences between model results and measurements are visible for the different NMTs used in this research. Although deviations are visible between the different NMTs, a relation with respect to area, type of ground or part of the flight route is not seen.

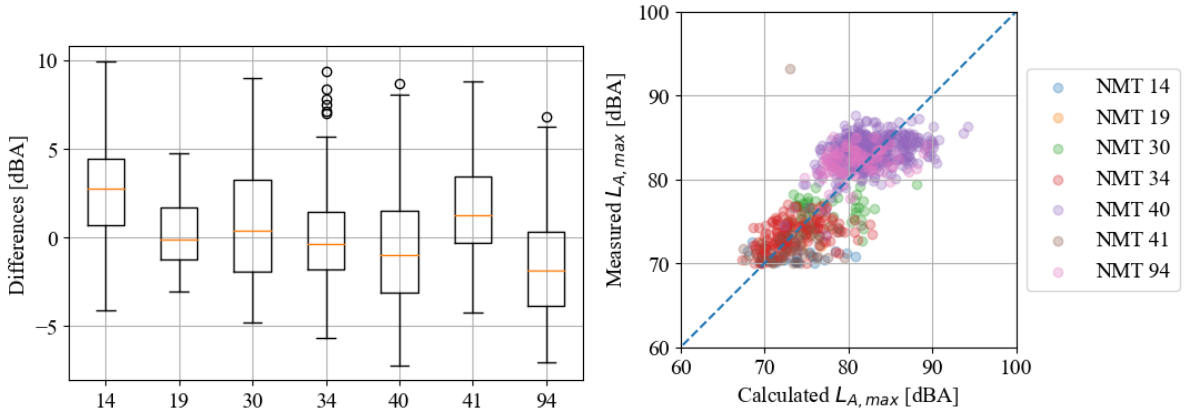

(a) Boxplot of differences between model results and measurements for the different NMTs.

(b) Scatter plot of model results and measurements sorted by NMT location.

Figure 1.5: Analysis of measurement location for the B737-800 data set for $L_{A,max}$.

As mentioned in Part I, the B737-800 aircraft used in this research do not all have the same engine. The different types of the CFM56-7B series have different maximum rated thrust $F_{n,max}$, which influences the N1% to thrust conversion. In Figure 1.6 the differences between model results and measurements for different engine types is plotted. A clear positive trend is visible in this plot. For the engine types with a higher $F_{n,max}$, the model estimated higher $L_{A,max}$ values than measured. While for the less powerful engines (CFM56-7B24 series), an underestimation of noise is modelled.

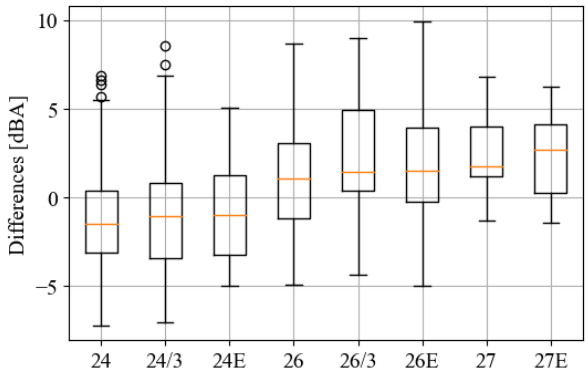

Figure 1.6: Boxplot of differences between model results and measurements for $L_{A,max}$ for different engine types CFM56-7B series.

When analysing the results for one specific engine type, the CFM56-7B24 for which 365 measurements are available, a slightly stronger thrust-noise relation is found. So when modelling noise, the engine type should thus be considered more carefully as it influences the results.

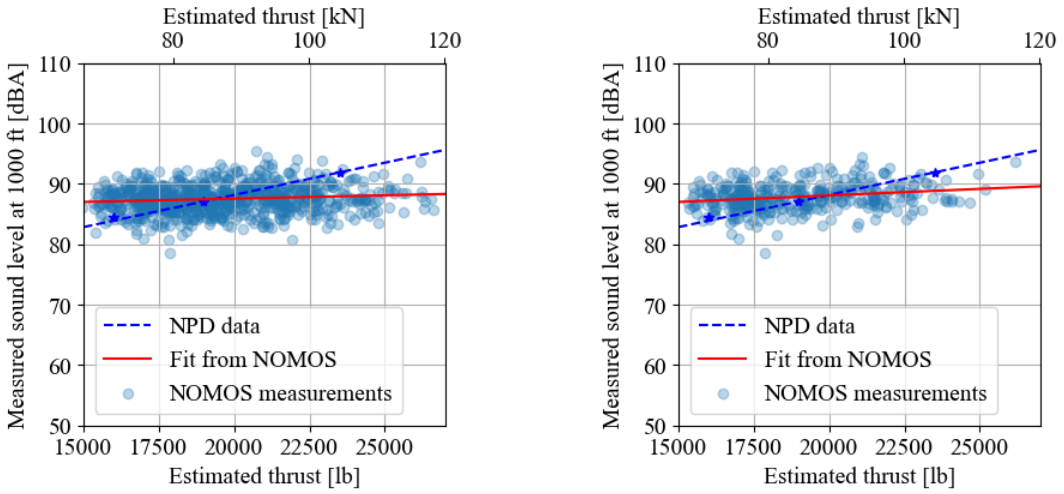

(a) $L_{A_{max}}$ measurements standardised to 1000 ft.

(b) $L_{A_{max}}$ measurements with a CFM56-7B24 engine standardised to 1000 ft.

Figure 1.7: Standardised measurements of B737-800 for reference distance of 1000 ft.

1.3. Standardised measurement

The measurements taken by the NOMOS are evaluated based on the found N1% and distance to the NMT. When the measurements are grouped based on their distance and plotted for found the N1% and sound level, a pattern shown in Figure 1.8 is found. Note that these N1% values and measurements are not corrected for different atmospheres or lateral attenuation, but pure raw measurement data. In these graphs, the slope of the fits are almost horizontal for the smaller distances and grow steeper for measurements with larger distances. A side note to this fit needs to be made. For larger distances, the number of measurements with a high thrust setting is small. This is in line with expectation, as thrust setting is reduced after the take-off phase.

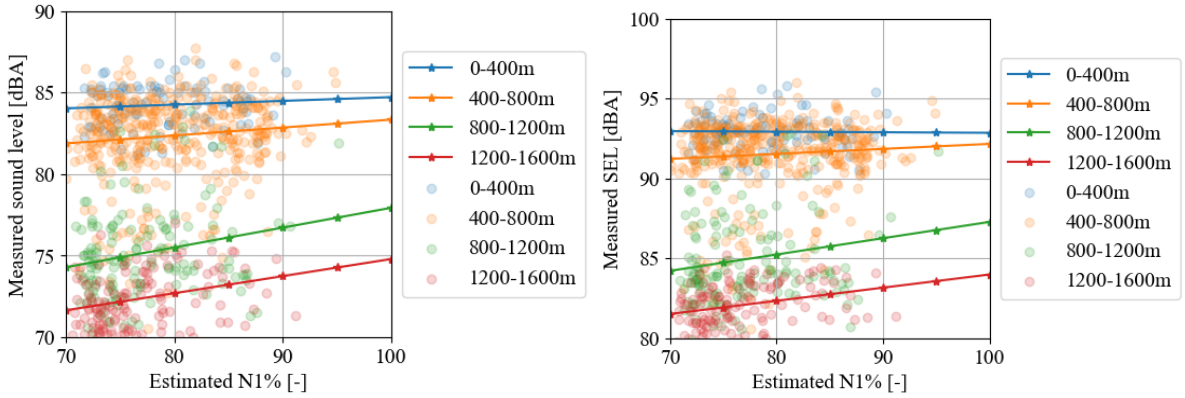

(a) Fit of $L_{A,max}$ to N1% data grouped per distance.

(b) Fit of SEL to N1% data grouped per distance.

Figure 1.8: Analysis of the B737-800 N1% with respect to measured $L_{A,max}$ and SEL grouped per distance.

When plotting the same relations for thrust instead of N1%, the graphs in Figure 1.9 become visible. The slopes are slightly less steep than for the N1%. A reason for this could be the different engine types used in this mix, each with its own maximum rated thrust. As N1 is a percentage of maximum thrust, this has an influence on the graphs. Further are in these thrust values a pressure correction applied to take into account the atmospheric effects. These plots are deemed more representative than the N1% plots.

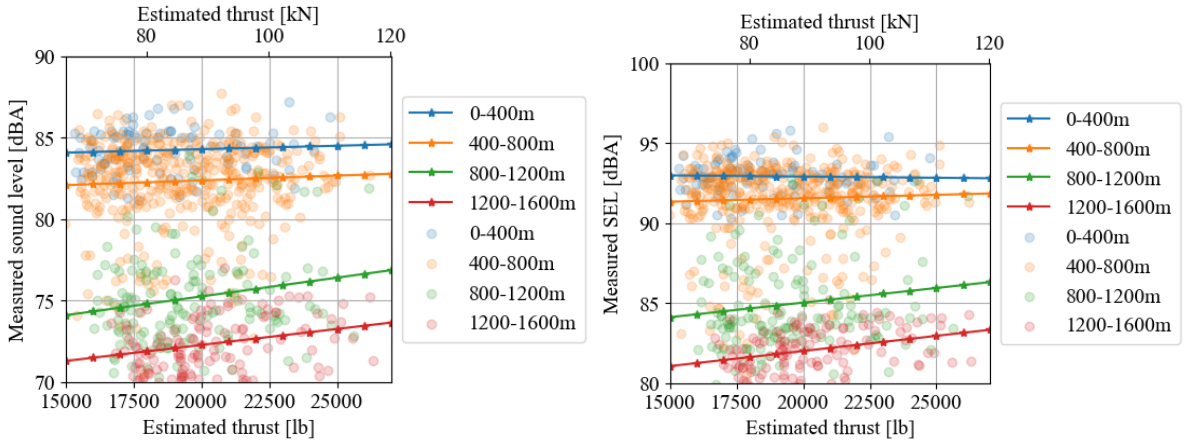

(a) Fit of $L_{A,max}$ to thrust data grouped per distance.

(b) Fit of SEL to thrust data grouped per distance.

Figure 1.9: Analysis of the B737-800 thrust with respect to measured $L_{A,max}$ and SEL grouped per distance.

To remove the effects of weather, distance and correction factor in total, the measurements are standardised to their NPD value. The method of standardising measurements is explained in Part I. This is applied to all measurements for the B737-800 for all distances in the NPD table. In Figure 1.10 and 1.11 these standardised measurements for $L_{A,max}$ and SEL are given, respectively. For $L_{A,max}$ the fit found from these data points is slightly positive but mainly horizontal for all distances.

For the standardised SEL measurements, an even more interesting phenomenon takes place. The slope of the fit changes with respect to the different distances. The slope becomes less steep when the distances become larger. This is contrary to what was expected when looking at Figure 1.9b. The cause of this deviation might be from the assumptions made with respect to the attenuation of noise during the standardisation of the measurements. Full acoustic measurements can result in better standardisation calculations and are advised to be performed to validate the used methods.

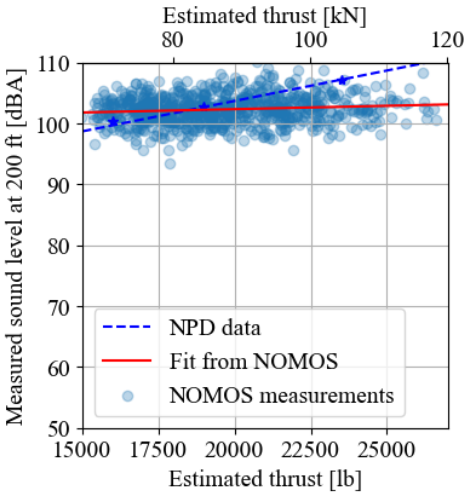

(a) $L_{A_{max}}$ measurements standardised to 200 ft (61m)

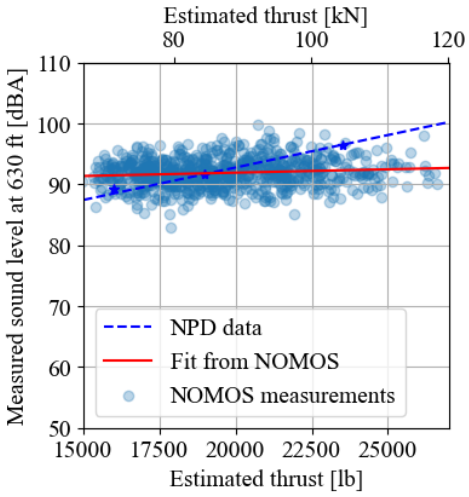

(b) $L_{A_{max}}$ measurements standardised to 630 ft (192m)

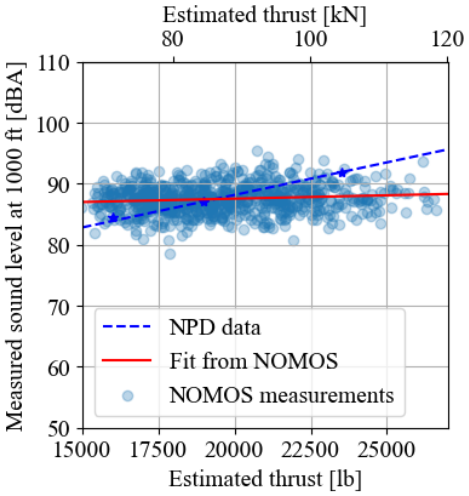

(c) $L_{A_{max}}$ measurements standardised to 1000 ft (305m)

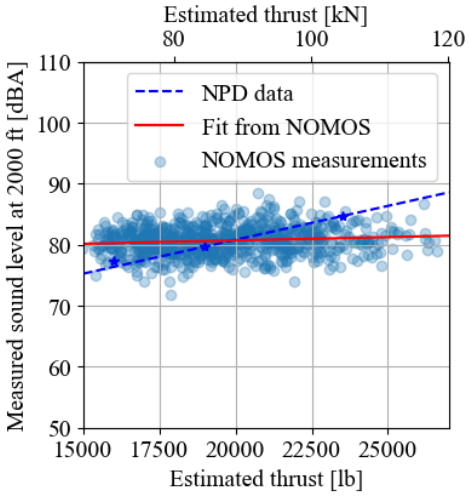

(d) $L_{A_{max}}$ measurements standardised to 2000 ft (610m)

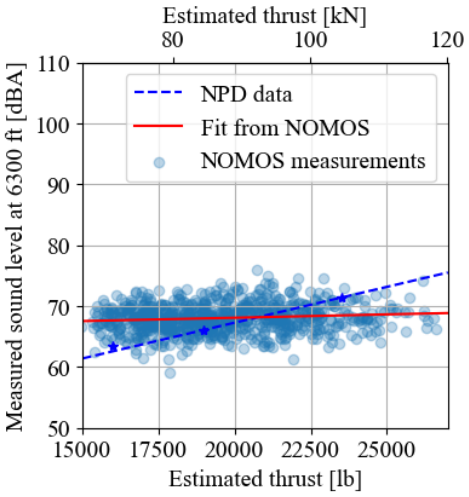

(e) $L_{A_{max}}$ measurements standardised to 6300 ft (1920m)

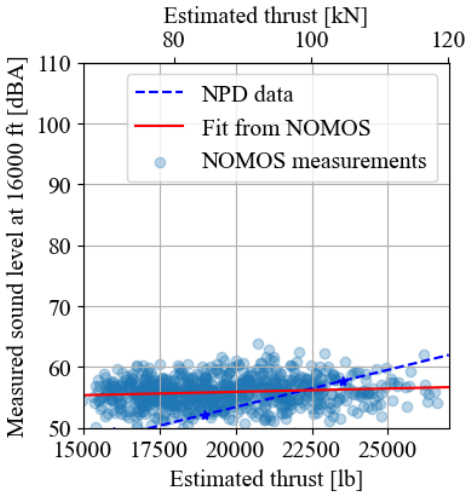

(f) $L_{A_{max}}$ measurements standardised to 16000 ft (4877m)

Figure 1.10: Standardised measurements of $L_{A_{max}}$ for different distances.

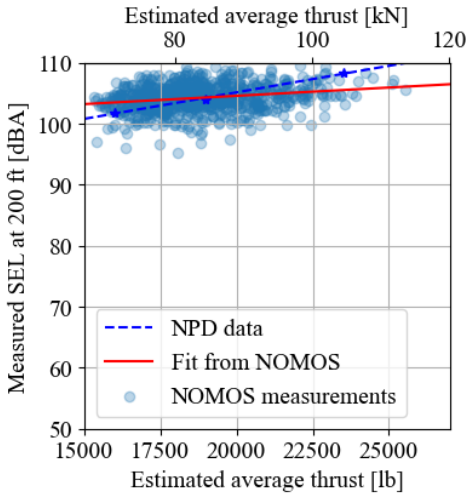

(a) SEL measurements standardised to 200 ft (61m)

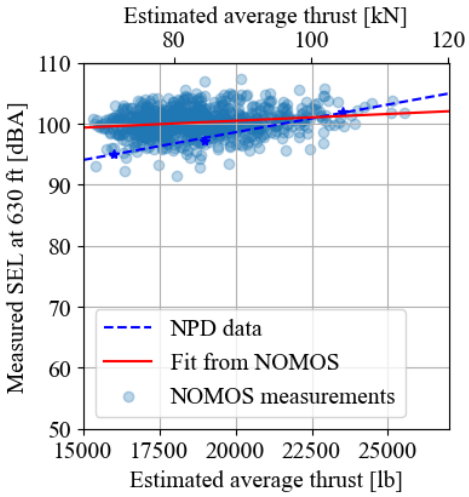

(b) SEL measurements standardised to 630 ft (192m)

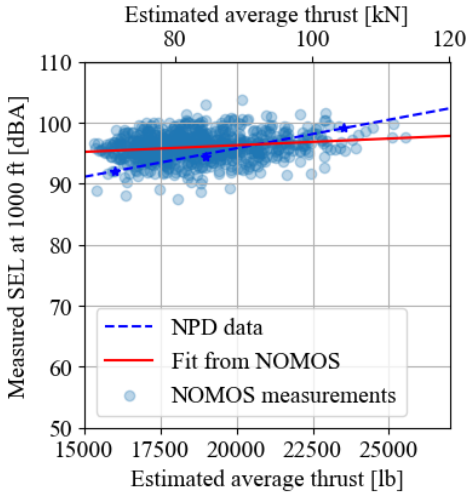

(c) SEL measurements standardised to 1000 ft (305m)

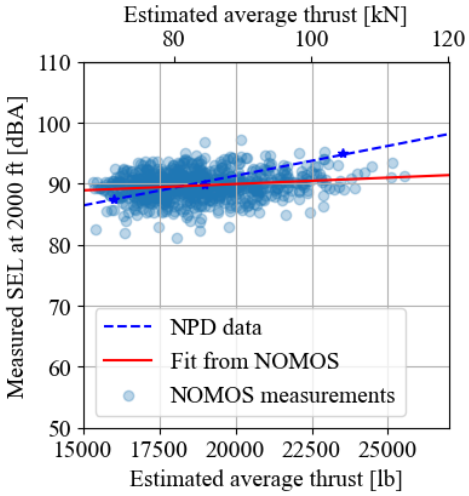

(d) SEL measurements standardised to 2000 ft (610m)

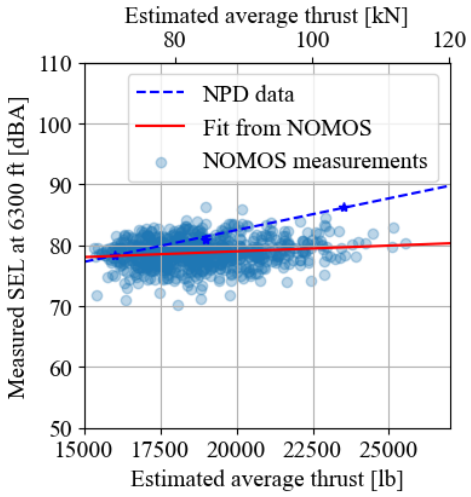

(e) SEL measurements standardised to 6300 ft (1920m)

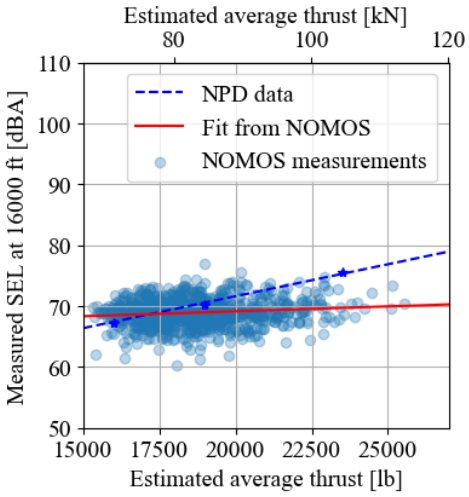

(f) SEL measurements standardised to 16000 ft (4877m)

Figure 1.11: Standardised measurements of SEL for different distances.

2

B737-700

The B737 Next-Generation consists of three aircraft types: -700,-800 and -900. These aircraft are in many ways similar but have different thrust profiles and ranges. The -800 is currently the most used aircraft in the series, but the -700 is also in use at Schiphol airport. As these two aircraft types make use of the same NPD values, an analysis of this aircraft is performed. In section 2.1 the model results are presented and the comparison with measurements is made. Finally, in section 2.2 the calibration of the model and their outcome are discussed.

2.1. Model results

The data set used for the B737-700 consist of 410 noise measurements from take-off procedures. In Figure 2.1 the measurements with their corresponding estimated N1% and distance are plotted in a colour graph. The same relations as seen in the B737-800 are visible where distance has a clear effect on the noise level, while estimated N1% does not. In Table 2.1 the results of the model compared to the measurements are given and these are visualised in Figure 2.2.

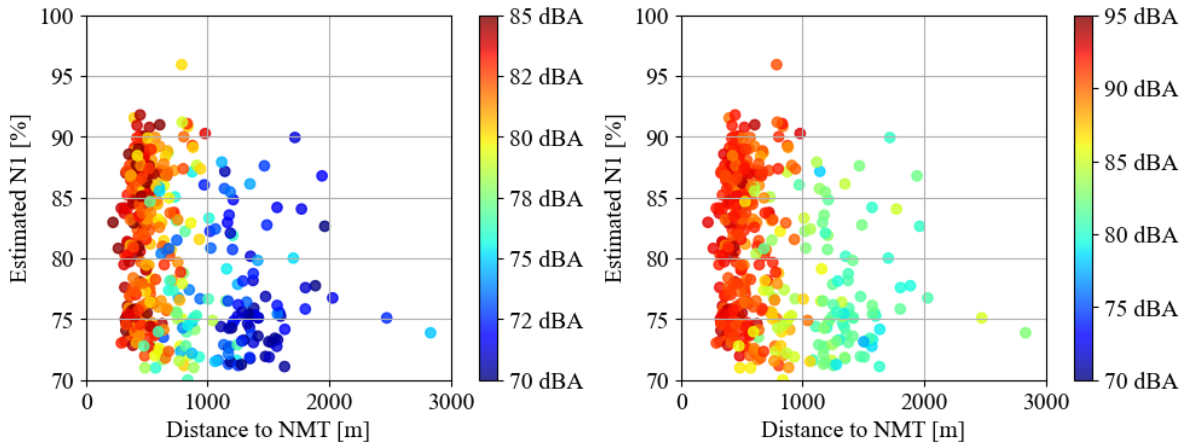

(a) $L_{A_{max}}$ measurements with respect to N1%.

(b) SEL measurements with respect to average N1%.

Figure 2.1: Measurements of B737-700 with respect to distance and N1%.

Table 2.1: Mean and standard deviation of the model results minus the measurements for the B737-700.

	μ [dBA]	σ [dBA]
$L_{A_{max}}$	-0.38	2.92
SEL	-0.11	2.67

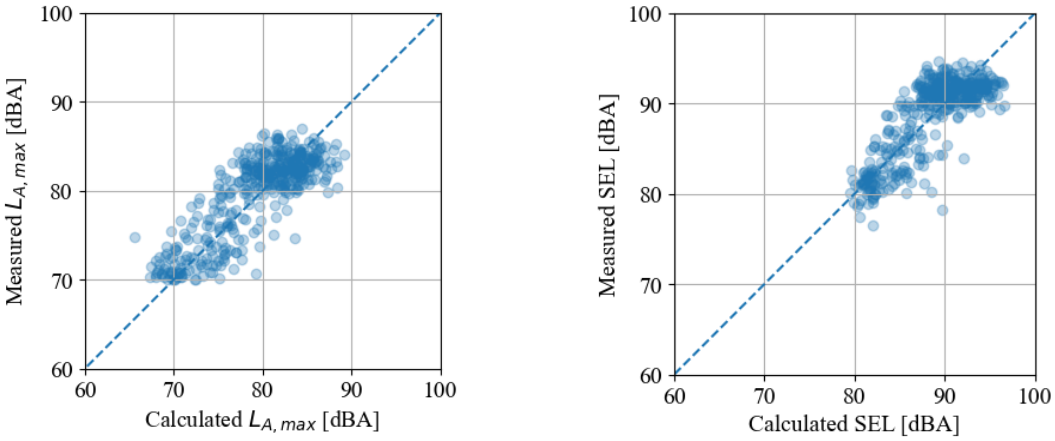

(a) L_{Amax} measurements compared to model results.

(b) SEL measurements compared to model results.

Figure 2.2: Measurements of B737-700 with respect to model results.

When looking at the differences between model results and measurements in Figure 2.3, a correlation is again found for the thrust setting. This is in line with what is found for the B737-800.

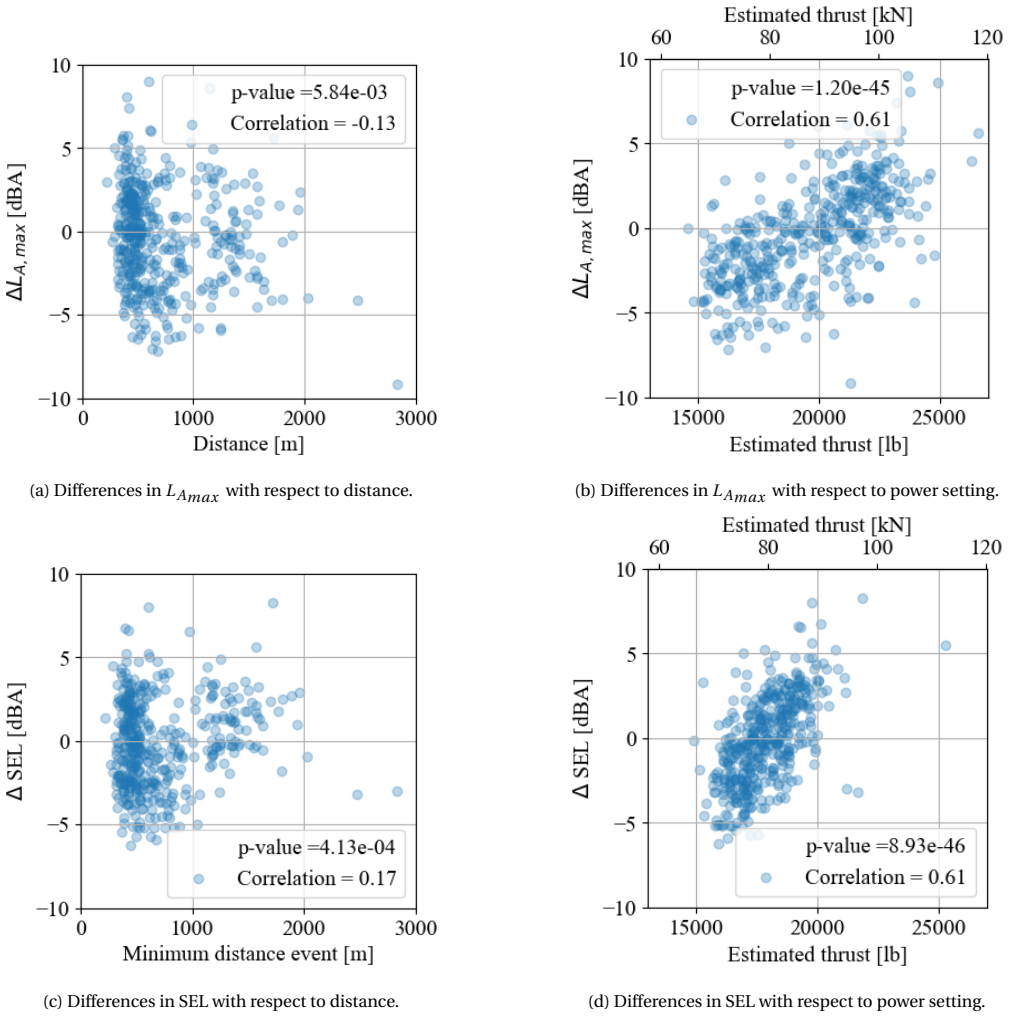

(a) Differences in L_{Amax} with respect to distance.

(b) Differences in L_{Amax} with respect to power setting.

(c) Differences in SEL with respect to distance.

(d) Differences in SEL with respect to power setting.

Figure 2.3: The differences between model results and measurements with respect to different parameters for the B737-700.

When applying the standardisation technique on the measurements for a reference distance of 1000 ft

(305 m), the relations in Figure 2.4 appear. These relations are similar to the relations found in Part I.

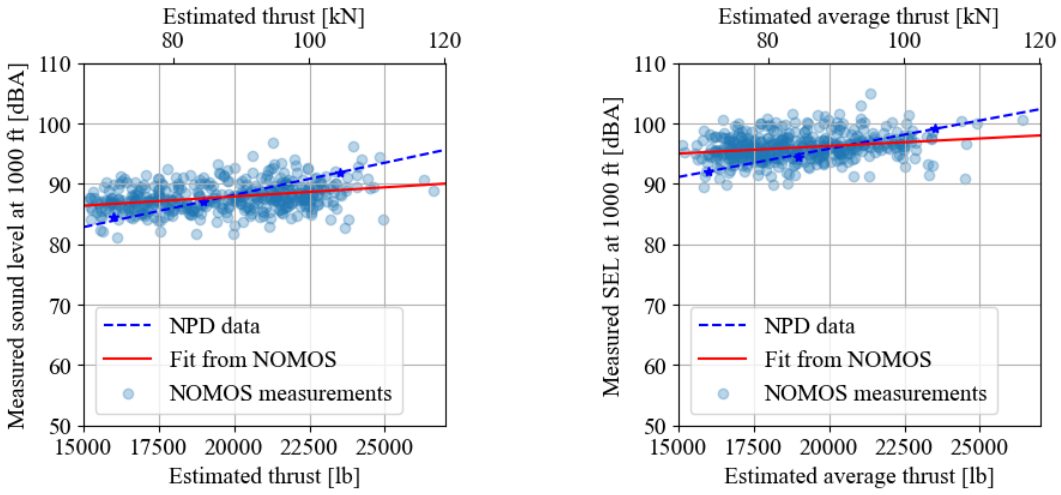

(a) $L_{A_{max}}$ measurements standardised to 1000 ft.

(b) SEL measurements standardised to 1000 ft.

Figure 2.4: Standardised measurements of B737-700 for reference distance of 1000 ft.

2.2. Calibration results

The two methods of calibration are applied to a calibration data set of the B737-700 and resulted in Table 2.2 and Figure 2.5. For the $L_{A,max}$, the first calibration method (based on altering the NPD tables using the differences between model and measurement) performs best concerning offset reduction and reaching a μ of almost 0 dBA. When looking at the standard deviation, the calibration method based on standardised measurements outperforms the first method with a 30% reduction with respect to a 20% reduction in standard deviation. For SEL the results between the two calibration methods are similar. Both reduce the already small offset and reduce the standard deviation by approximately 30%.

As mentioned, the -700 and the -800 make use of the same NPD table. This standard table can be found in Table 2.5. The calibrated table of the B737-700 using standardised measurements can be found in Table 2.3. The differences with the calibrated table for the B737-800 can be found in Table 2.4. The thrust-noise relation for the B737-700 is stronger than for the B737-800, which results in a somewhat steeper line. The differences found between the two aircraft means that using one NPD table is not as accurate as using specific NPD values for each aircraft type. For future modelling, type-specific NPD relations are advised.

Table 2.2: Results for the baseline and calibrated model using the both calibration methods.

	Data set	$L_{A,max}$ **[dBA]**		**SEL [dBA]**	
		μ	σ	μ	σ
Baseline	Calibration	-0.52	2.97	-0.21	2.65
	Validation	-0.06	2.85	0.15	2.69
Calibrated average diff	Calibration	-0.05	2.36	0.10	1.97
	Validation	0.52	2.57	0.26	1.98
Calibrated standardised	Calibration	0.14	2.08	-0.16	1.88
	Validation	0.53	1.90	0.00	1.91

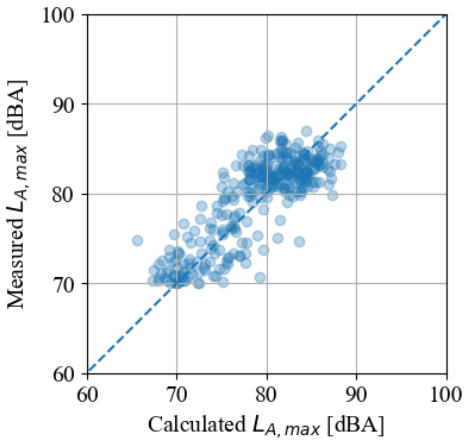

(a) L_{Amax} calibration data set baseline

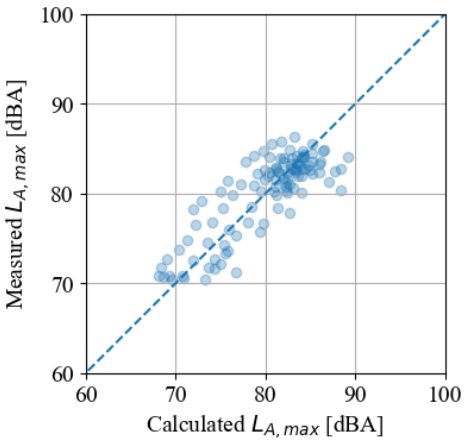

(b) L_{Amax} validation data set baseline.

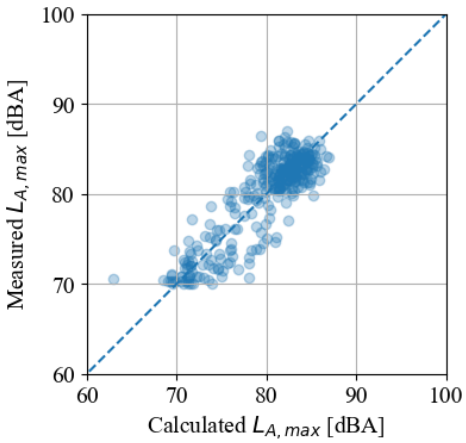

(c) L_{Amax} calibration data set calibrated using average differences.

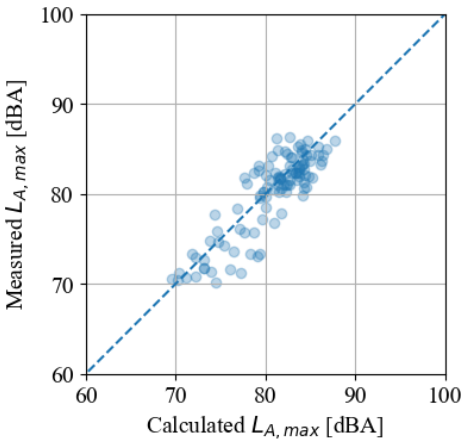

(d) L_{Amax} validation data set calibrated using average differences.

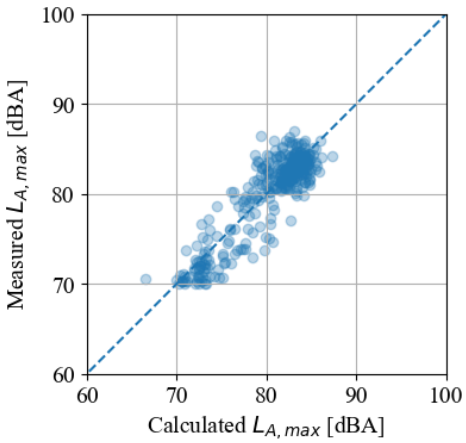

(e) L_{Amax} calibration data set calibrated using standardised measurements.

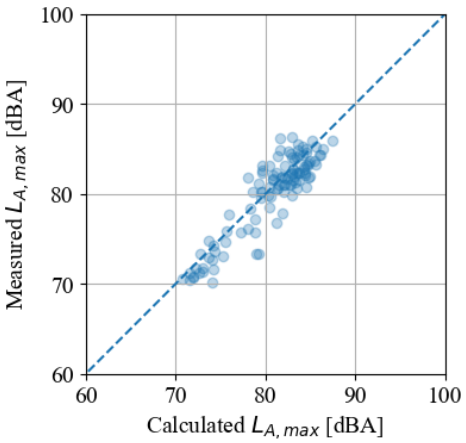

(f) L_{Amax} validation data set calibrated using standardised measurements.

Figure 2.5: Calibration and validation data set of the B737-700 before and after calibration using both calibration methods.

Table 2.3: Calibrated NPD table for the B737-700 using standardised measurements.

Power Setting (lb)	200ft	400ft	630ft	1000ft	2000ft	4000ft	6300ft	10000ft	16000ft	25000ft
10000	99.4	93.2	89	84.6	77.8	70.4	65.2	59.4	53	46.2
13000	100.1	93.9	89.7	85.3	78.5	71.1	65.9	60.1	53.7	46.9
16000	100.8	94.6	90.4	86	79.2	71.8	66.6	60.8	54.4	47.6
19000	101.5	95.3	91.1	86.7	79.9	72.5	67.3	61.5	55.1	48.3
23500	102.5	96.3	92.1	87.8	81	73.6	68.4	62.6	56.1	49.3

Table 2.4: Differences between the calibrated NPD table for the B737-800 and the B737-700.

Power Setting (lb)	200ft	400ft	630ft	1000ft	2000ft	4000ft	6300ft	10000ft	16000ft	25000ft
10000	1.3	1.3	1.3	1.4	1.3	1.3	1.3	1.3	1.3	1.3
13000	0.9	0.8	0.8	0.9	0.8	0.9	0.8	0.9	0.8	0.8
16000	0.4	0.3	0.4	0.4	0.4	0.4	0.4	0.4	0.4	0.4
19000	-0.1	-0.1	-0.1	-0.1	-0.1	-0.1	-0.1	-0.1	-0.1	-0.1
23500	-0.8	-0.8	-0.8	-0.8	-0.9	-0.8	-0.9	-0.8	-0.8	-0.8

Table 2.5: NPD table for B737NG departure procedures.

NPD_ID	Noise Metric	Op Mode	Power Setting (lb)	200ft	400ft	630ft	1000ft	2000ft	4000ft	6300ft	10000ft	16000ft	25000ft
CF567B	LAmax	D	10000	95.2	87.9	83.6	78.8	71.3	63	57.3	50.4	44.2	36.9
CF567B	LAmax	D	13000	98.1	91	86.7	82	74.5	66.3	60.7	53.9	46.9	39.6
CF567B	LAmax	D	16000	100.5	93.7	89.3	84.6	77.3	69.2	63.5	56.8	49.4	42.1
CF567B	LAmax	D	19000	102.7	96	91.7	87.1	79.7	71.7	66.1	59.5	52.2	44.9
CF567B	LAmax	D	23500	107.2	100.9	96.5	91.9	84.7	76.8	71.4	64.6	57.7	50.4
CF567B	SEL	D	10000	96.3	92.1	89.4	86.3	81.4	75.9	72	67	61.3	51.9
CF567B	SEL	D	13000	99.2	95.2	92.4	89.4	84.7	79.3	75.4	70.5	64.5	56.1
CF567B	SEL	D	16000	101.7	97.6	95	92.1	87.4	82.1	78.3	73.5	67.3	60
CF567B	SEL	D	19000	103.9	99.9	97.3	94.5	89.9	84.7	81	76.2	70.3	63.7
CF567B	SEL	D	23500	108.4	104.5	102	99.3	95	89.9	86.4	81.5	75.5	69.5

3

A330-300

The methods described in the paper in Part I are also applied to measurements of take-off operations of the A330-300 aircraft. In section 3.1 the measurements and their corresponding model results are given. In section 3.2 the baseline model is calibrated and the results of both calibration methods are given.

3.1. Model results

The data set used for the A330-300 consist of 167 noise measurements from take-off procedures. In Figure 3.1 the measurements with their corresponding estimated N1% and distance are plotted in a colour graph. The same relations as seen in the B737-800 are visible where distance has a clear effect on the noise level, while estimated N1% does not. In Table 3.1 the results of the model compared to the measurements are given and these are visualised in Figure 3.2.

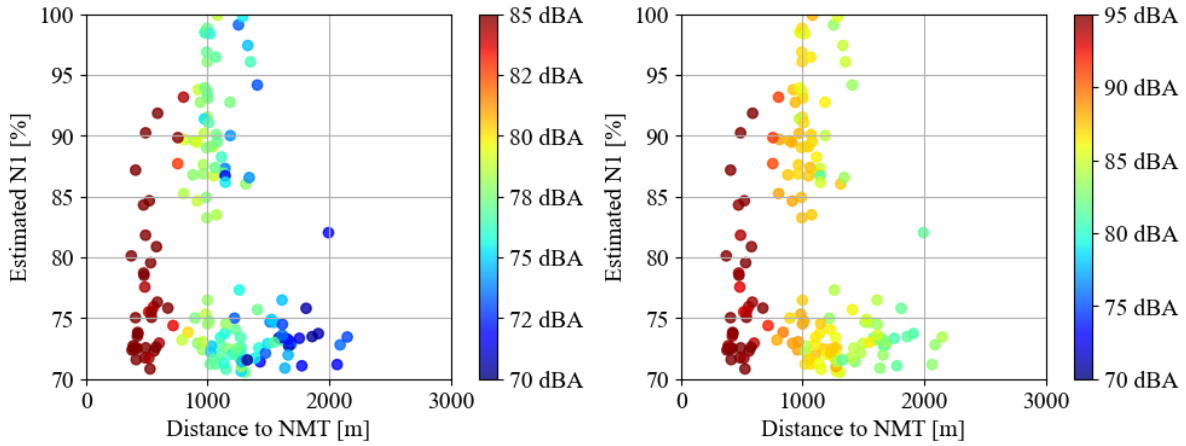

(a) $L_{A_{max}}$ measurements with respect to N1%.

(b) SEL measurements with respect to average N1%.

Figure 3.1: Measurements of A330-300 with respect to distance and N1%.

Table 3.1: Mean and standard deviation of the model results minus the measurements for the A330-300.

	μ [dBA]	σ [dBA]
$L_{A_{max}}$	-5.97	3.66
SEL	3.92	3.17

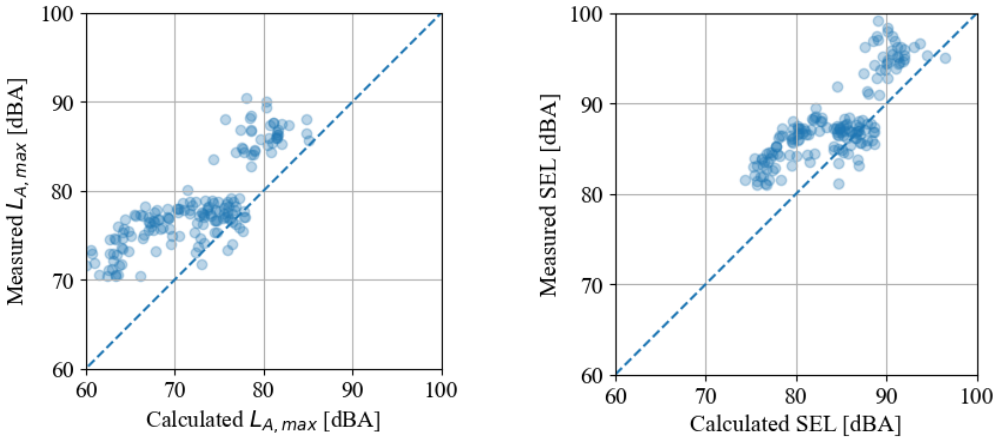

(a) L_{Amax} measurements compared to model results.

(b) SEL measurements compared to model results.

Figure 3.2: Measurements of A330-300 with respect to model results.

A large offset is present for this aircraft where the model underestimates the expected noise levels. When looking at the differences between model results and measurements in Figure 3.3, a correlation is again found for the thrust setting. This is in line with what is found for the B737-800.

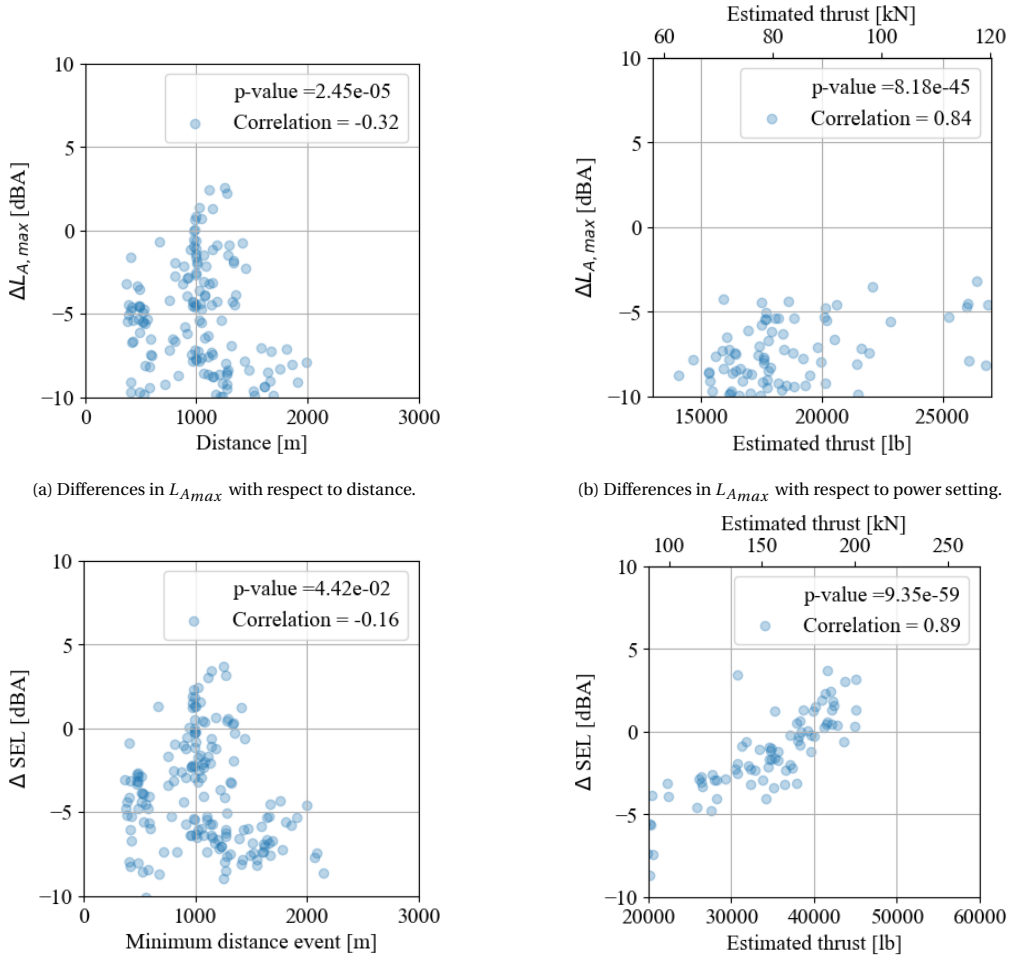

(a) Differences in L_{Amax} with respect to distance.

(b) Differences in L_{Amax} with respect to power setting.

(c) Differences in SEL with respect to distance.

(d) Differences in SEL with respect to power setting.

Figure 3.3: The differences between model results and measurements with respect to different parameters for the A330-300.

When applying the standardisation technique on the measurements for a reference distance of 1000 ft (305 m), the relations in Figure 3.4 appear. These relations are similar to the relations found in Part I.

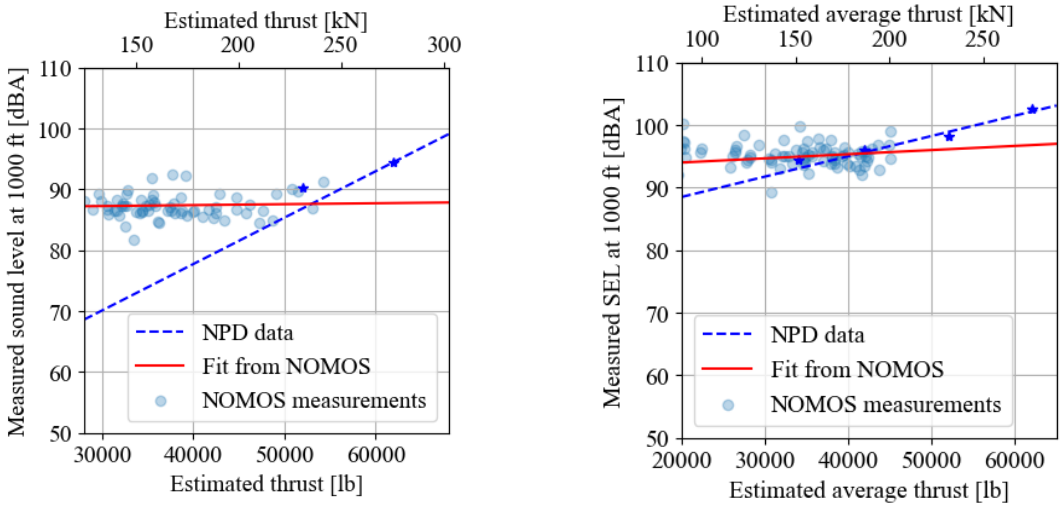

(a) $L_{A_{max}}$ measurements standardised to 1000 ft.

(b) SEL measurements standardised to 1000 ft.

Figure 3.4: Standardised measurements of A330-300 for reference distance of 1000 ft.

3.2. Calibration results

The two methods of calibration are applied to a calibration data set of the A330-300 and resulted in Table 3.2 and Figure 3.5. Both calibration methods reduce the large offset present in the calibration and validation data set, but not to 0 dBA. The calibration method based on the average differences results in better-estimated SEL values after calibration than the other calibration method, but worse on $L_{A,max}$. The cause of this difference could be attributed to the fact that the differences in the baseline model are too large. When altering the NPD table in the first calibration method, table logic must be kept (noise levels must decrease with larger distances and lower thrust setting and vice versa). When extreme outliers are present, causing table logic to fail, the table is not fully altered. This results in an offset present in the calibrated data set. For the second method, based on standardised measurements, this limitation is not present. The calibration for the SEL values for this method, however, is still based on assumptions, which might cause the offset in the calibrated data set.

The standard deviation of differences between the model results and the measurements in the baseline is large. The standard deviation reduces by 30-40% for the first calibration method and 45-55% for the second method. For this aircraft type, the calibration method based on standardised measurement performs best.

Table 3.2: Results for the A330-300 baseline and calibrated model using the both calibration methods.

	Data set	$L_{A,max}$ **[dBA]**		**SEL [dBA]**	
		μ	σ	μ	σ
Baseline	Calibration	-6.24	3.52	-4.14	3.00
	Validation	-5.16	3.92	-3.27	3.53
Calibrated average diff	Calibration	-2.14	2.51	-1.89	2.20
	Validation	-1.07	2.31	-1.16	2.09
Calibrated standardised	Calibration	0.19	1.90	-2.28	1.63
	Validation	0.72	1.81	-1.88	1.58

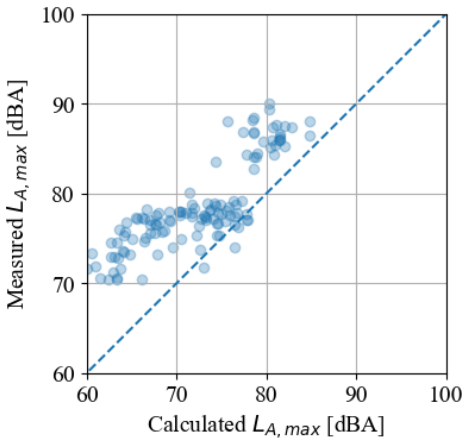

(a) L_{Amax} calibration data set baseline

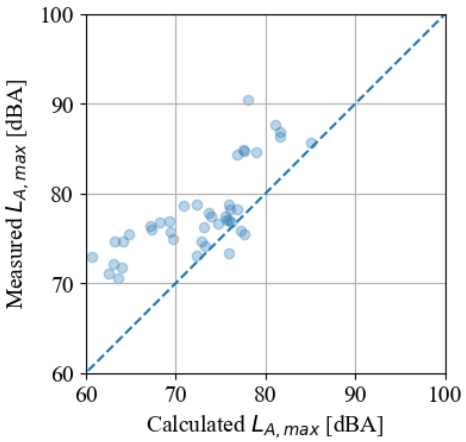

(b) L_{Amax} validation data set baseline.

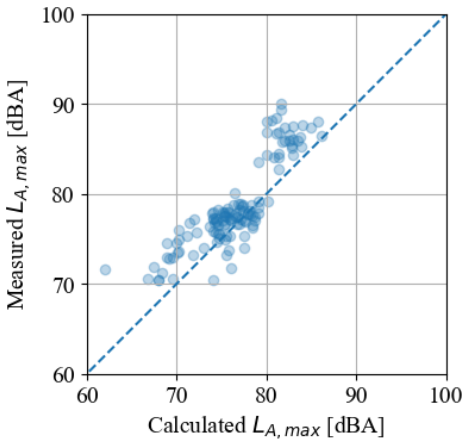

(c) L_{Amax} calibration data set calibrated using average differences.

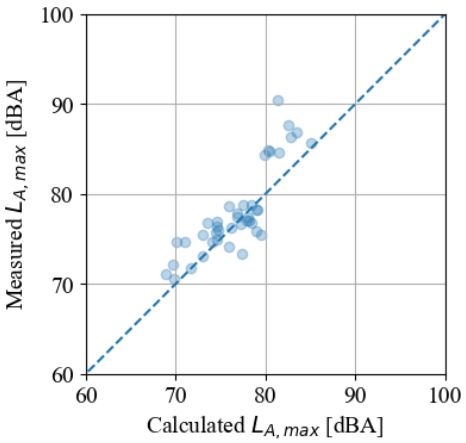

(d) L_{Amax} validation data set calibrated using average differences.

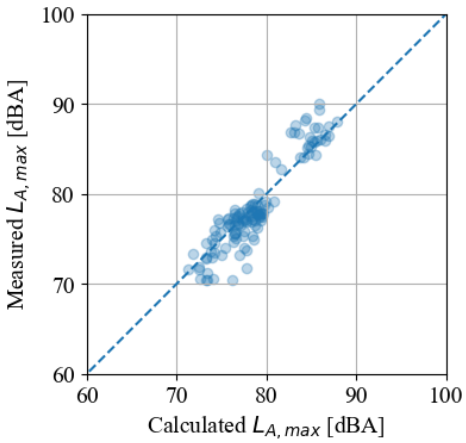

(e) L_{Amax} calibration data set calibrated using standardised measurements.

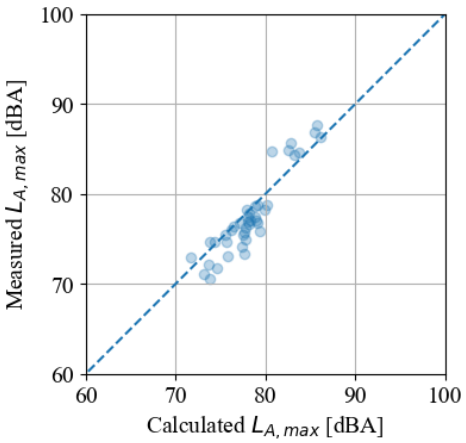

(f) L_{Amax} validation data set calibrated using standardised measurements.

Figure 3.5: Calibration and validation data set of the A330-300 before and after calibration using both calibration methods.

Bibliography

[1] Ian Jopson, Darren Rhodes, and Peter Havelock. *Aircraft noise model validation - How accurate do we need to be?* UK Civil Aviation Authority, Mar. 2003.

[2] European Civil Aviation Conference. *ECAC.CEAC Doc 29 4th Edition Report on Standard Method of Computing Noise Contours around Civil Airports Volume 1: Applications Guide*. Dec. 2016.

[3] Stephen Morrell, Richard Taylor, and David Lyle. "A review of health effects of aircraft noise". In: *Australian and New-Zealand Journal of Public Health* 21 (2 1997), pp. 221–257.

[4] Changwoo Lim et al. "Effect of background noise levels on community annoyance from aircraft noise". In: *The Journal of the Acoustical Society of America* 123 (2008), p. 766. DOI: 10.1121/1.2821985.

[5] D.H.T. Bergmans and H.W. Veerbeek. *Analyses of measurements to enforce and to reduce aircraft noise*. NLR, Dec. 2010, pp. 15–18.

[6] Prof D.G. Simons. *Introduction to Aircraft Noise*. Technical University Delft, 2019.

[7] Erlend Magnus Viggen. "The lattice Boltzmann method: Fundamentals and acoustics". Norwegian University of Science and Technology, Feb. 2014.

[8] ISO 9613. *Acoustics - Attenuation of sound during propagation outdoors - Part 1: Calculation of the absorption of sound by the atmosphere*. 1993.

[9] ISO 20906. *Acoustics - Unattended monitoring of aircraft sound in the vicinity of airports*. Reviewed and confirmed in 2020. 2009.

[10] Oksana Stalnov, Paruchuri Chaitanya, and Phillip F. Joseph. "Towards a non-empirical trailing edge noise prediction model". In: *Journal of Sound and Vibration* 372 (June 2016), pp. 50–68. ISSN: 10958568. DOI: 10.1016/j.jsv.2015.10.011.

[11] Antonio Filippone. "Aircraft noise prediction". In: *Progress in Aerospace Sciences* 68 (July 2014), pp. 27–63. ISSN: 03760421. DOI: 10.1016/j.paerosci.2014.02.001.

[12] Lothar Bertsch et al. "The Parametric Aircraft Noise Analysis Module-status overview and recent applications". In: *17th AIAA/CEAS Aeroacoustics Conference* (June 2011).

[13] S Guérin et al. "Airbus A319 Database from Dedicated Flyover Measurements to Investigate Noise Abatement Procedures". In: *AIAA/CEAS Aeroacoustics Conference* (May 2005). DOI: 10.2514/6.2005-2981.

[14] Michael Pott-Pollenske et al. "Airframe Noise Characteristics from Flyover Measurements and Predictions". In: American Institute of Aeronautics and Astronautics, May 2006. DOI: 10.2514/6.2006-2567.

[15] Society of Automotive Engineers. *SAE-AIR-1845A - Procedure for the Calculation of Airplane Noise in the Vicinity of Airports*. A-21 Aircraft Noise Measurement Aviation Emission Modeling, Aug. 2012. URL: https://doi.org/10.4271/AIR1845A.

[16] Sanford Fidell and Vincent Mestre. *A Guide To U.S. Aircraft Noise Regulatory Policy*. Springer Nature Switzerland, 2020. ISBN: 9783030399078. DOI: 10.1007/978-3-030-39908-5.

[17] ICAO. *Annex 16 - Environmental Protection - Volume 1 - Aircraft Noise*. July 2015.

[18] Ran Giladi and Eliav Menachi. "Validating Aircraft Noise Models". In: *OpenSky Symposium* 59 (Nov. 2020). DOI: 10.3390/proceedings2020059012.

[19] Christoph Struempfel and Josephin Hübner. "Aircraft Noise Modeling of Departure Flight Events based on Radar Tracks and Actual Aircraft Performance Parameters". In: *DAGA 2020 46. Jahrestagung für Akustik* (Mar. 2020). URL: https://www.researchgate.net/publication/340461180.

[20] Stanislaw Pietrzko and Rudolf Bütikofer. "FLULA - Swiss aircraft noise prediction program". In: *Annual Conference of the Australian Acoustical Society* (Nov. 2002), pp. 92–99.

[21] C Zellmann, B Schäffer, and J M Wunderli. "Aircraft Noise Emission Model Accounting for Aircraft Flight Parameters". In: *Journal of Aircraft* 55 (2 Mar. 2018), pp. 682–695. DOI: 10.2514/1.C034275.

[22] H.M.M. van der Wal, P. Vogel, and F.J.M. Wubben. *Voorschrift voor de berekening van de Lden en Lnight geluidbelasting in dB(A) ten gevolge van vliegverkeer van en naar de luchthaven Schiphol. Part 1: Berekeningsvoorschrift*. NLR, July 2001.

[23] European Civil Aviation Conference. *ECAC.CEAC Doc 29 4 th Edition Report on Standard Method of Computing Noise Contours around Civil Airports Volume 2: Technical Guide*. Dec. 2016.

[24] European Civil Aviation Conference. *ECAC.CEAC Doc 29 4th Edition Report on Standard Method of Computing Noise Contours around Civil Airports Volume 3, Part 1-Reference Cases and Verification Framework*. Dec. 2016.

[25] S.J. Heblij, J. Derei, and R.H. Hogenhuis. *Toepassing ECAC Doc29 voor het bepalen van de geluidbelasting van het vliegverkeer van Schiphol*. NLR, Feb. 2019.

[26] R.H. Hogenhuis and S.J. Heblij. *Trendvalidatie van Doc.29 berekeningen*. NLR, Oct. 2018.

[27] Antonio Filippone and Adrian Harwood. "Flyover Noise Measurements and Predictions of Commercial Airplanes". In: *Journal of Aircraft* 53 (2 Mar. 2016). DOI: 10.2514/1.C033370.

[28] Oleksandr Zaporozhets. *Aircraft noise models for assessment of noise around airports*. 2016. URL: https://www.researchgate.net/publication/319159360.

[29] James Trow and Claire Allmark. "The benefits of validating your aircraft noise model". In: *Euronoise* (2018). ISSN: 2226-5147.

[30] D Poles. *EUROCONTROL Base of Aircraft Data (BADA) Aircraft Performance Modelling Report*. EEC Technical/Scientific Report No. 2009-09, Mar. 2009.

[31] R. Alligier, D. Gianazza, and N. Durand. "Learning the aircraft mass and thrust to improve the ground-based trajectory prediction of climbing flights". In: *Transportation Research Part C: Emerging Technologies* 36 (Nov. 2013), pp. 45–60. ISSN: 0968090X. DOI: 10.1016/j.trc.2013.08.006.

[32] Max A. Heilig. "Aircraft Noise: Modelling & Measuring Using aircraft noise measurements for noise model prediction improvement". Delft University of Technology, July 2020.

[33] Ameya Behere et al. "Sensitivity Analysis of Airport Level Environmental Impacts to Aircraft Thrust, Weight, and Departure Procedures". In: *AIAA Scitech Forum* (Jan. 2020). DOI: 10.2514/6.2020-1731.

[34] Roberto Merino-Martínez et al. "Improving Aircraft Noise Predictions Considering Fan Rotational Speed". In: *Journal of Aircraft* 56 (1 Jan. 2018). DOI: 10.2514/1.C034849.

[35] Davey Hooijmeijer. "Dutch Aircraft Noise Model Analysis Classification comparison with measurements". Delft University of Technology, July 2019.

[36] Lothar Bertsch et al. "System Noise Assessment of a Tube-and-Wing Aircraft with Geared Turbofan Engines". In: *Journal of Aircraft* 56 (4 July 2019), pp. 1577–1596. DOI: 10.2514/1.C034935.

[37] Ulf Michel. "Correlation of aircraft certification noise levels EPNL with controlling physical parameters". In: 19th AIAA/CAES Aeroacoustics Conference, May 2013. DOI: 10.2514/6.2013-2014.

[38] Cyril M Harris. "Absorption of Sound in Air versus Humidity and Temperature". In: *The Journal of the Acoustical Society of America* 40 (1966), p. 148. DOI: 10.1121/1.1910031.

[39] M. Arntzen, M. Hordijk, and D.G. Simons. *Including atmospheric propagation effects in aircraft take-off noise modeling*. NLR, July 2015.

[40] Robbert P. F. Koster. "Using NOMOS measurements to assess improvements of ECAC Doc. 29 aircraft noise calculations". Delft University of Technology, Jan. 2020.

[41] Meritxell Genescà et al. "Measurement of aircraft noise in a high background noise environment using a microphone array". In: *Transportation Research Part D: Transport and Environment* 18 (1 Jan. 2013), pp. 70–77. ISSN: 13619209. DOI: 10.1016/j.trd.2012.09.002.

[42] W Soede. *Technische beschrijving vliegtuig geluidmeetsystemen: Luistervink, Nomos, Sensornet*. ARDEA Acoustics and consult, June 2012.

[43] Naoaki Shinohara and Ichiro Yamada. "Reliability of aircraft noise evaluation by measurement for comparison with prediction". In: InterNoise, Nov. 2014.

[44] S White. *Precision of Aircraft Noise Measurements at the London Airports*. ERCD Report 0506, Nov. 2005.

[45] D P Rhodes, S White, and P Havelock. *Validating the CAA aircraft noise model with noise measurements*. Environmental Research and Consultancy Department, CAA, 2002. URL: www.aviation.detr.gov.uk.

[46] Keith Adams. "Aircraft noise event detection - The threshold problem". In: InterNoise, 2004, pp. 686–1373.

[47] C. Asensio, M. Recuero, and M. Ruiz. "Aircraft noise-monitoring according to ISO 20906. Evaluation of uncertainty derived from the classification and identification of aircraft noise events". In: *Applied Acoustics* 73 (3 Mar. 2012), pp. 209–217. ISSN: 0003682X. DOI: 10.1016/j.apacoust.2011.09.002.

[48] Ran Giladi. "Real-time identification of aircraft sound events". In: *Transportation Research Part D: Transport and Environment* 87 (Oct. 2020), p. 102527. ISSN: 13619209. DOI: 10.1016/j.trd.2020.102527.

[49] Nur Asheila Taib and Busyairah Syd Ali. "An Analysis of Geometric Altitude Data in ADS-B Messages". In: International Technical Meeting of the Institute of Navigation, Feb. 2016. DOI: 10.33012/2016.13392.

[50] Luc Dekoninck. "Detecting and Correlating Aircraft Noise Events below Ambient Noise Levels Using OpenSky Tracking Data". In: OpenSky Symposium, Nov. 2020, pp. 12–13. DOI: 10.3390/proceedings2020059013.

[51] Christophe Rosin and Bertrand Barbo. "Aircraft noise monitoring: Threshold overstepping detection vs noise level shape and audio pattern recognition detection". In: 2011. URL: https://www.researchgate.net/publication/279527426.

[52] Keith Adams. "Towards Improving the Characterisation of Aircraft and Background Noise". In: 20th International Congress on Acoustics, Aug. 2010.

[53] Jorge Mariscal-Harana et al. "Audio-based aircraft detection system for safe rpas bvlos operations". In: *Electronics (Switzerland)* 9 (12 Dec. 2020), pp. 1–13. ISSN: 20799292. DOI: 10.3390/electronics9122076.

[54] C. Asensio, M. Ruiz, and M. Recuero. "Real-time aircraft noise likeness detector". In: *Applied Acoustics* 71 (6 June 2010), pp. 539–545. ISSN: 0003682X. DOI: 10.1016/j.apacoust.2009.12.005.

[55] Maciej Kłaczyński and Paweł Pawlik. "Automatic detection system of aircraft noise events during acoustic climate long-term monitoring near airport". In: *VibroEngineering Procedia* 6 (Oct. 2015), pp. 352–356. ISSN: 2345-0533.

[56] D P Rhodes and J B Ollerhead. *Aircraft Noise Model Validation*. 2001.

[57] H.W. Veerbeek and D.H.T. Bergmans. *Verification of Heathrow Noise and Track Keeping Systems*. NLR - Netherlands Aerospace Centre, July 2016.

[58] Commission Directive (EU). "Directive 2015/996: Assesment methods for the noise indicators". In: *Official Journal of the European Union* 168 (1 July 2015).

[59] Darren Rhodes. *Peer Review of Noise Modelling using ECAC Doc. 29 for Amsterdam Schiphol Airport*. UK Civil Aviation Authority, Oct. 2018.

[60] IEC 60942. *Electroacoustics - Sound calibrators*. 2017.

[61] Richard Payne. *Uncertainties associated with the use of a sound level meter*. National Physical Laboratory Report DQL-AC 002, 2004.

[62] Sanford Fidell and Paul Schomer. "Uncertainties in measuring aircraft noise and predicting community response to it". In: *Noise Control Engineering Journal* 55 (1 Jan. 2007), pp. 82–88. ISSN: 0736-2501.

[63] D Rhodes. *Guidance on comparing calculated aircraft noise levels with measurements*. UK Civil Aviation Authority, Dec. 2018.

[64] Deniz Sari et al. "Measuring the levels of noise at the Istanbul Atatürk Airport and comparisons with model simulations". In: *Science of the Total Environment* 482-483 (1 June 2014), pp. 472–479. ISSN: 18791026. DOI: 10.1016/j.scitotenv.2013.07.091.